

U.S. DEPARTMENT OF THE INTERIOR
U.S. GEOLOGICAL SURVEY

**METHANE IN COASTAL SEA WATER, SEA ICE, AND
BOTTOM SEDIMENTS, BEAUFORT SEA, ALASKA--
RESULTS FROM 1995**

Thomas D. Lorenson¹ and Keith A. Kvenvolden¹

Open-File Report 97-54

This report is preliminary and has not been reviewed for conformity with U.S. Geological Survey editorial standards (or with the North American Stratigraphic Code). Any use of trade, product, or firm names is for descriptive purposes only and does not imply endorsement by the U.S. Government.

¹Menlo Park, California 94025

Contents

	Page No.
Abstract	3
Introduction	3
Methods	4-9
Results	10
<i>Water Methane Concentrations</i>	10
<i>Water Methane Carbon Isotopic Compositions</i>	11-14
<i>Dissolved Inorganic Carbon in Water</i>	14
<i>Nutrients in Water</i>	14
<i>Methane in Ice cores</i>	14-17
<i>Methane in Sediments</i>	17-18
Summary	18
Acknowledgments	20
Table 1. Methane concentration, carbon isotopic composition, oxidation rates, and dissolved inorganic carbon concentration in sea water	21-23
Table 2. Seawater nutrient concentration	24-26
Table 3. Methane concentration in sea ice	27
Table 4. Hydrocarbon gas concentration in sediments	28
References	29-31
Appendix 1	32-50
<i>Water Temperature - Salinity - Methane Concentrations plotted with water depth for each station</i>	51-59
Appendix 2	60-68
<i>Methane concentrations in water plotted with water depths grouped by transects from each survey</i>	69-71
Appendix 3	72-74
<i>Water column cross sections of methane concentrations and carbon isotopic composition grouped by transects from each survey</i>	75-77
Appendix 4	75-77
<i>Dissolved inorganic carbon in water plotted with water depth grouped in transects conducted in August 1995</i>	75-77
Appendix 5	75-77
<i>Methane oxidation rates of water plotted with water depth grouped in transects conducted in each survey</i>	75-77
Appendix 6	75-77
<i>Methane concentrations of ice plotted with ice depth, grouped in transects</i>	75-77

Abstract

This report summarizes data acquired in 1995 for the gas-hydrate portion of the USGS project "Permafrost and gas hydrate as possible sources of methane" of the USGS Global Change and Climate History program. The report is the final addition to data summarized in the initial report entitled "Methane in coastal sea water, sea ice, and bottom sediments, Beaufort Sea, Alaska." (USGS Open-File Report 95-70) which covers the years 1990-1994.

The objective of this project has been to test the hypothesis that methane hydrate deposits of the Beaufort Sea continental shelf are destabilized by the ~ 10°C temperature increase that has resulted from the Holocene transgression of the Arctic Ocean. To test this idea we have selected an area off the north coast of Alaska between Harrison Bay and Camden Bay. During 1995 we concentrated on the central part of this area between the Colville River and Sagavanirktok River. We measured the concentration of methane in surficial sediments, in the water column when ice is present and absent, and in seasonal sea ice. Our results show that more methane is present in the water when ice is present than when ice is absent, and that methane is also present within the ice itself, often at higher concentrations than in the water. The Beaufort Sea shelf of Alaska is a likely seasonal source of methane. The primary source of this methane is probably microbial ($\delta^{13}\text{C} = -51.0$ to $-77.0\text{\textperthousand}$), but a small, ephemeral source of thermal methane ($\delta^{13}\text{C} = -46.4\text{\textperthousand}$), possibly from dissociated methane hydrate, may also contribute.

Introduction

Methane is an important trace component of the atmosphere. Its concentration is increasing at a rate of about 0.9% per year (Khalil and Rasmussen, 1983; Steele et al., 1987; Blake and Rowland, 1988), although this rate has decreased recently (Steele, et al., 1992). Because methane is radiatively active, it is a "greenhouse" gas that has a global warming potential 20 times larger than an equivalent weight of carbon dioxide when integrated over a 100-yr. span of time (Shine et al., 1990). The earth's atmosphere has a wide variety of sources and sinks for methane (Cicerone and Oremland, 1988), including gas hydrate. Gas hydrate exists in metastable equilibrium with its environment and is affected by changes in pressure and temperature. The amount of methane that is trapped in gas hydrate is perhaps 3,000 times the amount in the atmosphere (Kvenvolden, 1988). A large release of methane from gas hydrate could have a significant impact on atmospheric composition and thus on the radiative properties of the atmosphere and likely warm the earth (MacDonald, 1990).

Gas hydrate deposits of polar continental shelves are currently believed to be the most vulnerable to climate change (Kvenvolden, 1988).

These areally extensive shelves, formerly exposed to very cold surface temperatures (yearly average -10° to -20° C) have been and are being transgressed by a much warmer polar ocean (~0° C). As a result, the polar shelf surface in water depths greater than ~5 m, has experienced an approximately 10° C or more temperature increase over the past 10,000 years. Although pressure on shelfal gas hydrate deposits has increased owing to a rise in sea level of about 100 m, this pressure increase which would stabilize the gas hydrate, is more than offset by the large temperature increase that destabilizes the gas hydrate. The amount of methane released by this process has been estimated to be about 4 Tg (10^{12} grams) year⁻¹ (Kvenvolden, 1991) or about 1% of all current sources of atmospheric methane. If this suggestion and estimate are correct, then escape of methane from gas hydrate deposits of polar continental shelves should be observable. To test this idea, beginning in 1990 we conducted surveys of methane in sediment, water, and ice in an area of the Beaufort Sea continental shelf offshore from the north coast of Alaska. Previously, measurements of atmospheric methane concentrations at Barrow, Alaska, about 200 km northeast of the study area, showed a seasonal increase during August through February, perhaps due in part to methane venting from Arctic shelfal waters (Figure 1). This report summarizes our data collected in 1995. Data from the years 1990-1994 can be found in the companion report of Lorenson and Kvenvolden (1995).

Methods

In our 1995 survey, we measured methane concentration in sea water under the ice on four primary transects from nearshore to the shelf break at water depths ranging from 2.5 to 58 m from the Colville River Delta east to the Endicott oil production facility, Alaska (Figure 2). The surveys were undertaken during the first week of May 1995, and the later portion of August 1995. At each station in May, a 23-cm diameter hole was drilled through the 2-m thick ice. Niskin bottles (1.7 L) were attached at intervals to a line lowered to the seafloor and subsequently tripped to collect water samples for methane determinations. In August 1995, when partially open water was present, a boat was used to transit to stations. As each Niskin bottle was recovered, 100 cm³ of water was transferred to a 140 cm³ syringe. At the end of each day's field work, 40 cm³ of ultra-pure nitrogen was added to each of the syringes, and methane was extracted from the water into the nitrogen at room temperature by shaking the syringe, following a method modified from McAullife (1971). A portion of the resulting gas mixture was measured for methane content by gas chromatography. Multiple extractions were used on several samples to

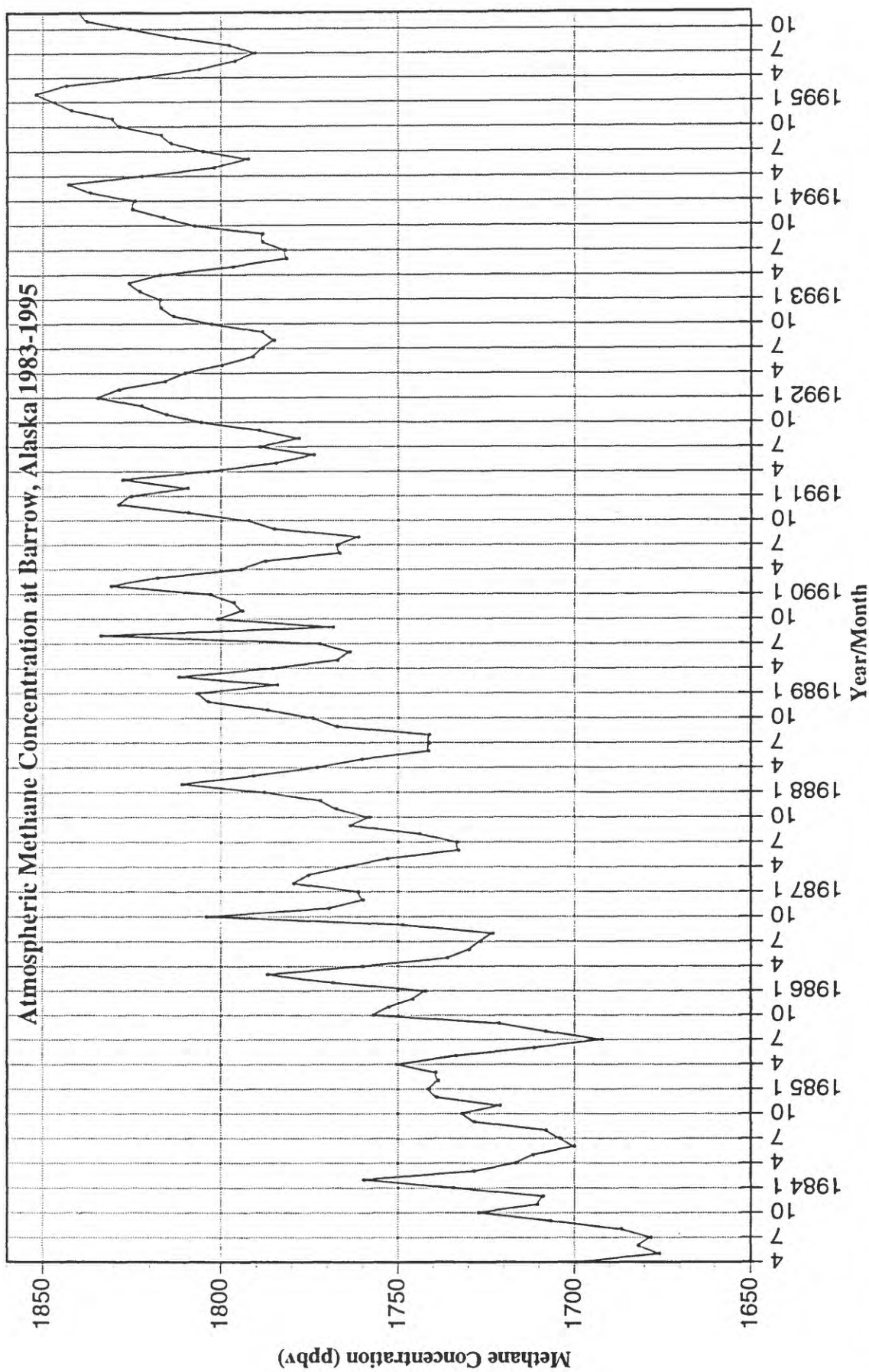


Figure 1. Mean monthly atmospheric methane concentration (ppb-v, parts per billion by volume) measured at Barrow, Alaska from 1983-1995. Measurements are made by the National Oceanic and Atmospheric Administration (NOAA), Climate Monitoring and Diagnostics Laboratory (CMDL).

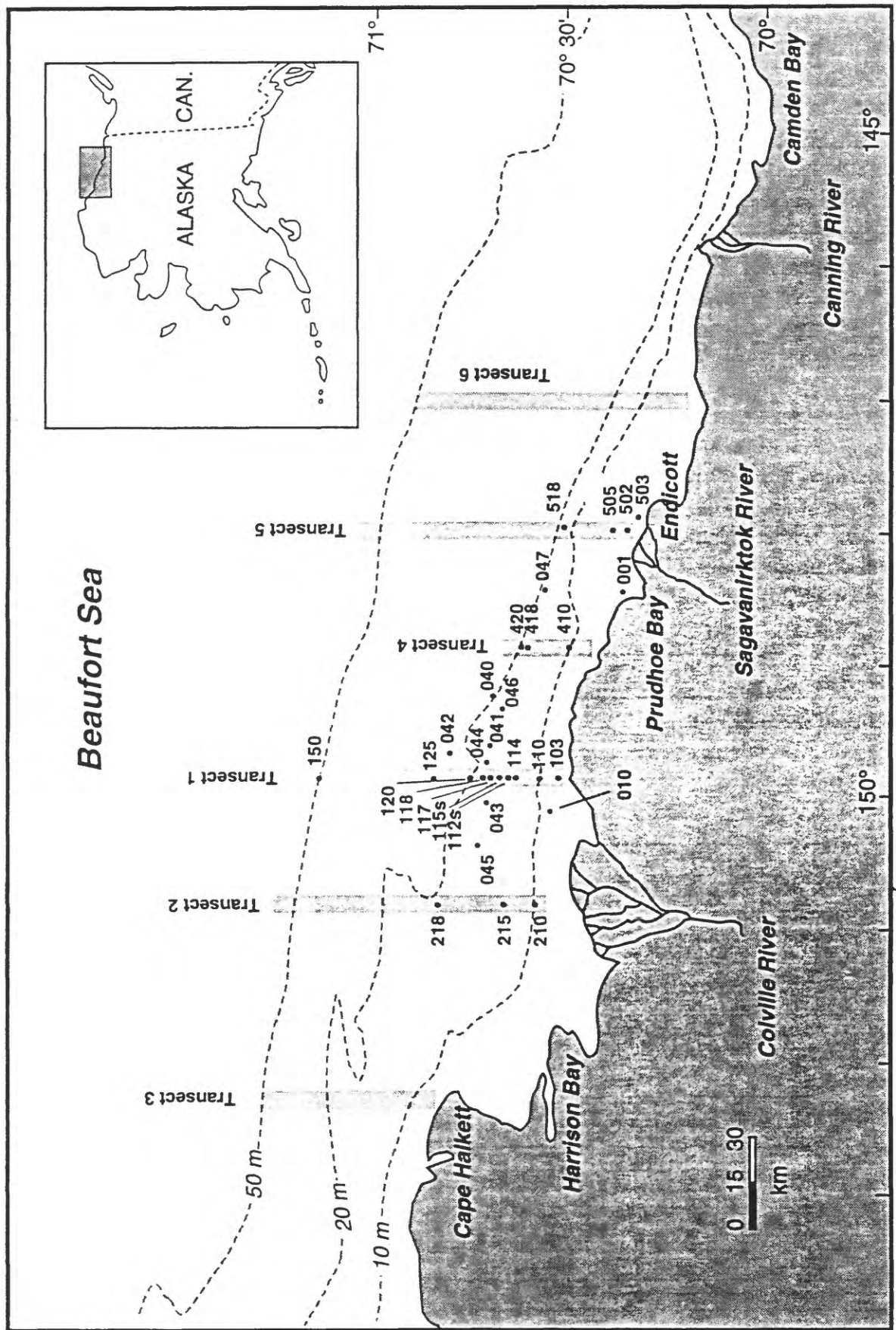


Figure 2. Station numbers and locations for the survey conducted in 1995. Also shown are transects 1 through 6 where similar surveys were conducted over the past 5 years.

determine an empirical extraction efficiency coefficient which was utilized with the remainder of the samples that were extracted only once. Our analyzed gas standard contained $10 \text{ ppm} \pm 2\%$ methane in nitrogen. Duplicate samples were analyzed for each water depth with an average standard deviation of $\pm 0.6 \text{ nM}$.

Methane oxidation was measured on water samples that were taken directly from Niskin bottles in approximately 50 ml aliquots leaving about 15 ml of headspace in the sample container. Each sample was shaken to remove the ambient methane that was present in the original water sample. A portion of each sample was transferred to a 14-ml vial leaving no headspace and inoculated with $^{14}\text{CH}_4$ equilibrated water. The vials were incubated at in situ temperatures in darkness, allowing the bacteria to oxidize $^{14}\text{CH}_4$ to $^{14}\text{CO}_2$ as well as incorporate ^{14}C into the bacterial biomass. While incubating, the ambient CH_4 concentrations were measured using a portable gas chromatograph (GC). The concentration of $^{14}\text{CH}_4$ added to the vials was also measured by GC. The incubations were ended at roughly eight hour intervals for a total of 24 hours by addition of 6N NaOH. The samples were then stored in 40-ml vials for later laboratory analysis. In the laboratory, the samples were transferred to 50-ml serum and sealed with a septa that was fitted with a basket containing a piece of accordion folded filter paper (approx. 3 cm x 5 cm). The filters were then soaked with 0.4 ml of 6N NaOH and the liquid sample was acidified using 0.4ml of 10N H_2SO_4 . The $^{14}\text{CO}_2$ derived from methane oxidizing bacteria entered the headspace as a gas and was trapped on the filter paper. Along with the samples, known standards were run under the same conditions. The serum bottle was filled with 20 ml of distilled water and then 0.3 ml of 6N NaOH was added. Next, 10 μl of a standard radiolabeled bicarbonate solution was added to the solution. The samples and standard were occasionally swirled for at least 24 hours. After complete $^{14}\text{CO}_2$ gas evolution, the baskets and filter paper were placed into 40 ml scintillation vials. Finally, 15 ml of Cytoscint brand scintillation flour was added to the vials and placed in a Packard Series Liquid Scintillation Counter (LSC) which measures disintegrations per minute (DPM). In addition to this procedure, the liquid sample that contained the biomass was filtered using a $0.22 \mu\text{m}$ membrane filter to trap the biomass. The filters were dried and flooded with 10 ml of Cytoscint and counted on the LSC as well. The results are presented as nM methane oxidized per day and related to DPM by the following relationship:

$$\begin{aligned} \text{nM CH}_4 \text{ oxidized/L day}^{-1} = \\ (\text{DPM/sample vol. L}) * (1\text{Curie}/2.2 \times 10^{12} \text{DPM}) * (1 \text{ M}/55 \text{ Curies}) * (10^9 \text{ nM}/1\text{M}) \end{aligned}$$

Dissolved inorganic carbon (DIC) was measured in selected water samples from 8 stations mainly along Transect 1 in August, 1995. Water samples were collected onboard-ship from Niskin bottles equipped with a short latex hose attached to the spigot. The hose, once flowing with sample was placed into a 200 ml glass flask equipped with a ground-glass stopper and flushed with 2-3 volumes of sample. Air bubbles were avoided by placing the hose at the bottom of the bottle. Once filled, about 3 ml of water was removed and a small amount of aqueous mercuric chloride was added as a biocide. Finally the bottle was capped with the stopper which had been lubricated with silicone grease. The samples were kept at ambient temperature until analyses at a shore-based laboratory. In the laboratory the samples were measured for DIC by a UIC model 5011 CO₂ coulometer described in detail by Dickson and Goyet, 1994. Accuracy/precision for the system is about 1.0 µmole/kg.

CTD (conductivity, temperature, depth) casts were made at most stations. CTD data was recorded internally by a Seacat 19 (May 1995) or 25 (August 1995) CTD probe made by Sea Bird of Seattle Washington. The data was downloaded onto a computer where it was processed using Seasoft Version 4.016. The sub-programs DATCNV, BINAVE, then SPLITCTD were utilized to process the raw data. The data were averaged into 0.5 m intervals. The upcast and downcast were evaluated, and only upcast is plotted. The upcast was used because the sensors showed less fluctuation. The results are plotted for each station and appended with dissolved water methane concentrations in Appendix 1, pg. 32-50.

The methods utilized to measure nutrients in this study were adapted from older colorimetric procedures and are described in detail by Whittlege and others, (1981). A basic description of each method, conducted on a Technicon Autoanalyzer System, follows:

Phosphate is determined as phosphomolybdic acid which in its reduced form in the presence of antimony has an absorption maximum at 880 nm. The method is basically an automated version of the procedure of Murphy and Riley (1962).

Orthosilicic acid is determined by its reaction with molybdate in aqueous acidic solution to form silicomolybdic acid. In this procedure, which is basically that of Armstrong and others (1967), where stannous chloride is used to reduce silicomolybdic acid to the heteropolylic acid which has an absorption maximum at 820 nm.

Nitrite is determined by the Greiss reaction in which sulfanilamide and N-(1-Naphthyl)ethylenediamine dihydrochloride react with nitrite in aqueous acidic solution to form an intensely pink diazo dye with an absorption maximum at 540 nm. Nitrate, after it is reduced to nitrite by passage through a column of copperized cadmium filings, is determined in an identical manner to nitrite (Wood and others 1967). This analysis gives

the sum of nitrate + nitrite, and nitrate is determined by difference.

Ammonium is determined by the Berthelot reaction in which hypochlorous acid and phenol react with ammonia in aqueous alkaline solution to form indophenol blue, an intensely blue chromophore with an absorption maximum at 637 nm. The method utilized is a modification of the procedure reported by Slawyk and MacIsaac (1972).

The methane content of sea ice was measured at 7 stations in 1995 as compared to 51 stations in 1993 to 1994. The stations were located along transect 1, and at stations 010 and 503; the latter two stations were chosen because of their historically elevated methane concentrations. A 1 m long by 7.6 cm diameter ice corer with an extension was used to core through the ice to sea water. The ice core was laid out on the sea ice, measured and cut into 10 cm sections. Selected intervals were chosen, then placed in 1-liter friction sealed cans equipped with 2 septa ports, sealed, and kept frozen. At the field laboratory, each sample was weighed, then the headspace within the can was purged with ultra pure nitrogen for 5 minutes at flow rates exceeding 500 ml/min. Tests on the methane content of the purged headspace with the frozen ice core inside yielded concentrations less than 0.1 ppm. The cans containing ice samples were placed in hot water baths and stabilized at approximately 20° C. Each can was shaken by hand for about 30 seconds to partition the dissolved methane between the water and the nitrogen headspace. Next, a syringe containing 30 ml of ultra pure grade nitrogen was injected into the can, then 30 ml of the resulting mixture of headspace and gas was removed and analyzed for methane content in the same manner as described for sea water samples. The volume of headspace in the can was determined by the weight of the ice sample, assuming that once melted the water occupied a volume of 1 ml/gm.

Sediment samples were taken in May 1995 operating from the ice canopy. A hole was augured in the ice, through which a 45 x 7.5 cm core barrel with an auger cutting head was lowered. The core barrel was attached to 1.5-m long connecting stems in series up to a maximum length of 15.5 m. Once on the ocean bottom, the core barrel was rotated by hand with the aid of a T bar until no further penetration was achieved. Upon retrieval, the liner containing sediment was extruded onto the ice. A 10 cm section of the core was placed in a septa-equipped 1-liter sample can. Seawater was added to the brim of the can, then 200 ml of water was removed, creating a 200 ml headspace. About 2-3 grams of sodium azide was added as a biocide. The can was sealed, then purged with helium at a flow rate estimated to be greater than 500 ml/min. for 5 minutes. The samples were kept frozen until analysis at our Menlo Park laboratories.

Results

Stations in water depths from 2.5 to 58 m were reoccupied on four of the previously established six north-south transect lines as shown in Figure 2. Three digit, abbreviated station numbers are shown on the transect lines. Many stations were reoccupied on subsequent surveys. Each station is given 3 additional numbers making a total of six digits per station. The first two refer to the year, the third to the month of sample collection, the fourth to the transect number, and the last two represent the approximate water depth at each station. For example, station 955120 can be read as 1995, May, Transect 1, at 20 meters water depth. When the same station was reoccupied on a subsequent survey only the first 3 digits change denoting a different sampling date; i.e., 958120 was completed in August, 1995. Stations off transect lines are given a 0 in the fourth digit place.

Water Methane Concentrations and related measurements

In 1995 we concentrated our efforts around the previously described methane anomaly located near station 120 (Transect 1, Oliktok Point, 20 m; Lorenson and Kvenvolden, 1995). At station 120 we had observed an anomalously high methane concentration near the bottom on two occasions: 94 nM in May 1992, and 149 nM ($\delta^{13}\text{C} = -46.4\text{\textperthousand}$) in August, 1994. The anomalous occurrence on two occasions and the isotopic composition expected from destabilizing "Kuparuk" gas hydrate led us to believe that there might be an ephemeral seep leaking methane into the ocean from a gas hydrate source. To date, this remains the most compelling observation in favor of destabilizing gas hydrate on the Arctic shelf; however, we were not able to confirm this observation by locating the seep site, nor did we see any evidence of a seep in 1995.

Water methane concentrations, carbon isotopic composition, methane oxidation rates, and total dissolved inorganic carbon were measured and are listed in Table 1, pg. 21-23. Graphs of methane vs. water depth at each transect are given in Appendix 2, pg. 51-59, and water mass transect cross sections are shown in Appendix 3, pg. 60-68. DIC concentrations vs. depth at Transect 1 and nearby 18 m deep stations measured in August 1995 are given in Appendix 4 pg. 69-71. Measurements of methane in ice-covered sea water were made in May 1995. The results are compared with measurements taken in partially ice-free water during August 1995.

Analyses of 66 samples from ice-covered waters demonstrate that methane concentrations in the water column are supersaturated with respect to the equilibrium solubility of methane with the atmosphere (~4 nM). Maximum methane concentrations at a given station ranged from 18 to 197 nM (12 to 275 nM in 1992-1994) and were typically about 30 to 45 nM (15 to 25 nM in 1992-1994) throughout the water column (Figure 3). The highest methane concentrations were commonly found near the bottom;

however, a significant number of stations had the highest concentrations in the upper 10 m. This observation is unique in this five-year study. In May 1995 a large area of grounded ice was seen at about the location of 955115s. We think that the ice keeling into the bottom sediment may have had an effect on the methane concentration by suspending methane-rich sediment in the water column. The more typical observation of maximum methane concentration near the bottom was seen in other areas. Maximum methane concentrations are given in map view in Figure 3.

Methane concentrations from ice-free water were determined in 82 samples. Maximum methane concentrations at a given station ranged from 6 to 56 nM (5 to 44 nM in 1993-1994 excluding anomalies) (Figure 4). Typically, methane concentrations were at a minimum at the surface, remained nearly constant or increased with depth to concentrations ranging from 21 to 56 nM (9 to 44 nM in 1993-1994 excluding anomalies). In sharp contrast to previous ice-free surveys, during the period of August 1995, the pack ice receded only to about the 20 m isobath. From about the 15 m to the 20 m isobath the ice content of the water grew progressively greater. This situation produced a 2 to 6 m layer of fresher (about 12 to 20 ‰ salinity, see Appendix 1) water over more saline, marine water. Melting ice is believed to be the source of most of the fresh water, with some input from rivers. As a consequence, methane in the deeper, more saline water was shielded from the atmosphere, where it would most likely have escaped. Methane concentrations in the upper 3 m of water ranged from 7 to 36 nM. Methane concentrations in the upper 3 m of ice-free water in the 1993-1994 surveys never exceeded 18 nM and were commonly between 6 and 14 nM.

Water Methane Carbon Isotopic Composition

Measurements of the carbon isotopic composition ($\delta^{13}\text{C}$) of methane in 128 water samples were made at the University of Hawaii. The results are shown in Table 1. Values range from -51.0 to -77.0 ‰ with one outlier of -37.1 ‰. The results strongly suggest that the source of methane is from microbial degradation of organic material in bottom sediments. No distinct seasonality between the May survey and the August survey was noted and there are variable trends of isotopic composition with depth. During the May survey the carbon isotopic composition is nearly equal throughout the water column at transect 2, although along transects 1 and 4 there is a tendency toward heavier values with depth, whereas at transect 5 the values become lighter with depth. During the August survey, again, the carbon isotopic composition is nearly equal throughout the water column; however, in transects 1, 4, and 5 there is a slight tendency toward lighter values with depth, whereas at transect 2 the values are mixed. Appendix 3 contains cross sections along transects depicting both methane concentration and isotopic composition isopleths. In addition an inset contains a similar cross

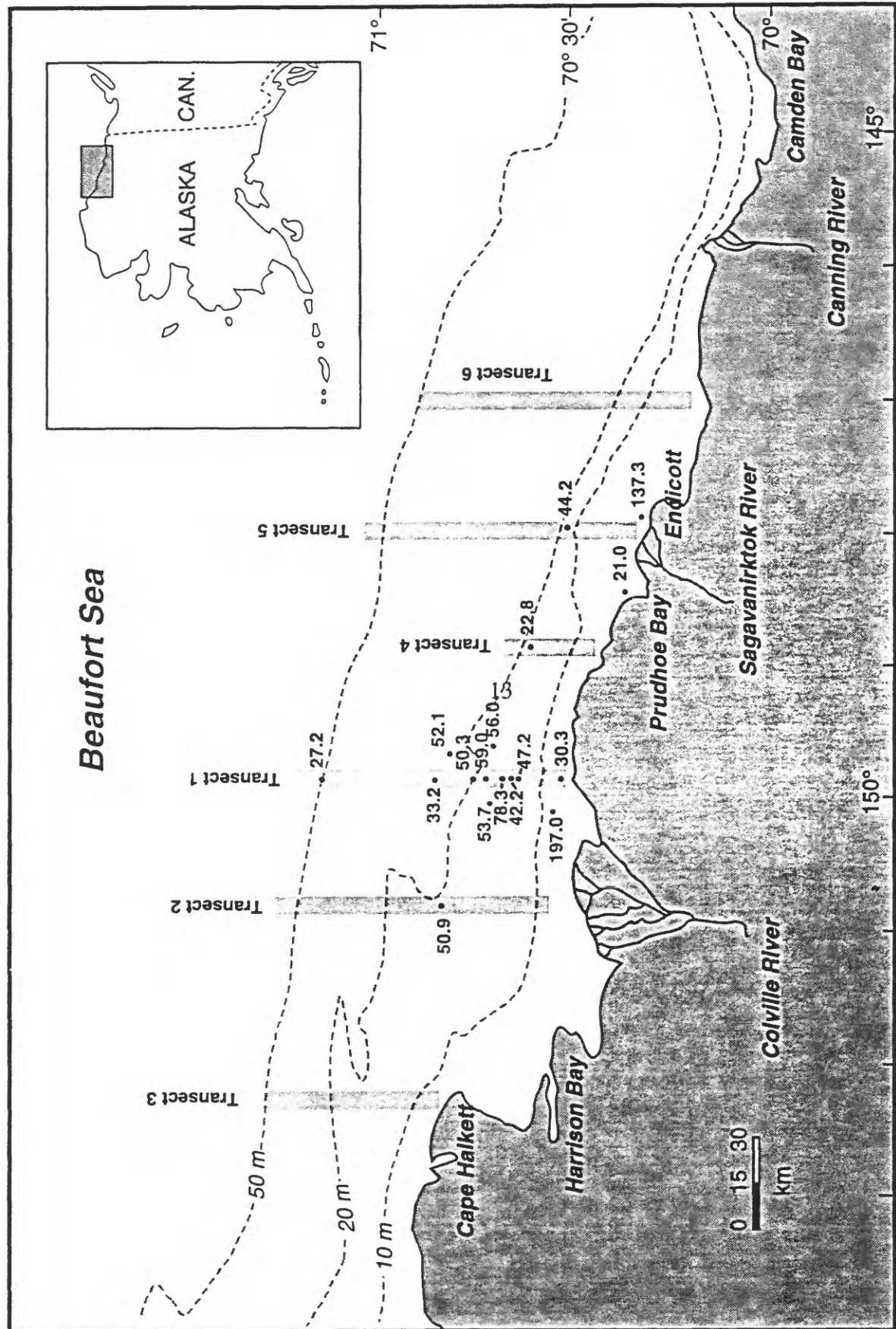


Figure 3. Maximum methane concentrations (nM) in water, May 1995

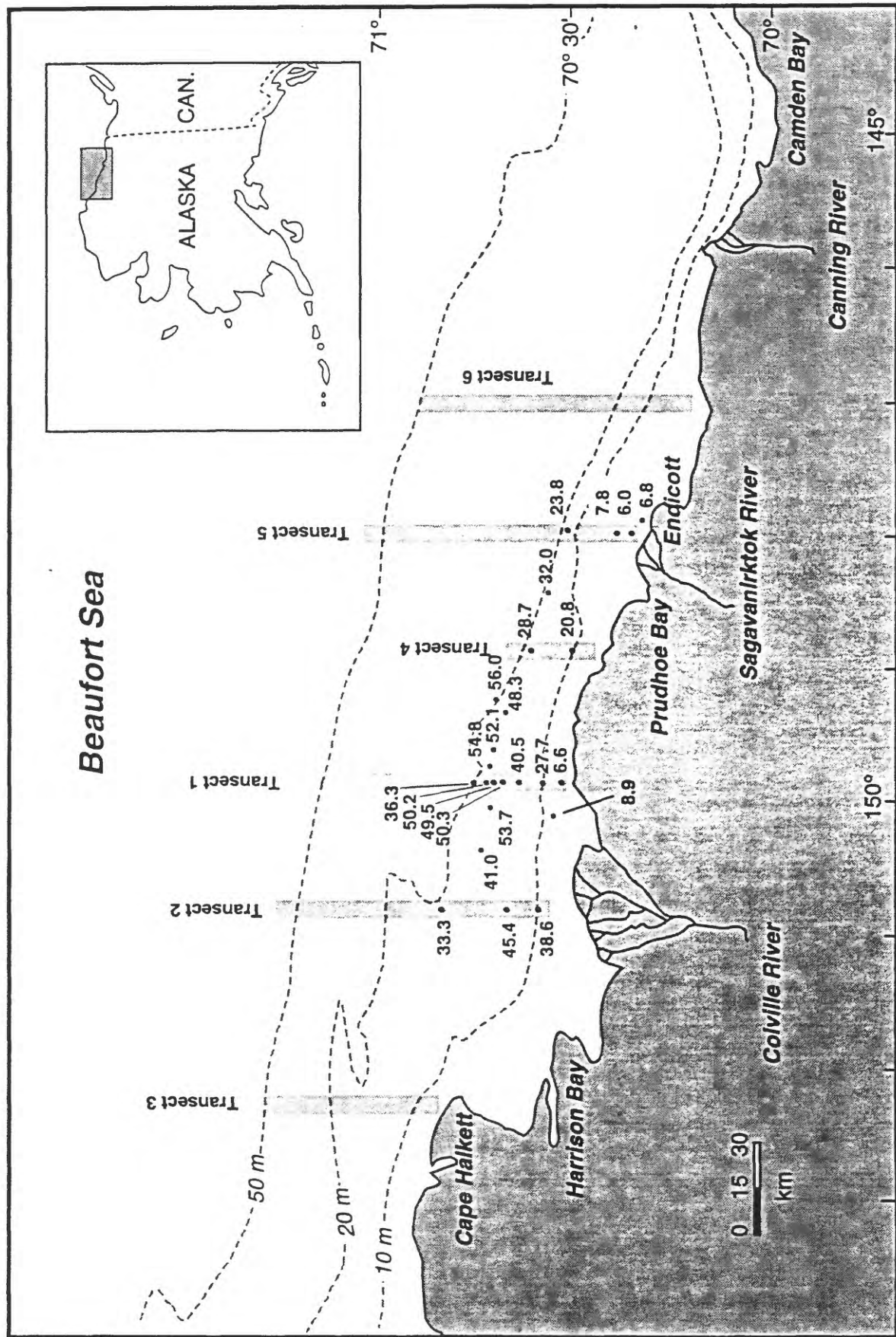


Figure 4. Maximum methane concentrations (nM) in water, August 1995

section from the last survey during the same season for comparison. In general these composite pictures look very different attesting to the changing nature of the environment and its effect on methane dynamics in the Beaufort Sea.

Methane oxidation rates were determined in selected samples (Table 1) and are given graphically in Appendix 5, pg. 72-74. Our results show that specific oxidation rates for methane found in the Beaufort Sea are comparable to estuarine and oxic/anoxic boundary layer values (10^{-4} to 10^{-3} per day). While these rates are generally higher than typical open ocean rates ($<10^{-4}$ per day), methane loss due to oxidation is small compared to other losses such as flux to the atmosphere. These oxidation rates would account for only 1 to 2% of the methane available in the water column. These results further support our previous conclusions that the methane accumulated during the winter months is mostly ventilated to the atmosphere during the summer and probably contributes to the observed seasonal atmospheric methane cycle (McLaughlin et al., 1996). The results from the May 1995 and previous surveys show that during ice covered times methane oxidation rates are much higher than in ice free periods (September, 1993), when the oxidation rates were undetectable. Thus a seasonality exists regarding the oxidation of methane by bacteria living in the water column.

Dissolved Inorganic Carbon in water

The dissolved inorganic carbon (DIC) content of the water column was measured on the August 1995 survey. The results show a correlation between methane concentration and DIC (Figure 5). A correlation also exists between salinity and DIC, reflecting the addition of ice melt-water and river water to the ocean. DIC values within the 1200 to 1900 μM range correlate with lower salinities (diluted sea water) in the upper 6 m of the water column. This water layer acts like a cap over the more saline, methane-rich water beneath it and likely prevents methane from escaping into the atmosphere much like the ice canopy does. Profiles of DIC vs. depth along and near transect 1 are given in Appendix 4, pg. 69-71.

Nutrients in water

The nutrients, phosphate (PO_4), silica (Si, measured as H_4SiO_4), ammonium (NH_4), nitrite (NO_2), and nitrate (NO_3) were measured at many stations throughout the study period. We collected samples as a service to oceanographers studying the Arctic Ocean and merely report the data here with no interpretation. The results are given in Table 2, pg. 24-26.

Methane in ice cores

We measured the methane content of samples from the ice canopy in

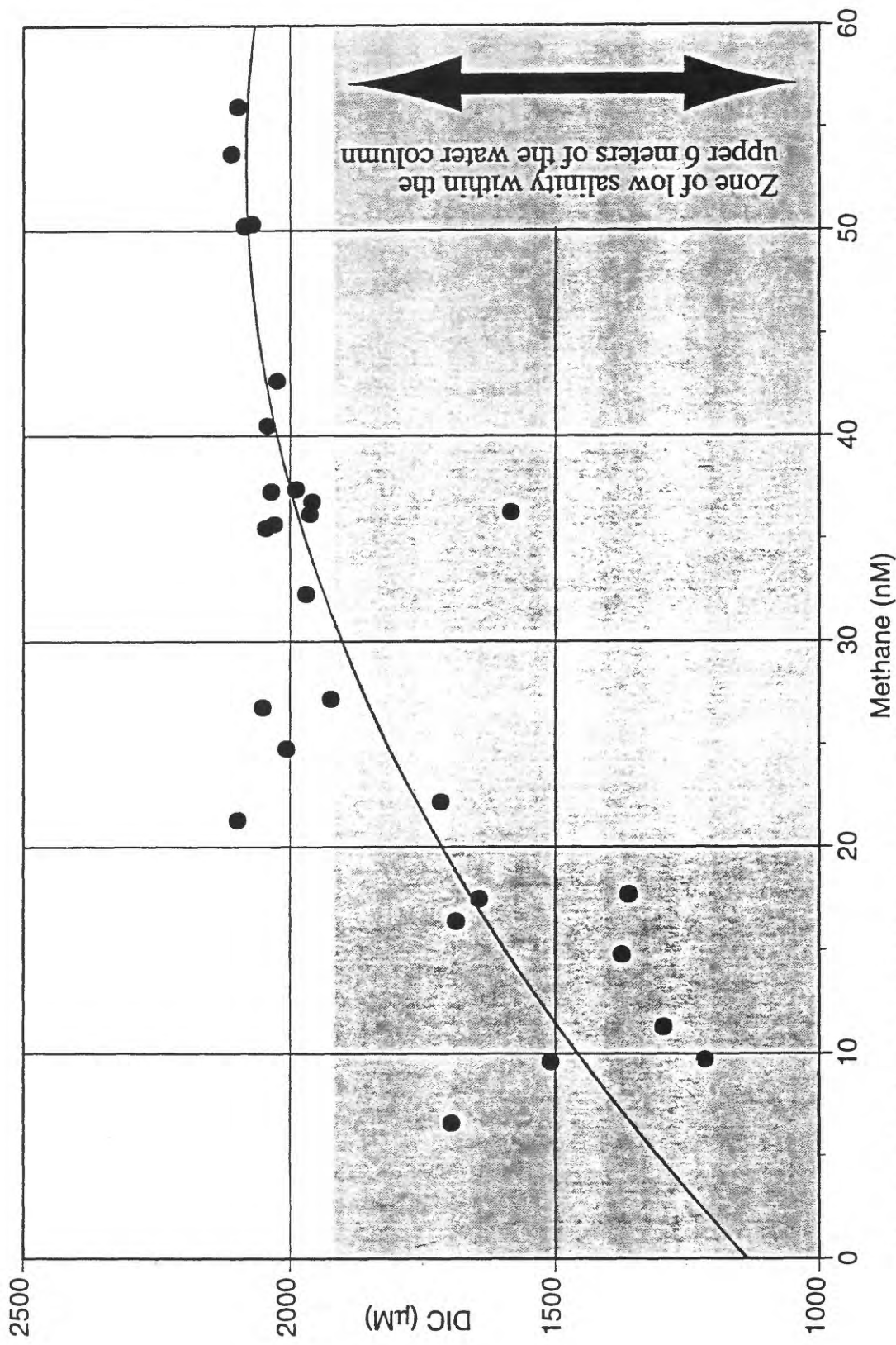


Figure 5. Methane concentration versus dissolved inorganic carbon concentration (DIC) in water along and near transect 1 for August 1995. The good correlation between the two components is most likely related to the salinity of the water. DIC values within the 1200 to 1900 μM are consequent with lower salinities (diluted sea water) in the upper 6 m of the water column, a water layer that acts like a cap over the more saline, methane rich water beneath it.

May 1995. Typically coastal sea ice inshore from 15 m water depth initially forms as a mobile mass of frazil, anchor, and brash ice a few decimeters thick. This mass gradually solidifies into granular "fast" or stationary ice by late fall. Subsequently the fast ice grows to a thickness of about 2 m over a fixed point on the seafloor. Ice seaward of about 15 m water depth (the seasonal ice pack) is formed in a similar manner but is subject to intense deformation and is mobile throughout the winter. Thus, fast ice is more likely to trap methane in transit from sea water to the atmosphere at a fixed location, whereas offshore ice more likely traps methane from non-fixed locations as it thickens.

We sampled fast ice and seasonal pack ice at 7 stations in 1995 (compared to 51 stations in 1993 to 1994): five stations along transect 1, and at stations 010 and 503, the latter two stations were chosen because of their historically elevated methane concentrations. Water depths ranged from 2 to 20 m. Methane concentrations are listed in Table 3. Methane concentration profiles along transects are given in Appendix 6, pg. 75-77.

Methane concentration profiles through the ice within the upper 50 cm interval and from water depths less than about 10 m contained the highest concentrations of methane (7 to 806 nM), with highly variable values. Even in two ice cores drilled 2 meters apart (955503 and 955503R), the values for the same intervals varied by as much as 66% and commonly by about 20-30%. In the ice interval from 50 to 200 cm, methane concentration ranged from 3 to 10 nM, with typical values of about 4-5 nM. In contrast to the 1995 samples, those from April 1993, and 1994 had concentrations of methane (7 to 1260 nM), with typical values of about 30 to 40 nM within the upper 50 cm interval and from water depths less than about 10 m. In 1993-1994, in the ice interval from 50 to 200 cm, the methane concentration ranged from 5 to 286 nM, with typical values of about 15 nM.

Ice that formed where water depths are greater than 15 m shows the same trend of decreasing methane with increasing depth in the ice core; however, the methane concentrations were less varied and were always lower. Within the 0 to 50 cm interval methane concentrations ranged from 6 to 10 nM (8 to 14 nM in 1993-94) and from 3 to 5 nM (5 to 14 nM in 1993-94) within the 50 to 200 cm interval.

The large differences in methane concentrations between 1993-94 and 1995 may be related to sample handing. The headspace in the 1995 sample set was purged with helium at a higher rate (>500 ml/min in 1995 as compared with 200 ml/min in 1993-1994) than those of previous years. Hence the concentrations seen in the 1995 samples, likely represent more closely the actual concentration in ice, whereas those measurements from previous years are likely too high and reflect some contamination by atmospheric methane.

Measurements of the carbon isotopic composition of methane in ice are

shown in Table 3 and reveal a wide range of values from -39.5 to -87.6‰. Core samples were measured at the highest concentrations of methane which occur within the upper 50 cm of the ice layer. At station 010, the carbon isotopic composition of methane was -87.6 ‰ (708 nM) at 0-10 cm, remaining nearly constant at -85.0 ‰ (806 nM) at 30-40 cm. The correspondence of high methane concentration and very light carbon isotopic composition of methane strongly suggests a microbial source for methane.

In contrast, at station 955503, very near Endicott Island, an oil production facility, the carbon isotopic composition of methane ranges from -70.0 to -39.2 ‰. In addition there is an increase of methane concentration with depth from 11.7 to 88.9 nM corresponding to increasing heaviness of the carbon isotopic composition of methane in the upper 40 cm. This relationship suggests that thermogenic methane was added to some background concentration of microbial methane during initial freeze-up. However, at station 955503R, cored two meters from 955503, methane concentrations were lower in the same interval (8.5 to 64.6 nM), and the carbon isotopic composition of methane became lighter with depth. Regardless of the discrepancies, when the concentration of methane is highest, the corresponding carbon isotopic value of methane is heaviest indicating that the aforementioned suggestion concerning a thermal methane source is valid. The differences in methane concentration over such a short distance underscores the heterogeneous distribution of methane in sea ice.

Methane in sediments

In May 1990, our initial study of gas sources in Harrison Bay concentrated on surficial sediments. It was thought that if methane from destabilized gas hydrates were accumulating and migrating, the gas would transit through the sea floor. As a guide to sampling locations we reviewed the work of Neave and Sellman (1982), who seismically mapped subsea (drowned) permafrost and shallow gas anomalies. Our working model of gas hydrate occurrence in permafrost (Kvenvolden, 1988) requires that gas hydrate and permafrost coexist. Holocene sea level rise has, within the last 10,000 years, flooded the area now known as Harrison Bay. About a 10° C temperature rise over this area has initiated a downward migrating thermal pulse capable of melting permafrost and destabilizing gas hydrate. With the additional thermal insulation of the ocean, the geothermal gradient creeps upward and causes an upward migration of warmer temperatures (Lachenbruch and others, 1988). Osterkamp and Fei (1993) have shown that the combined effect of the temperature increases above and below the permafrost should have begun to melt the outer portions of the subsea permafrost, corresponding to approximately the 20 m isobath.

In May 1995 we again sampled surficial sediment for methane and

other hydrocarbon gases, the results are given in Table 4 and shown in Figure 6. In contrast to the 1990 survey, we concentrated our efforts mainly on transect 1 and in very shallow areas that had usual concentrations of methane incorporated in the sea ice. In addition, we cored most sites down to at least 30 cm, thereby allowing us to measure a deeper portion of the sediment column than in the previous survey. Methane concentration ranged from 3.3 to 18.4 $\mu\text{L/L}$ wet sediment and increased with depth in the sediment. In 1990 methane concentrations ranged from 2.2 to 10.1 $\mu\text{L/L}$. In addition to methane, trace concentrations of ethane, ethene, propane, and propene (see Table 4) in the sediment are likely formed by microbial action. Carbon isotopic measurements of methane in the water and ice above the sediment indicate that the methane is formed by microbial degradation of organic matter. Methane most likely enters the water column and sea ice from the sediment by a variety of processes of which ice keeling and anchor ice formation (the process by which bottom forming ice builds up and eventually floats upward, often with sediment adhering to the ice clumps) play an important role.

Summary

This report documents the concentrations of methane in sediment, water, and sea ice in an area of the Beaufort Sea continental shelf offshore northern Alaska for the year of 1995. This report extends and completes the data collected during field surveys conducted from 1990 to 1994. In addition to methane concentrations, information regarding carbon isotopic composition of methane in water and ice, methane oxidation rates, dissolved inorganic carbon, nutrients, salinity, and temperature of the water column are also tabulated. In general, more methane is present in the water when ice forms a seal over the water column than when ice is absent. A fresh water cap from melting ice and river discharge can also form a seal, albeit more permeable to methane transit to the atmosphere. Methane is also present in ice often in concentrations exceeding those in water. Fast ice forming in place over water depths less than about 10 m can contain methane concentrations an order of magnitude higher than that of the underlying water. Measurements of the carbon isotopic composition of methane in water and ice were initiated in 1994 and continued in 1995 as an attempt to define the source or sources of methane. These data represent the first ever collected in such a setting. The data thus far demonstrate a wide range of values from -31.6(measured 4-94 at station 503) to -87.6‰ indicating that there may be complex variety of sources; however, the preponderance of the data suggest that most of the methane is from a microbial source and most likely from the bottom sediment. The methane is incorporated into water and ice mainly by interactions of ice and bottom sediment of which ice keeling and anchor ice formation play an important role.

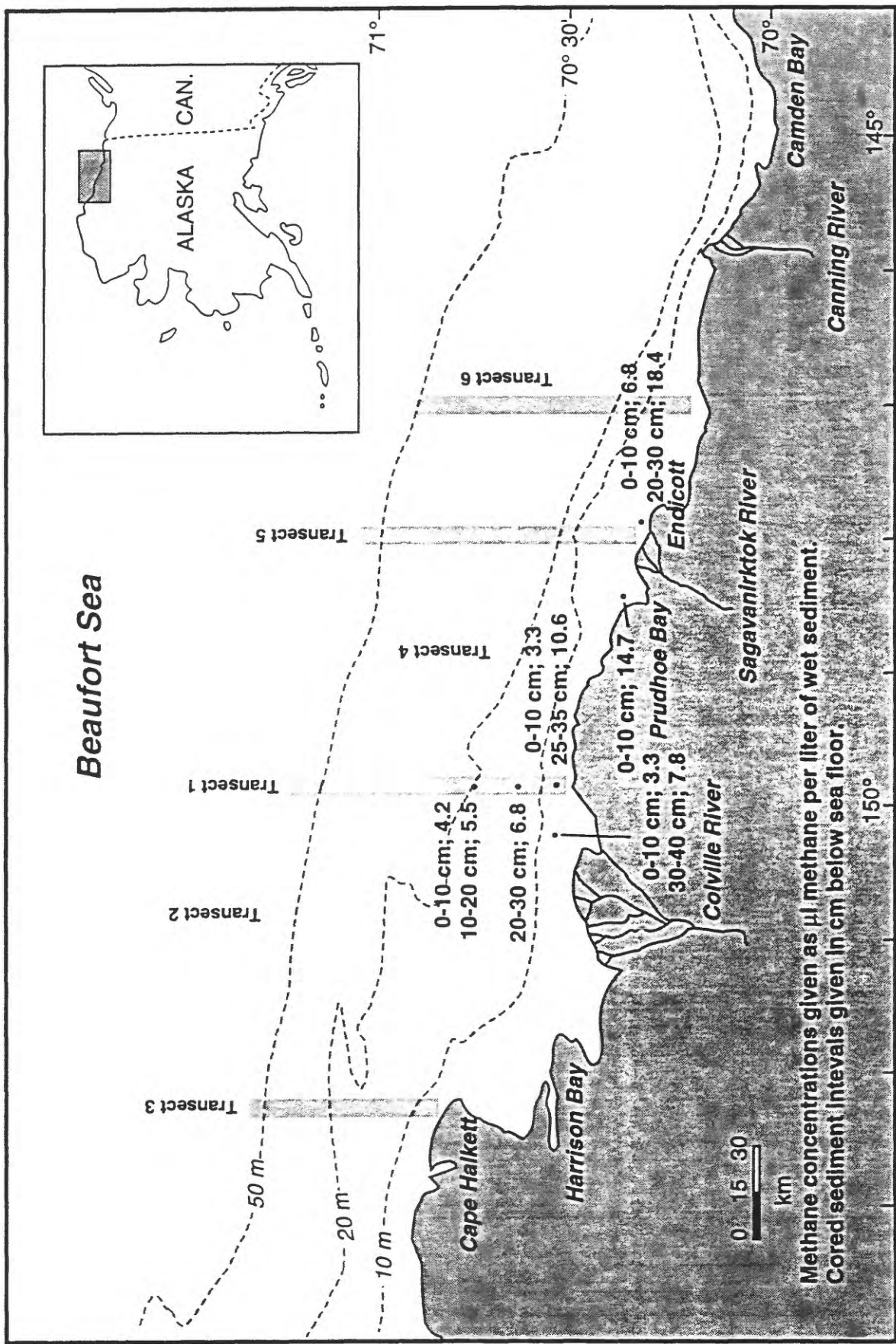


Figure 6. Methane concentrations in sediment ($\mu\text{L/L}$ wet sediment), in May 1995. Methane concentration increases with depth in the sediment. Isotopic measurements in the water and ice above the sediment indicate that the methane is formed by microbial degradation of organic matter.

Acknowledgments

The project has been conducted in collaboration with the University of Washington and the University of Hawaii. We thank (1) M.D. Lilley, E.J. Olson, E. McLaughlin, and K. A. Krogslund, School of Oceanography, University of Washington, for the information on methane concentrations, methane oxidation rates, and nutrient concentrations in seawater; (2) T. Rust, F. J. Sansone, and B.N. Popp, SOEST, University of Hawaii, for the isotopic analyses of methane and field assistance. (3) Rolf G. Schottle and Chris Winn, also with the University of Hawaii for DIC measurements and interpretations. We are grateful to P.W. Barnes, U.S. Geological Survey, for guidance in Arctic operations. This work was supported by the USGS Global Change and Climate History Program.

Table 1. Methane concentrations (nM methane per liter seawater), methane carbon isotopic composition, methane oxidation rates (nanoM methane per liter per day), and dissolved inorganic carbon (microM carbon per kilogram seawater).

Station	Latitude N.	Longitude W.	Date	Sample	Methane	Methane	DIC	Comments
					depth (m)	(nM)	Isotopic	
							Composition	
					(ppt)			
955001	70 24.540	148 31.470	5/6/95	3	21.0	-63.43	0.007	West Dock, Prudhoe Bay
955010	70 30.008	150 08.860	5/5/95	3	197.0	-60.26	8.668	5 km SW of Thetis Island
955040	70 44.068	150 13.434	5/7/95	3	33.6			18m contour about 6 nm west of Transect 1 Oliktok
955040	70 44.068	150 13.434	5/7/95	10	54.8			18m contour about 6 nm west of Transect 1 Oliktok
955040	70 44.068	150 13.434	5/7/95	17	35.4	-67.87	0.177	18m contour about 6 nm west of Transect 1 Oliktok
955041	70 42.035	149 39.986	5/7/95	3	46.7		0.043	18m contour about 6 nm east of Transect 1 Oliktok
955041	70 42.035	149 39.986	5/7/95	9	43.0		0.019	18m contour about 6 nm east of Transect 1 Oliktok
955041	70 42.035	149 39.986	5/7/95	14	45.5	bdl		18m contour about 6 nm east of Transect 1 Oliktok
955041	70 42.035	149 39.986	5/7/95	17	32.9	-62.63	0.027	18m contour about 6 nm east of Transect 1 Oliktok
955042	70 48.959	149 39.784	5/7/95	3	21.4		0.018	24m contour about 6 nm east of Transect 1 Oliktok
955042	70 48.959	149 39.784	5/7/95	10	31.2		0.134	24m contour about 6 nm east of Transect 1 Oliktok
955042	70 48.959	149 39.784	5/7/95	17	45.9		0.225	24m contour about 6 nm east of Transect 1 Oliktok
955042	70 48.959	149 39.784	5/7/95	23	35.0	-61.96	0.025	24m contour about 6 nm east of Transect 1 Oliktok
955103	70 31.950	149 53.210	5/5/95	2	30.3		bdl	Transect 1 3 m Oliktok Point
955114	70 38.094	149 53.014	5/5/95	3	47.2	-71.58	bdl	Transect 1 14 m Oliktok Point
955114	70 38.094	149 53.014	5/5/95	7	43.1	-63.07	bdl	Transect 1 14 m Oliktok Point
955114	70 38.094	149 53.014	5/5/95	11	36.0	-68.54	bdl	Transect 1 14 m Oliktok Point
955114	70 38.094	149 53.014	5/5/95	14	40.0	-56.83	0.014	Transect 1 14 m Oliktok Point
955112S	70 40.041	149 53.064	5/7/95	12	42.4	-66.68		Transect 1 Oliktok 12 m shoal outboard ice island
955115S	70 41.065	149 54.540	5/8/95	3	78.3		0.023	Transect 1 15 m Oliktok Point shoal outboard ice island
955115S	70 41.065	149 54.540	5/8/95	7	53.2	-79.40	0.064	Transect 1 15 m Oliktok Point shoal outboard ice island
955115S	70 41.065	149 54.540	5/8/95	12	48.6		0.131	Transect 1 15 m Oliktok Point shoal outboard ice island
955115S	70 41.065	149 54.540	5/8/95	14	42.8	-63.30	0.141	Transect 1 15 m Oliktok Point shoal outboard ice island
955118	70 42.431	149 53.768	5/5/95	17	48.7			Transect 1 18 m Oliktok Point
955118R	70 42.431	149 53.768	5/7/95	3	58.6			Transect 1 18 m Oliktok Point
955118R	70 42.431	149 53.768	5/7/95	9	59.0		0.313	Transect 1 18 m Oliktok Point
955118R	70 42.431	149 53.768	5/7/95	14	56.3	bdl		Transect 1 18 m Oliktok Point
955118R	70 42.431	149 53.768	5/7/95	17	44.9	-60.31	0.808	Transect 1 18 m Oliktok Point
955118X	70 42.431	149 53.768	5/8/95	3	58.3	-73.53		Transect 1 18 m Oliktok Point repeat #2
955118X	70 42.431	149 53.768	5/8/95	7	63.0	-72.10		Transect 1 18 m Oliktok Point repeat #2
955118X	70 42.431	149 53.768	5/8/95	10	52.1	-73.90		Transect 1 18 m Oliktok Point repeat #2
955118X	70 42.431	149 53.768	5/8/95	14	51.6	-70.03		Transect 1 18 m Oliktok Point repeat #2
955118X	70 42.431	149 53.768	5/8/95	17	46.2	-65.49		Transect 1 18 m Oliktok Point repeat #2
955120	70 47.074	149 52.852	5/4/95	3	19.8	-71.20	bdl	Transect 1 20 m Oliktok Point
955120	70 47.074	149 52.852	5/4/95	7	21.9	-71.06	bdl	Transect 1 20 m Oliktok Point
955120	70 47.074	149 52.852	5/4/95	11	28.3	-70.65	bdl	Transect 1 20 m Oliktok Point
955120	70 47.074	149 52.852	5/4/95	15	32.0	-70.99	bdl	Transect 1 20 m Oliktok Point
955120	70 47.074	149 52.852	5/4/95	19	21.0	-68.54	0.020	Transect 1 20 m Oliktok Point
955120R	70 47.074	149 52.852	5/7/95	3	21.6		0.004	Transect 1 20 m Oliktok Point repeat #1
955120R	70 47.074	149 52.852	5/7/95	9	22.8	bdl		Transect 1 20 m Oliktok Point repeat #1
955120R	70 47.074	149 52.852	5/7/95	14	50.3		0.080	Transect 1 20 m Oliktok Point repeat #1
955120R	70 47.074	149 52.852	5/7/95	19	45.2	-63.36	0.565	Transect 1 20 m Oliktok Point repeat #1
955125	70 51.246	149 52.692	5/5/95	3	18.4	-66.20	0.004	Transect 1 25 m Oliktok Point
955125	70 51.246	149 52.692	5/5/95	10	18.9	-66.61	bdl	Transect 1 25 m Oliktok Point
955125	70 51.246	149 52.692	5/5/95	15	20.9	-61.53	bdl	Transect 1 25 m Oliktok Point
955125	70 51.246	149 52.692	5/5/95	20	24.0	-64.28	0.003	Transect 1 25 m Oliktok Point
955125	70 51.246	149 52.692	5/5/95	25	33.2	-62.85	bdl	Transect 1 25 m Oliktok Point

Table 1. Methane concentrations (nM methane per liter seawater), methane carbon isotopic composition, methane oxidation rates (nanoM methane per liter per day), and dissolved inorganic carbon (microM carbon per kilogram seawater).

Station	Latitude N.	Longitude W.	Date	Sample depth (m)	Methane	Methane	DIC (µM/kg)	Comments
					(nM)	Isotopic Composition (ppt)		
					Oxidation Rate (nM/day)			
955150	71 11.132	149 52.994	5/4/95	3	22.2	lost	0.003	Transect 1 58 m Oliktok Point
955150	71 11.132	149 52.994	5/4/95	10	22.5	-61.76	bdl	Transect 1 58 m Oliktok Point
955150	71 11.132	149 52.994	5/4/95	20	25.9	-63.04	bdl	Transect 1 58 m Oliktok Point
955150	71 11.132	149 52.994	5/4/95	30	21.0	-57.81	bdl	Transect 1 58 m Oliktok Point
955150	71 11.132	149 52.994	5/4/95	40	27.2	-55.04	bdl	Transect 1 58 m Oliktok Point
955150	71 11.132	149 52.994	5/4/95	50	21.5	-52.55	bdl	Transect 1 58 m Oliktok Point
955150	71 11.132	149 52.994	5/4/95	57	19.7	-52.02	0.008	Transect 1 58 m Oliktok Point
955218	70 46.989	150 49.122	5/8/95	3	50.9	-71.24	0.031	Transect 2 18 m Colville River Delta
955218	70 46.989	150 49.122	5/8/95	9	44.3	-72.19	0.013	Transect 2 18 m Colville River Delta
955218	70 46.989	150 49.122	5/8/95	14	48.0	-71.07	0.043	Transect 2 18 m Colville River Delta
955218	70 46.989	150 49.122	5/8/95	17	50.6	-72.16	0.005	Transect 2 18 m Colville River Delta
955418	70 36.17	148 44.45	5/8/95	3	21.7	-63.05	bdl	Transect 4 18 m Kaparuk River
955418	70 36.17	148 44.45	5/8/95	9	22.2	-61.12	0.009	Transect 4 18 m Kaparuk River
955418	70 36.17	148 44.45	5/8/95	14	22.8	-65.42	0.007	Transect 4 18 m Kaparuk River
955418	70 36.17	148 44.45	5/8/95	17	19.8	-56.57	0.123	Transect 4 18 m Kaparuk River
955503	70 21.176	147 57.041	5/2/95	3	137.3	-75.08		Transect 5 3 m Endicott
955518	70 32.018	147 57.006	5/8/95	3	20.6	-67.00		Transect 5 18 m Endicott
955518	70 32.018	147 57.006	5/8/95	9	21.8	-66.53	0.009	Transect 5 18 m Endicott
955518	70 32.018	147 57.006	5/8/95	14	22.9	-68.29	0.011	Transect 5 18 m Endicott
955518	70 32.018	147 57.006	5/8/95	18	44.2	-76.96	0.044	Transect 5 18 m Endicott
958010	70 30.88	150 08.95	8/18/95	2	8.9	-61.29		5 km SW of Thetis Island
958040	70 44.08	149 13.17	8/17/95	3	17.7	-62.80		1359.9:7.0 nm bearing 104° true from 958118
958040	70 44.08	149 13.17	8/17/95	8	36.8	-54.99		1958.6:7.0 nm bearing 104° true from 958118
958040	70 44.08	149 13.17	8/17/95	13	37.3	-54.13		2035.0:7.0 nm bearing 104° true from 958118
958040	70 44.08	149 13.17	8/17/95	18	56.0	-63.26		2097.8:7.0 nm bearing 104° true from 958118
958041	70 42.03	149 39.56	8/19/95	3	27.6	-62.08		About 6 nm east of station 958118, 18m contour
958041	70 42.03	149 39.56	8/19/95	8	30.4	-56.52		About 6 nm east of station 958118, 18m contour
958041	70 42.03	149 39.56	8/19/95	13	46.3	-62.67		About 6 nm east of station 958118, 18m contour
958041	70 42.03	149 39.56	8/19/95	17	52.1	-67.85		About 6 nm east of station 958118, 18m contour
958043	70 43.46	150 02.52	8/18/95	1	9.7	-60.23		1215.4:3.49 nm bearing 108° true from 958118
958043	70 43.46	150 02.52	8/18/95	3	11.3	-63.42		1293.3:3.49 nm bearing 108° true from 958118
958043	70 43.46	150 02.52	8/18/95	8	37.4	-57.98		1988.9:3.49 nm bearing 108° true from 958118
958043	70 43.46	150 02.52	8/18/95	13	35.5	-58.52		2045.6:3.49 nm bearing 108° true from 958118
958043	70 43.46	150 02.52	8/18/95	17	53.7	-65.58		2109.5:3.49 nm bearing 108° true from 958118
958044	70 42.65	149 48.68	8/19/95	3	22.2	-69.23		About 3 nm east of station 958118, 18m contour
958044	70 42.65	149 48.68	8/19/95	8	41.3	-60.86		About 3 nm east of station 958118, 18m contour
958044	70 42.65	149 48.68	8/19/95	13	41.2	-60.27		About 3 nm east of station 958118, 18m contour
958044	70 42.65	149 48.68	8/19/95	17	54.8	-67.37		About 3 nm east of station 958118, 18m contour
958045	70 45.00	150 23.35	8/18/95	3	12.4	-59.56		About 10 nm west of 958118
958045	70 45.00	150 23.35	8/18/95	8	37.2	_____		About 10 nm west of 958118
958045	70 45.00	150 23.35	8/18/95	13	36.3	-56.09		About 10 nm west of 958118
958045	70 45.00	150 23.35	8/18/95	17	41.0	-56.76		About 10 nm west of 958118
958046	70 40.49	149 19.88	8/19/95	3	24.2	-65.00		About 9 nm east of station 958118, 18m contour
958046	70 40.49	149 19.88	8/19/95	8	32.2	-57.50		About 9 nm east of station 958118, 18m contour
958046	70 40.49	149 19.88	8/19/95	13	45.9	-66.97		About 9 nm east of station 958118, 18m contour
958046	70 40.49	149 19.88	8/19/95	17	48.3	-68.14		About 9 nm east of station 958118, 18m contour
958047	70 33.05	148 28.89	8/20/95	3	14.0	-59.67		About 6 nm east of station 958420, 18m contour
958047	70 33.05	148 28.89	8/20/95	8	27.2	-61.85		about 6 nm east of station 958420, 18m contour
958047	70 33.05	148 28.89	8/20/95	13	31.9	-62.85		about 6 nm east of station 958420, 18m contour
958047	70 33.05	148 28.89	8/20/95	17	32.0	-62.64		about 6 nm east of station 958420, 18m contour
958103	70 32.10	149 53.04	8/17/95	2	6.6	-56.32		1695.7 Transect 1 3 m Oliktok Point

Table 1. Methane concentrations (nM methane per liter seawater), methane carbon isotopic composition, methane oxidation rates (nanoM methane per liter per day), and dissolved inorganic carbon (microM carbon per kilogram seawater).

Station	Latitude N.	Longitude W.	Date	Sample	Methane	Methane	DIC	Comments
					depth (m)	(nM)	Isotopic	
							Composition	
						(ppt)	(nM/day)	
958110	70 53.16	149 52.75	8/19/95	3	9.6	-66.31		1508.9 Transect 1 10 m Oliktok Point
958110	70 53.16	149 52.75	8/19/95	6	16.4	-66.67		1686.5 Transect 1 10 m Oliktok Point
958110	70 53.16	149 52.75	8/19/95	9	27.2	-69.52		1923.5 Transect 1 10 m Oliktok Point
958114	70 38.20	149 53.08	8/17/95	3	17.5	-64.92		1643.1 Transect 1 14 m Oliktok Point
958114	70 38.20	149 53.08	8/17/95	8	32.3	-67.50		1970.3 Transect 1 14 m Oliktok Point
958114	70 38.20	149 53.08	8/17/95	13	40.5	-70.19		2043.3 Transect 1 14 m Oliktok Point
958115s	70 40.89	149 52.71	8/17/95	3	14.8	-64.76		1373.2 Transect 1 15 m Oliktok Point shoal
958115s	70 40.89	149 52.71	8/17/95	8	36.2	-59.14		1963.4 Transect 1 15 m Oliktok Point shoal
958115s	70 40.89	149 52.71	8/17/95	12	42.7	-63.56		2024.5 Transect 1 15 m Oliktok Point shoal
958115s	70 40.89	149 52.71	8/17/95	16	50.3	-71.08		2071.6 Transect 1 15 m Oliktok Point shoal
958117	70 41.19	149 52.75	8/19/95	3	25.1	—		Transect 1 17 m Oliktok Point
958117	70 41.19	149 52.75	8/19/95	8	37.9	-61.16		Transect 1 17 m Oliktok Point
958117	70 41.19	149 52.75	8/19/95	13	40.9	-61.81		Transect 1 17 m Oliktok Point
958117	70 41.19	149 52.75	8/19/95	17	49.5	-66.94		Transect 1 17 m Oliktok Point
958118	70 42.48	149 52.55	8/17/95	3	22.2	-65.80		1715.6 Transect 1 18 m Oliktok Point
958118	70 42.48	149 52.55	8/17/95	8	37.4	-59.37		1989.3 Transect 1 18 m Oliktok Point
958118	70 42.48	149 52.55	8/17/95	12	35.7	-60.66		2029.6 Transect 1 18 m Oliktok Point
958118	70 42.48	149 52.55	8/17/95	16	50.2	-70.11		2086.3 Transect 1 18 m Oliktok Point
958118X	70 42.43	149 53.12	8/19/95	3	33.4	-69.53		Transect 1 18 m Oliktok Point repeat
958118X	70 42.43	149 53.12	8/19/95	8	39.8	-59.93		Transect 1 18 m Oliktok Point repeat
958118X	70 42.43	149 53.12	8/19/95	13	40.7	-58.30		Transect 1 18 m Oliktok Point repeat
958118X	70 42.43	149 53.12	8/19/95	17	48.4	-64.67		Transect 1 18 m Oliktok Point repeat
958120	70 45.68	149 52.67	8/17/95	3	36.3	-61.50		1582.9 Transect 1 20 m Oliktok Point
958120	70 45.68	149 52.67	8/17/95	8	24.8	-53.43		2006.5 Transect 1 20 m Oliktok Point
958120	70 45.68	149 52.67	8/17/95	13	26.8	-54.28		2051.1 Transect 1 20 m Oliktok Point
958120	70 45.68	149 52.67	8/17/95	18	21.3	-63.12		2098.1 Transect 1 20 m Oliktok Point
958210	70 35.01	150 49.05	8/18/95	3	18.8	-70.93		Transect 2 10 m Colville River
958210	70 35.01	150 49.05	8/18/95	7	38.6	-74.72		Transect 2 10 m Colville River
958215	70 40.92	150 49.20	8/18/95	3	11.3	-62.30		Transect 2 15 m Colville River
958215	70 40.92	150 49.20	8/18/95	7	26.8	-64.17		Transect 2 15 m Colville River
958215	70 40.92	150 49.20	8/18/95	11	37.6	-58.67		Transect 2 15 m Colville River
958215	70 40.92	150 49.20	8/18/95	14	45.4	-61.87		Transect 2 15 m Colville River
958218	70 46.89	150 49.31	8/18/95	3	10.8	-57.84		Transect 2 18 m Colville River
958218	70 46.89	150 49.31	8/18/95	8	33.3	-49.19		Transect 2 18 m Colville River
958218	70 46.89	150 49.31	8/18/95	13	32.8	-45.89		Transect 2 18 m Colville River
958218	70 46.89	150 49.31	8/18/95	17	29.2	-37.08		Transect 2 18 m Colville River
958410	70 29.35	148 43.62	8/19/95	3	8.5	-56.91		Transect 4 10 m Kuparuk River
958410	70 29.35	148 43.62	8/19/95	6	9.9	-57.30		Transect 4 10 m Kuparuk River
958410	70 29.35	148 43.62	8/19/95	9	20.8	-62.67		Transect 4 10 m Kuparuk River
958420	70 36.25	148 44.27	8/19/95	3	10.2	-57.86		Transect 4 20 m Kuparuk River
958420	70 36.25	148 44.27	8/19/95	8	24.5	-58.23		Transect 4 20 m Kuparuk River
958420	70 36.25	148 44.27	8/19/95	14	23.7	-60.13		Transect 4 20 m Kuparuk River
958420	70 36.25	148 44.27	8/19/95	19	28.7	-62.41		Transect 4 20 m Kuparuk River
958502	70 21.51	147 57.54	8/20/95	2	6.0	-51.02		Transect 5 2 m Endicott
958503	70 21.33	174 56.65	8/20/95	2	6.8	-55.81		Endicott Dock
958505	70 23.04	147 56.78	8/20/95	1	7.8	-50.36		Transect 5 5 m Endicott
958505	70 23.04	147 56.78	8/20/95	4	6.7	-55.98		Transect 5 5 m Endicott
958518	70 32.41	148 01.31	8/20/95	3	7.4	-53.46		Transect 5 18 m Endicott
958518	70 32.41	148 01.31	8/20/95	8	18.3	-55.95		Transect 5 18 m Endicott
958518	70 32.41	148 01.31	8/20/95	13	23.8	-59.28		Transect 5 18 m Endicott
958518	70 32.41	148 01.31	8/20/95	18	23.4	-59.27		Transect 5 18 m Endicott

bdl=

<

0.0001

1/day)

Table 2. Seawater nutrient concentrations (mM, millimoles nutrient per liter seawater) measured in 1995.

Station	Depth (m)	PO4 (mM)	Si (mM)	NO3 (mM)	NO2 (mM)	NH4 (mM)
955001	2	0.86	15.50	1.83	0.14	0.12
955010	3	1.08	19.00	3.87	0.07	0.32
955040	3	0.75	12.84	1.50	0.11	0.16
955040	10	0.84	11.66	1.71	0.10	0.03
955040	17	1.06	20.56	5.21	0.06	0.10
955041	3	0.91	13.54	2.23	0.09	0.19
955041	9	0.86	13.63	2.28	0.09	0.76
955041	14	0.88	13.99	2.39	0.08	0.06
955041	17	1.00	19.91	4.27	0.06	0.08
955042	3	0.78	13.62	1.54	0.12	0.01
955042	10	0.76	12.63	1.82	0.09	0.00
955042	17	0.91	13.67	2.61	0.06	0.07
955042	23	0.96	19.66	4.57	0.06	0.06
955103	2	0.89	24.68	3.64	0.10	0.32
955114	3	0.88	13.58	2.47	0.06	0.65
955114	7	0.86	13.53	2.43	0.05	0.08
955114	11	0.96	13.63	2.58	0.05	0.10
955114	14	0.95	17.74	3.48	0.05	0.06
955115	3	0.80	0.78	1.39	0.08	0.09
955115	7	0.85	15.37	2.24	0.06	0.01
955115	12	0.88	13.93	2.44	0.05	0.00
955115	14	0.93	17.79	3.22	0.05	0.04
955118	3	0.97	11.88	2.38	0.06	0.03
955118	3	0.79	15.87	0.00	0.12	0.00
955118	7	0.86	15.33	2.33	0.06	0.00
955118	9	0.88	14.58	2.37	0.07	0.00
955118	10	0.87	14.15	2.38	0.06	0.10
955118	14	0.95	12.75	2.53	0.06	0.02
955118	14	0.90	14.78	2.73	0.05	0.00
955118	17	1.02	15.31	3.51	0.05	0.08
955118	17	0.83	14.89	3.02	0.05	0.02
955120	3	1.12	20.33	5.20	0.06	0.00
955120	3	0.91	8.77	1.39	0.12	0.21
955120	7	0.87	12.64	2.49	0.11	0.00
955120	9	0.82	8.50	1.39	0.12	0.08
955120	11	0.87	12.31	2.48	0.12	0.05
955120	14	0.87	11.97	2.18	0.07	0.00
955120	15	0.83	12.12	2.67	0.13	0.05
955120	19	0.84	11.79	1.38	0.12	0.23
955120	19	0.97	18.16	4.34	0.06	0.03
955125	3	0.79	11.18	1.35	0.13	0.01
955125	10	0.81	11.83	1.35	0.13	0.01

Table 2. Seawater nutrient concentrations (mM, millimoles nutrient per liter seawater) measured in 1995.

Station	Depth (m)	PO4 (mM)	Si (mM)	NO3 (mM)	NO2 (mM)	NH4 (mM)
955125	15	0.82	12.48	1.45	0.12	0.02
955125	20	1.01	17.39	3.22	0.06	0.01
955125	25	1.10	22.40	5.73	0.06	0.00
955150	3	0.96	13.04	1.88	0.07	0.06
955150	10	0.91	13.42	1.88	0.06	0.09
955150	20	0.92	13.66	1.97	0.06	0.03
955150	30	1.03	19.86	3.92	0.01	0.00
955150	40	1.31	24.47	6.27	0.06	0.90
955150	50	1.50	33.30	8.71	0.06	1.55
955150	57	1.84	38.56	9.49	0.08	2.58
955218	3	0.79	12.84	1.40	0.11	0.04
955218	9	0.80	12.82	1.45	0.11	0.00
955218	14	0.96	19.91	3.37	0.04	0.00
955218	17	0.79	15.89	0.00	0.12	0.00
955418	3	0.78	13.63	1.35	0.11	0.00
955418	9	0.76	14.65	1.49	0.12	0.03
955418	14	0.80	12.95	1.74	0.12	0.00
955418	17	0.91	17.33	3.13	0.09	0.00
955518	1	0.77	13.04	1.27	0.10	0.00
958010	2	0.27	12.91	0.01	0.00	0.00
958013	2	0.26	14.84	0.09	0.00	0.08
958040	3	0.30	8.20	0.02	0.00	0.10
958040	8	0.99	15.91	0.05	0.00	1.13
958040	13	0.39	14.79	0.13	0.13	2.25
958040	18	0.57	9.39	0.05	0.00	0.17
958043	1	0.04	4.65	0.13	0.04	0.00
958043	3	0.17	5.02	0.03	0.00	0.45
958043	8	0.48	11.82	0.02	0.00	0.02
958043	13	0.51	7.24	0.01	0.01	0.02
958043	17	0.76	17.91	0.00	0.01	0.00
958045	3	0.26	5.72	0.00	0.00	0.46
958045	8	0.46	6.36	0.00	0.01	0.00
958045	13	0.54	7.00	0.35	0.15	0.07
958045	17	0.88	6.04	0.00	0.03	0.32
958047	3	0.36	7.29	0.00	0.00	0.00
958047	8	0.52	11.60	0.00	0.00	0.09
958047	13	0.57	7.37	0.00	0.00	0.09
958047	17	0.72	7.60	0.06	0.00	1.14
958110	3	0.20	7.97	0.01	0.00	0.04
958110	6	0.38	7.01	0.00	0.00	0.40
958110	9	0.39	12.82	0.00	0.00	0.00

Table 2. Seawater nutrient concentrations (mM, millimoles nutrient per liter seawater) measured in 1995.

Station	Depth (m)	PO4 (mM)	Si (mM)	NO3 (mM)	NO2 (mM)	NH4 (mM)
958114	3	0.37	9.58	0.06	0.02	0.55
958114	8	0.33	16.46	0.07	0.01	0.11
958114	13	0.61	6.92	0.03	0.00	0.04
958115	3	0.21	12.27	0.07	0.00	0.01
958115	8	0.63	9.91	0.06	0.00	0.93
958115	12	1.75	15.27	0.00	0.08	9.27
958115	16	0.79	11.67	0.06	0.00	0.00
958117	3	0.28	6.03	0.00	0.00	0.76
958117	8	0.51	7.86	0.00	0.01	0.26
958117	12	0.52	6.91	0.00	0.02	0.61
958117	16	0.73	10.58	0.00	0.01	0.21
958118	3	0.40	14.63	0.09	0.00	0.00
958118	8	0.55	12.27	0.08	0.00	0.37
958118	12	0.57	8.93	0.02	0.00	0.08
958118	16	0.73	9.47	0.01	0.01	0.33
958120	3	0.49	11.80	0.03	0.00	0.14
958120	8	0.66	15.37	0.05	0.02	0.22
958120	13	0.59	11.76	0.07	0.00	0.01
958120	18	0.84	12.02	0.20	0.01	0.88
958210	3	0.34	10.05	0.00	0.00	0.17
958210	7	0.35	5.50	29.13	0.17	0.23
958215	3	0.32	7.77	0.02	0.00	0.00
958215	7	0.49	6.67	0.00	0.00	0.91
958215	11	0.63	5.58	0.00	0.01	0.03
958215	14	0.76	5.56	0.00	0.01	0.44
958218	3	0.26	5.48	0.01	0.00	0.22
958218	8	0.40	5.72	0.00	0.01	0.18
958218	13	0.63	6.22	0.00	0.01	0.00
958218	17	0.93	7.13	0.00	0.02	0.32
958502	2	0.21	7.48	0.14	0.03	0.91
958503	2	0.36	10.29	0.09	0.00	1.27
958505	1	0.34	10.49	0.00	0.00	-0.01
958505	4	0.47	8.48	0.00	0.00	0.28
958518	3	0.20	8.32	0.00	0.00	0.22
958518	8	0.53	8.69	0.01	0.06	0.31
958518	13	0.37	9.59	0.00	0.01	0.02
958518	18	0.65	6.92	0.00	0.00	0.88

Table 3. Methane concentrations (nM, nanomoles methane per liter melted ice water), and methane carbon isotopic composition in ice.

Station	Latitude N.	Longitude W.	Date	Core	Methane	Carbon	Carbon	Description
					interval	(nM)	Isotopic	
					(cm)		Composition (ppt)	
955001	70 24.54	148 31.47	5/6/95	0-10	15.32			West Dock
					40-50	7.36		West Dock
					80-90	4.99		West Dock
					120-130	4.03		West Dock
					180-190	4.91		West Dock
955010	70 30.008	150 08.860	5/4/95	0-10	708.35	-87.61		5 Km SW of Thetis I.
					30-40	805.58	-84.99	5 Km SW of Thetis I.
					80-90	21.88		5 Km SW of Thetis I.
					130-140	9.54		5 Km SW of Thetis I.
					180-190	4.80		5 Km SW of Thetis I.
955103	70 31.950	149 53.210	5/5/95	0-10	324.88	-84.73		Transect 1 03 m Oliktok Point
					20-30	10.48		Transect 1 03 m Oliktok Point
					40-50	10.25		Transect 1 03 m Oliktok Point
					90-100	3.13		Transect 1 03 m Oliktok Point
					150-160	3.70		Transect 1 03 m Oliktok Point
955114	70 38.094	149 53.014	5/5/95	0-10	8.87			Transect 1 14 m Oliktok Point
					40-50	5.91		Transect 1 14 m Oliktok Point
					100-110	4.24		Transect 1 14 m Oliktok Point
					160-170	3.27		Transect 1 14 m Oliktok Point
955120	70 47.074	149 52.852	5/4/95	0-10	9.98			Transect 1 20 m Oliktok Point
					40-50	5.67		Transect 1 20 m Oliktok Point
					80-90	4.60		Transect 1 20 m Oliktok Point
					120-130	3.95		Transect 1 20 m Oliktok Point
					160-170	5.13		Transect 1 20 m Oliktok Point
955150	71 11.132	149 52.944	5/4/95	0-10	4.72			Transect 1 50 m Oliktok Point
					40-50	3.33		Transect 1 50 m Oliktok Point
					90-100	4.70		Transect 1 50 m Oliktok Point
					140-150	2.78		Transect 1 50 m Oliktok Point
					180-190	4.41		Transect 1 50 m Oliktok Point
955503	70 21.176	147 57.041	5/3/95	0-10	11.71	-56.71		Endicott Dock
					10-20	32.25	-69.99	Endicott Dock
					20-30	57.13	-47.76	Endicott Dock
					30-40	88.91	-39.49	Endicott Dock
					40-50	22.55		Endicott Dock
					50-60	7.39		Endicott Dock
					60-70	9.02		Endicott Dock
					70-80	8.03		Endicott Dock
					80-90	8.03		Endicott Dock
					90-100	8.09		Endicott Dock
					100-110	5.73		Endicott Dock
					110-120	5.44		Endicott Dock
					120-130	6.66		Endicott Dock
					130-140	6.63		Endicott Dock
					140-150	6.59		Endicott Dock
					150-160	5.49		Endicott Dock
					160-170	4.74		Endicott Dock
					170-180	4.47		Endicott Dock
					180-190	4.45		Endicott Dock
					190-203	5.56		Endicott Dock
955503R	70 21.176	147 57.041	5/6/95	0-10	8.53			Endicott Dock repeat
					10-20	20.35		Endicott Dock repeat
					20-30	64.58	-47.76	Endicott Dock repeat
					30-40	30.45	-59.29	Endicott Dock repeat
					40-50	19.63		Endicott Dock repeat
					50-60	12.71		Endicott Dock repeat
					60-70	10.80		Endicott Dock repeat
					70-80	14.47		Endicott Dock repeat
					80-90	10.93		Endicott Dock repeat
					90-100	10.88		Endicott Dock repeat

Table 4. Hydrocarbon gas concentration in sediments (μM gas per liter wet sediment).

Sample	Location	Water depth m	Date	Lat. N.	Long W.	Core	C1	C2	C2:1		C3	C3:1	iC4	nC4
									Interval cm	$\mu\text{L/L}$ wet sediment				
955001	West Dock	3	5/6/95	70 24.540	148 31.470		0-10	14.71	0.13	0.21	0.17	0.04	0.00	0.02
955010	5km. SW Thetis I.	3	5/5/95	70 30.008	150 08.860		0-10	3.34	0.00	0.00	0.07	0.00	0.00	0.00
955010	5km. SW Thetis I.	3	5/5/95	70 30.008	150 08.860		30-40	7.75	0.13	0.29	0.17	0.45	0.01	0.01
955103	Transect 1 3m	3	5/5/95	70 31.950	149 53.210		0-10	3.34	0.00	0.00	0.00	0.00	0.00	0.00
955103	Transect 1 3m	3	5/5/95	70 31.950	149 53.210		25-35	10.62	0.01	0.00	0.05	0.00	0.00	0.00
955114	Transect 1 14m	14	5/5/95	70 38.094	149 53.014		20-30	6.84	0.05	0.00	0.07	0.00	0.00	0.00
955120	Transect 1 20m	20	5/4/95	70 47.074	149 52.852		0-10	4.15	0.00	0.00	0.00	0.00	0.00	0.00
955120	Transect 1 20m	20	5/4/95	70 47.074	149 52.852		20-30	5.53	0.00	0.00	0.00	0.00	0.00	0.00
955503	Endicott Dock	3	5/2/95	70 21.176	147 57.041		0-10	6.81	0.05	0.00	0.04	0.00	0.00	0.00
955503	Endicott Dock	3	5/2/95	70 21.176	147 57.041		20-30	18.42	0.20	0.00	0.04	0.00	0.00	0.00

References

- Armstrong, F.A.J., C.R. Stearns, and J.D.H. Strickland, 1967, The measurement of upwelling and subsequent biological processes by means of the Technicon Autoanalyzer and associated equipment: Deep-Sea Research, v. 14, p. 381-389.
- Blake, D.R. and F.S. Rowland, 1988, Continuing worldwide increase in tropospheric methane, 1978 to 1987: Science, v. 240, p. 634-637.
- Cicerone, R.J. and R.S. Oremland, 1988, Biogeochemical aspects of atmospheric methane, Global Biogeochem. Cycles: v. 2, p. 299-327.
- Dickson, A. G., and Goyet, C., 1994, Handbook of Methods for the Analysis of the Various Parameters of the Carbon Dioxide System in Sea Water, 1994 Version 2 A. G. Dickson and C. Goyet, eds. DOE 1994 (unpublished manuscript). SOP 2.
- Khalil, M.A.K. and R.A. Rasmussen, 1983, Sources, sinks, and seasonal cycles of atmospheric methane: J. Geophys. Res., v. 88(C9), p. 5232-5144.
- Kvenvolden, K.A., 1991, A review of Arctic gas hydrates as a source of methane in global change: in Weller, G., Wilson, C.L., and Severin, B.A.B. (eds.), International Conference on the Role of the Polar Regions in Global Change: Proceedings of a conference held June 11-15, 1990 at the University of Alaska Fairbanks, Geophysical Institute and Center for Global Change and Arctic System Research, University of Alaska Fairbanks, v. II, p. 696-701.
- Kvenvolden, K.A., 1988, Methane hydrates and global climate: Global Biogeochem. Cycles, v. 2, p 221-229.
- Lachenbruch, A.H., Sass, J.H., Lawver, L.A., Brewer, M.C., Marshall, V., Munroe, R.J., Kennelley, Jr., J.P., Galanis, Jr., S.P., and Moses, Jr., T.H., 1988, Temperature and depth of permafrost on the Arctic Slope of Alaska: in Geology and exploration of the National Petroleum Reserve in Alaska, 1974-82: U.S. Geological Survey Professional Paper 1399, p. 645-656.
- Lorenson, T. D., and Kvenvolden, K.A., 1995, Methane in coastal sea water, sea ice, and bottom sediments, Beaufort Sea, Alaska: U.S.G.S Open-File Report 95-70 84 p.

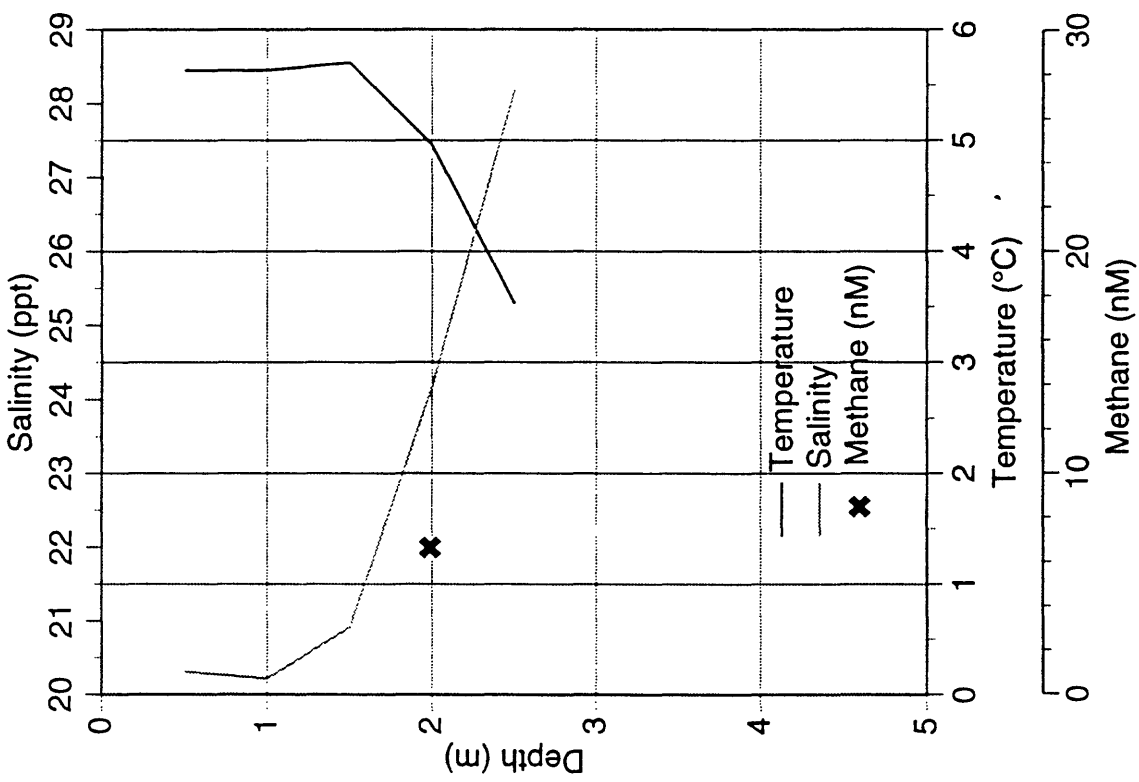
- McLaughlin, E.A., Lilley, M.D., Olson E.J., Kvenvolden, K.A., and Lorenson T.D., 1996 Methane Oxidation in the Beaufort Sea: EOS abstract with programs, American Geophysical Union annual meeting, San Francisco, CA, Dec., 1996 in press.
- MacDonald, G.J., 1990, Role of methane clathrates in past and future climates: *Climatic Change*, v. 16, p. 247-281.
- McAullife, C., 1971, GC determination of solutes by multiple phase equilibration: *Chem. Tech.*, v. 1, p. 46-51.
- Murphy, J. and J.P. Riley, 1962, A modified single solution method for the determination of phosphate in natural waters: *Anal. Chim. Acta.*, v. 27, p. 31-36.
- Neave, K.G. and P.V. Sellmann, 1982, Subsea permafrost in Harrison Bay, Alaska; CRREL Report 82-24, 62 p.
- Osterkamp, T.E. and T. Fei, Potential occurrence of permafrost and gas hydrates in the continental shelf near Lonely, Alaska: Proc. 6th Int. Conf. on Permafrost, Beijing, China, July 1993, p. 500-505.
- Shine, K.P., Derwent, R. G. Wuebbles, D. J. and Morcrette, J-J., 1990, Radiative forcing of climate: *in Climate Change*, The IPCC Scientific Assessment. edited by J. T. Houghton, G. L. Jenkins, and J. J. Ephraums: Cambridge University Press, New York, p. 41-68,
- Steele, L.P., E.J. Dlugokencky, P.M. Lang, P.P. Tans, R.C. Martin and K.A. Masarie, 1992, Slowing down of the global accumulation of atmospheric methane during the 1980s: *Nature*, v. 358, p. 313-316.
- Steele, L.P., P.J. Fraser, R.A. Rasmussen, M.A.K. Khalil, T.H. Conway, A.J. Crawford, R.H. Gammon, K.A. Masarie and K.W. Thoning, 1987, The global distribution of methane in the troposphere: *J. Atmos. Chem.* v. 5, p. 125-171.
- Slawyk, G., and J.J. MacIsaac, 1972, Comparison of two automated ammonium methods in a region of coastal upwelling, *Deep-Sea Res.*, 19, p. 521-524.
- Whitledge, T.E., S.C. Malloy, C.J. Patton, and C.D. Wirick, 1981, Automated Nutrient Analyses in Seawater, BNL 51398, Brookhaven National Laboratory, 216 p.

Wood, E.D., F.A.J. Armstrong, and F.A. Richards, 1967, Determination of nitrate in seawater by cadmium-copper reduction to nitrite: J. Mar. Biol. Assoc. U.K., v. 47, p. 23-31.

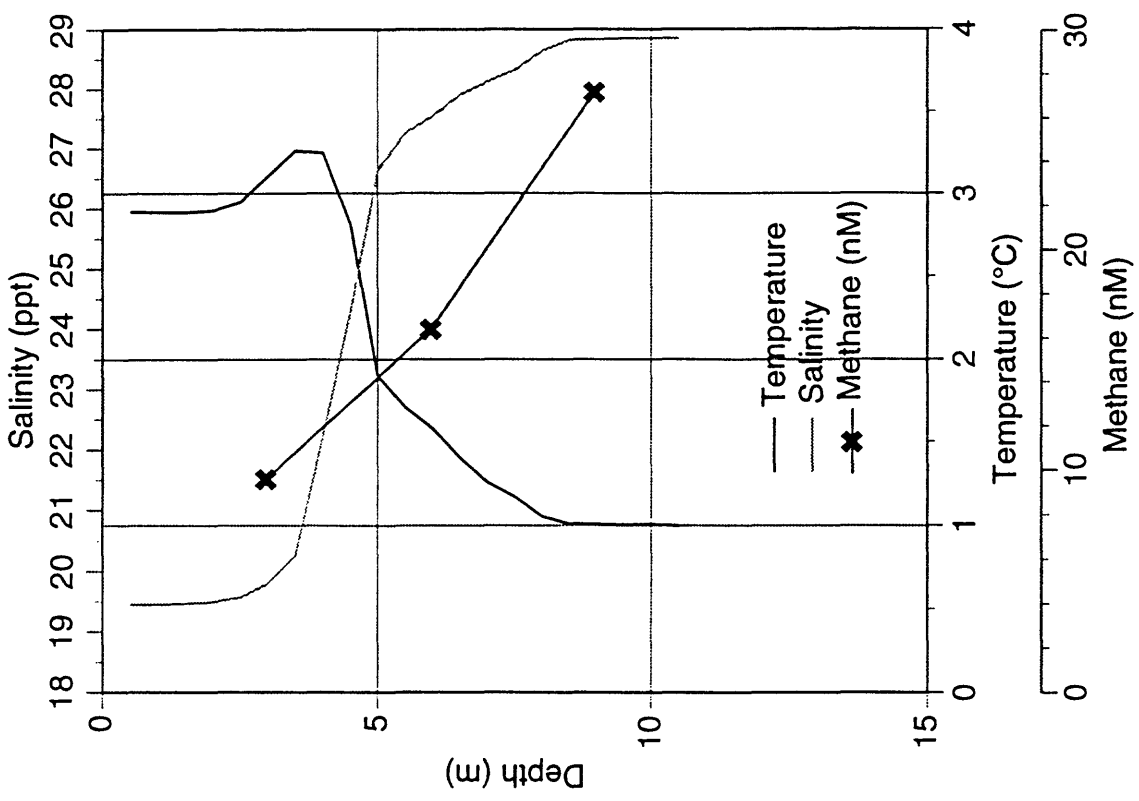
Appendix 1

Water Temperature - Salinity - Methane concentrations plotted with
water depth for each station

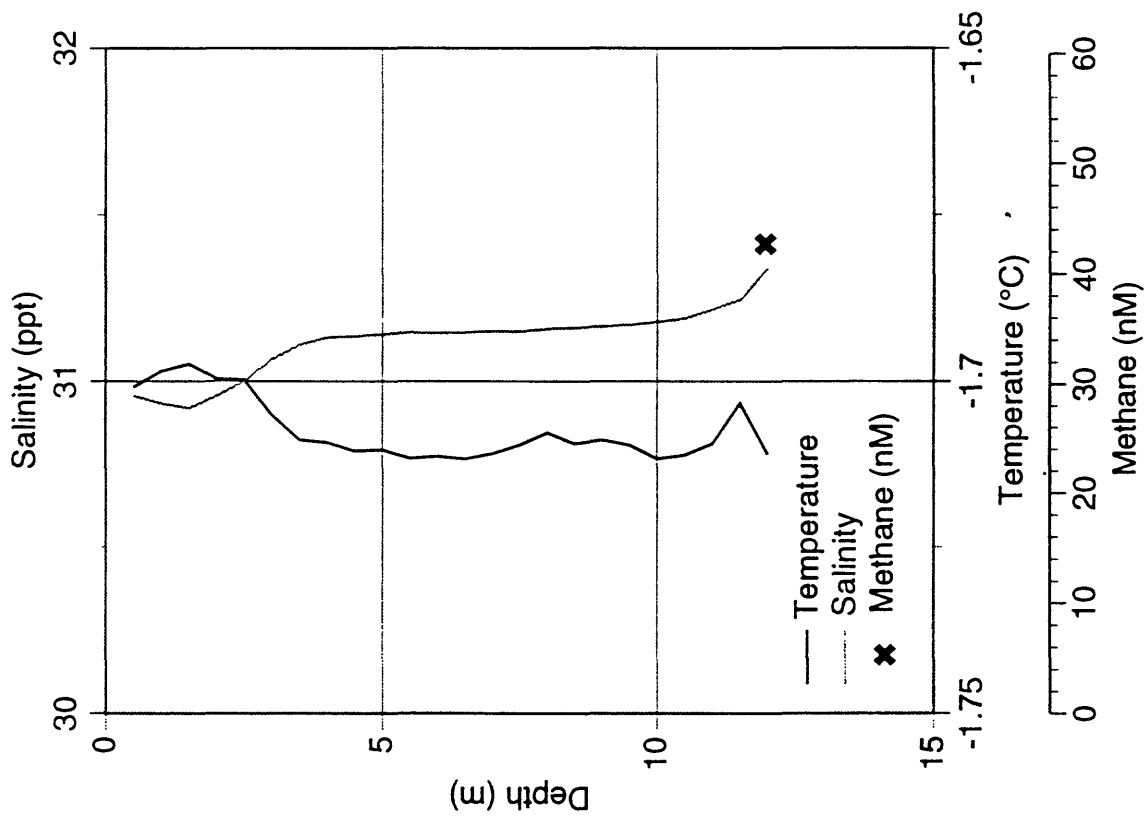
958103 T1 Oliktok Pt. 3m August 1995



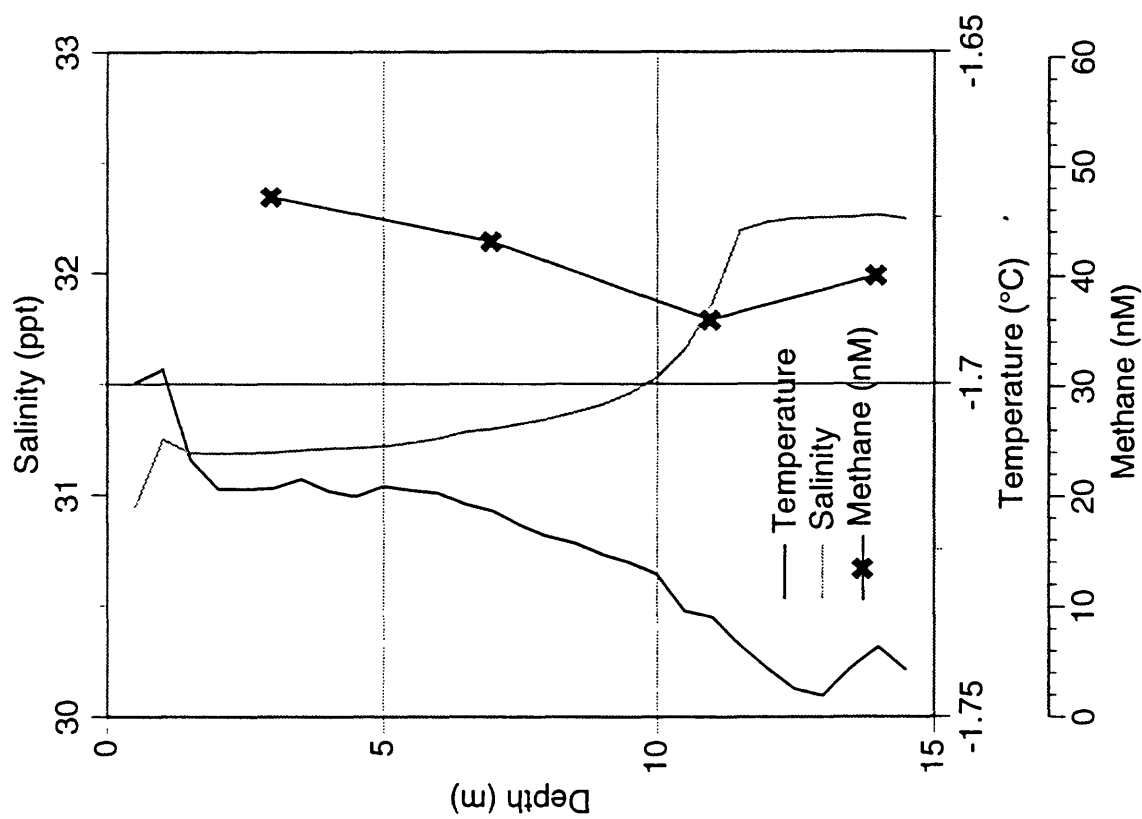
958110 T1 Oliktok Pt. 10m August 1995



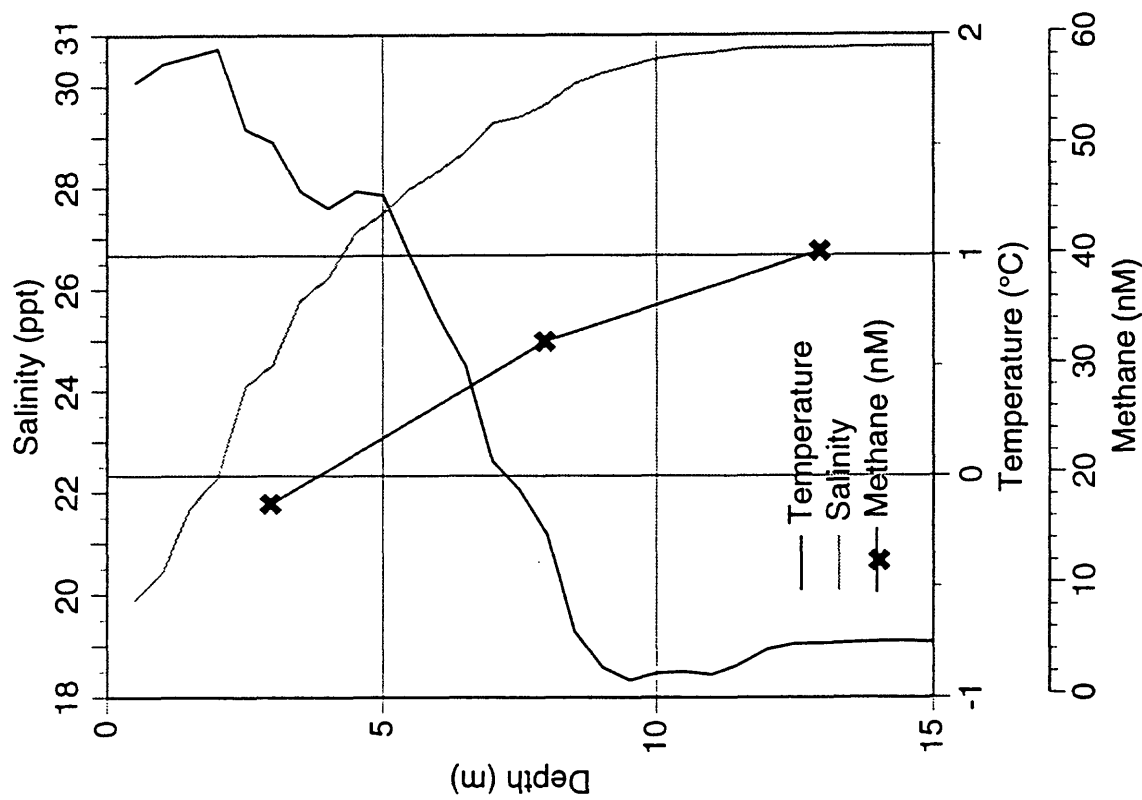
955112s T1Oliktok Pt. 12m May 1995



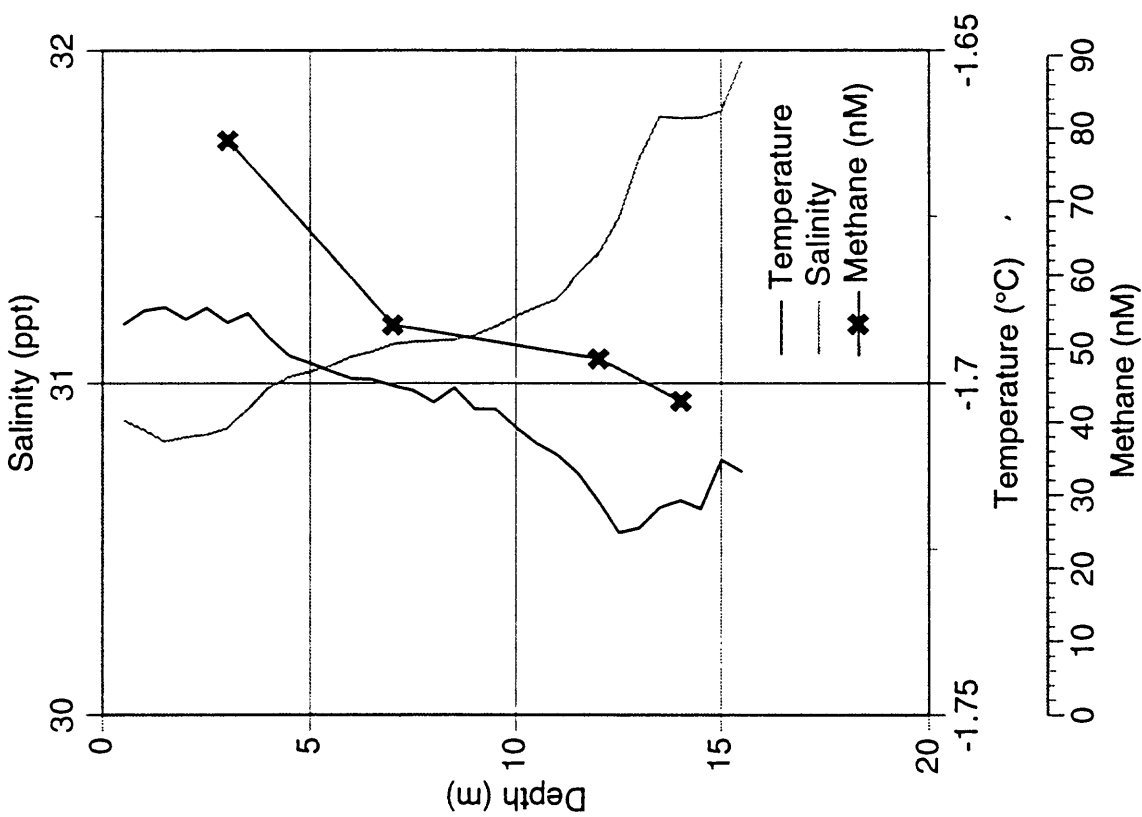
955114T1 Oliktok Pt. 14m May 1995



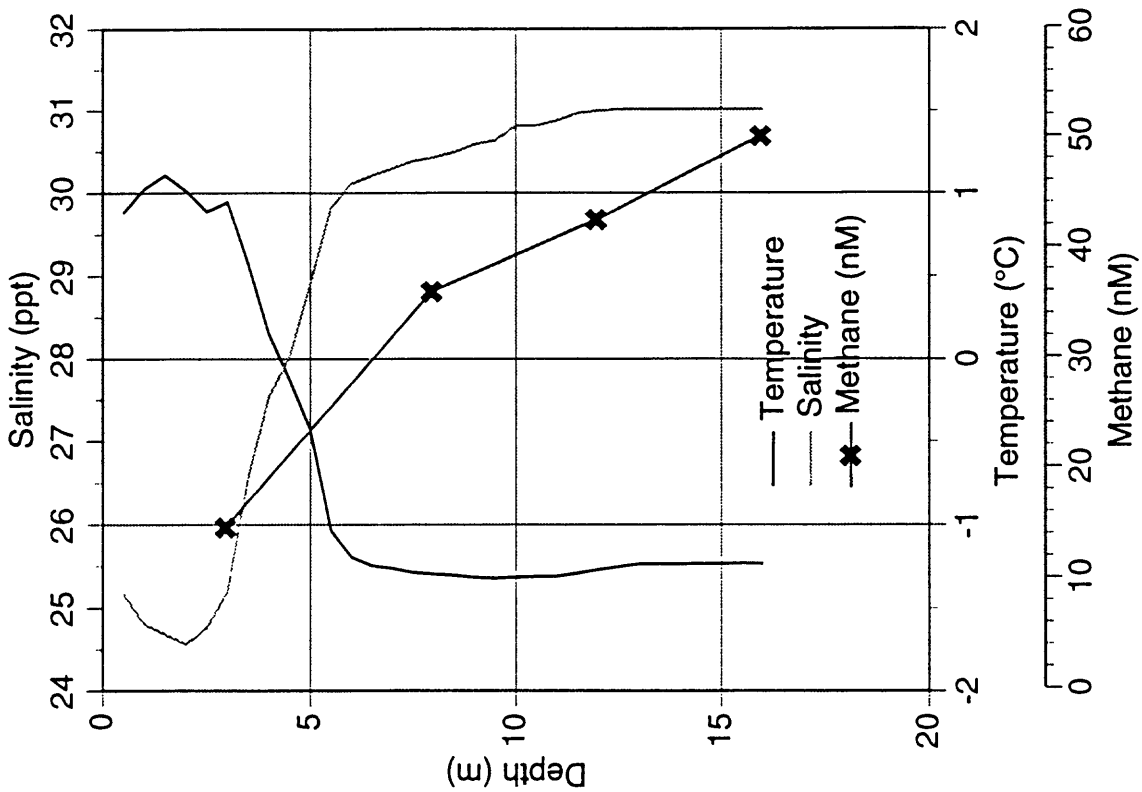
958114 T1 Oliktok Pt. 14m August 1995



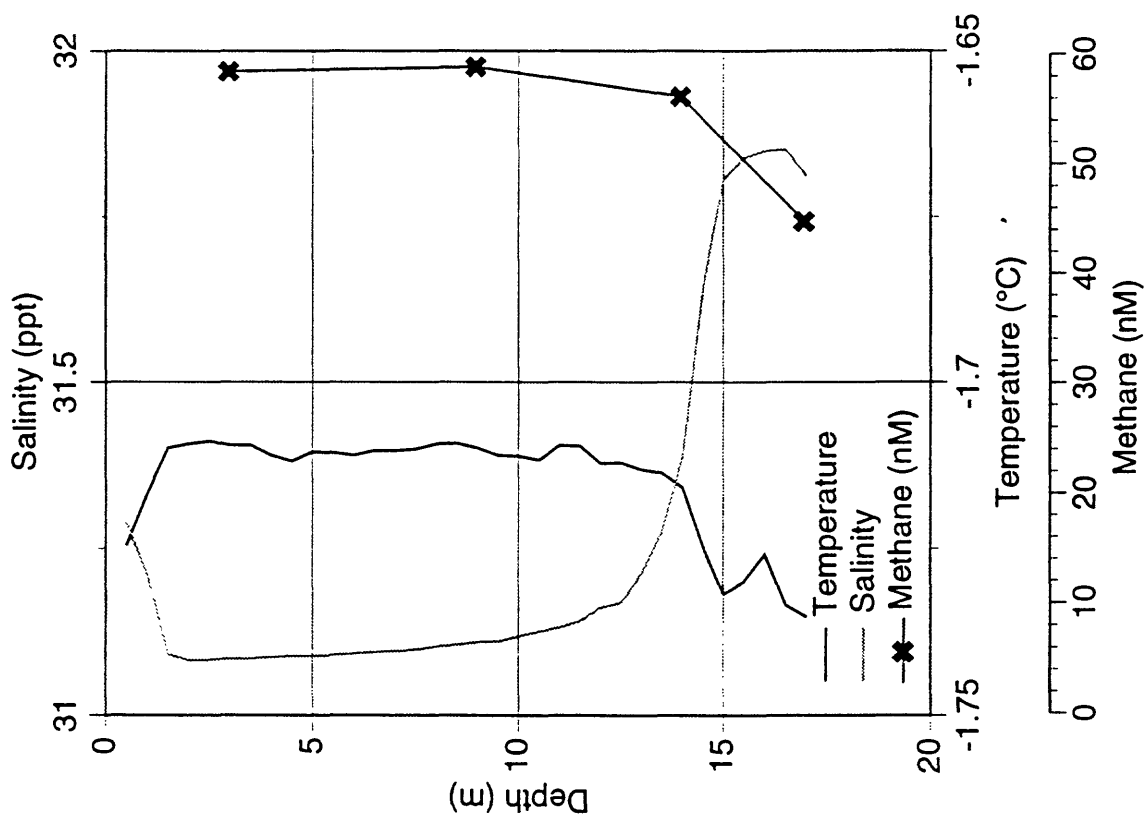
955115 T1 Oliktok Pt. 15m May 1995



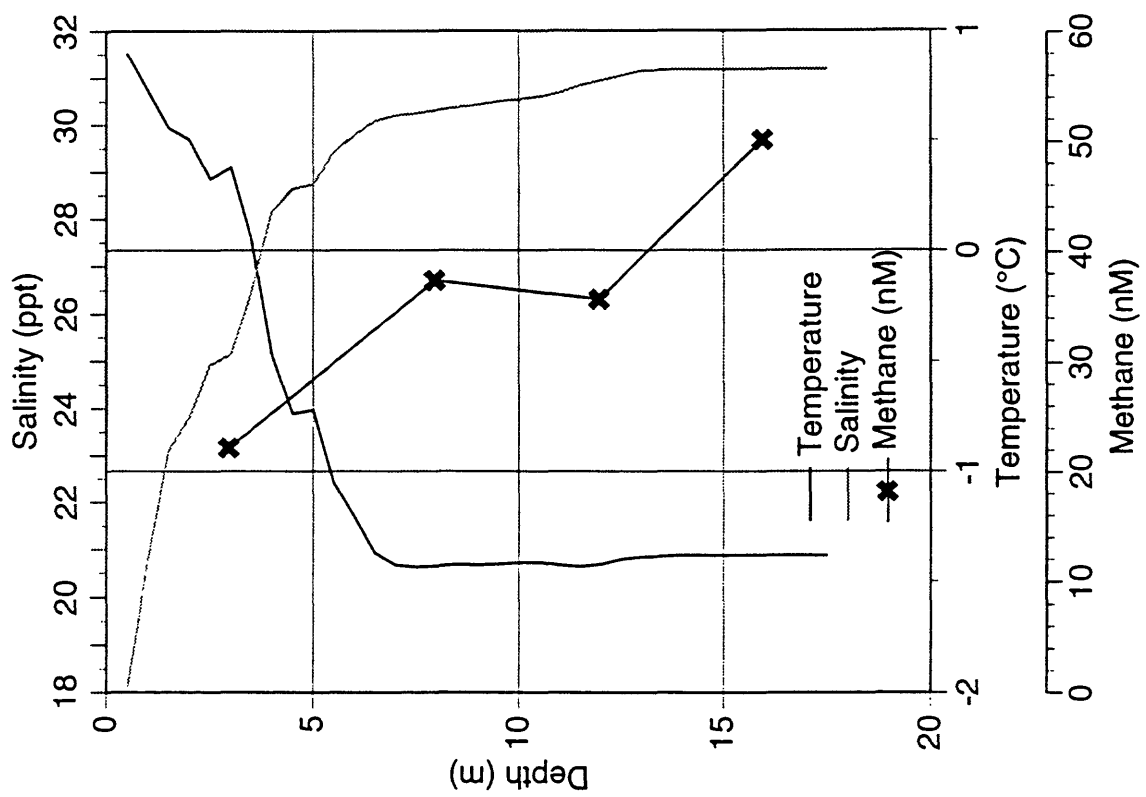
958115s T1 Oliktok Pt. 15m August 1995



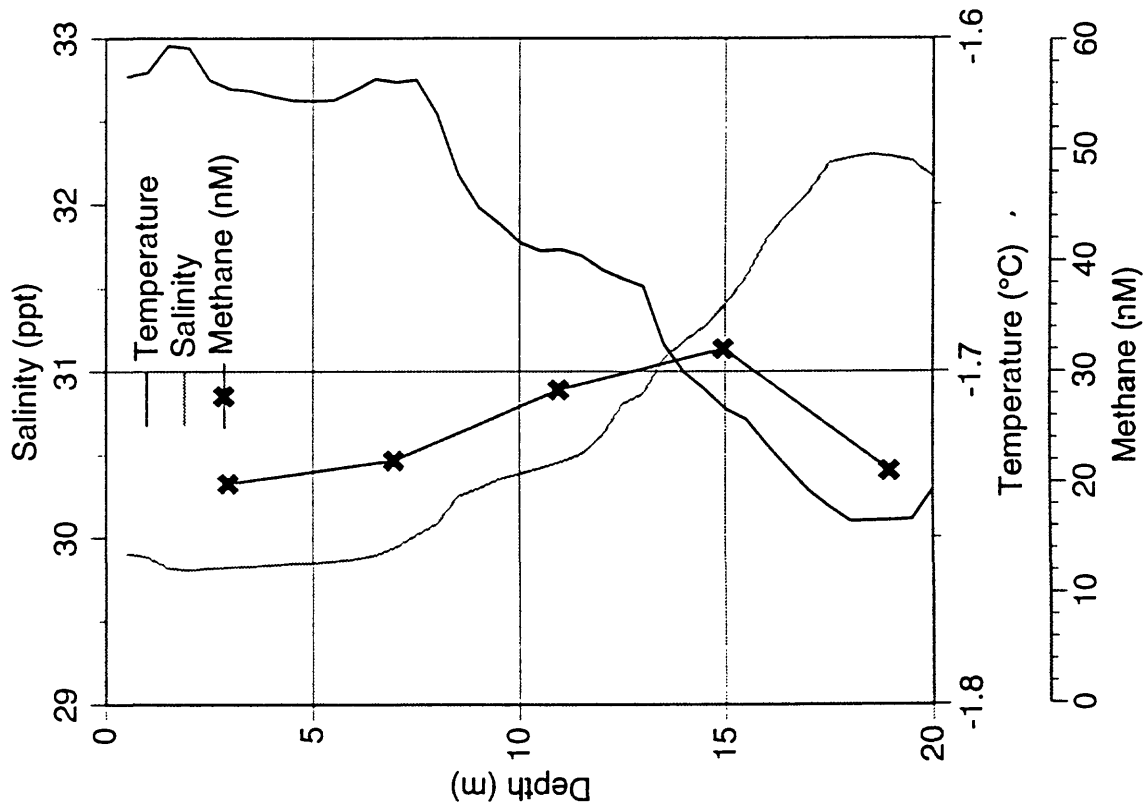
955118R T1 Oliktok Pt. 18m May 1995



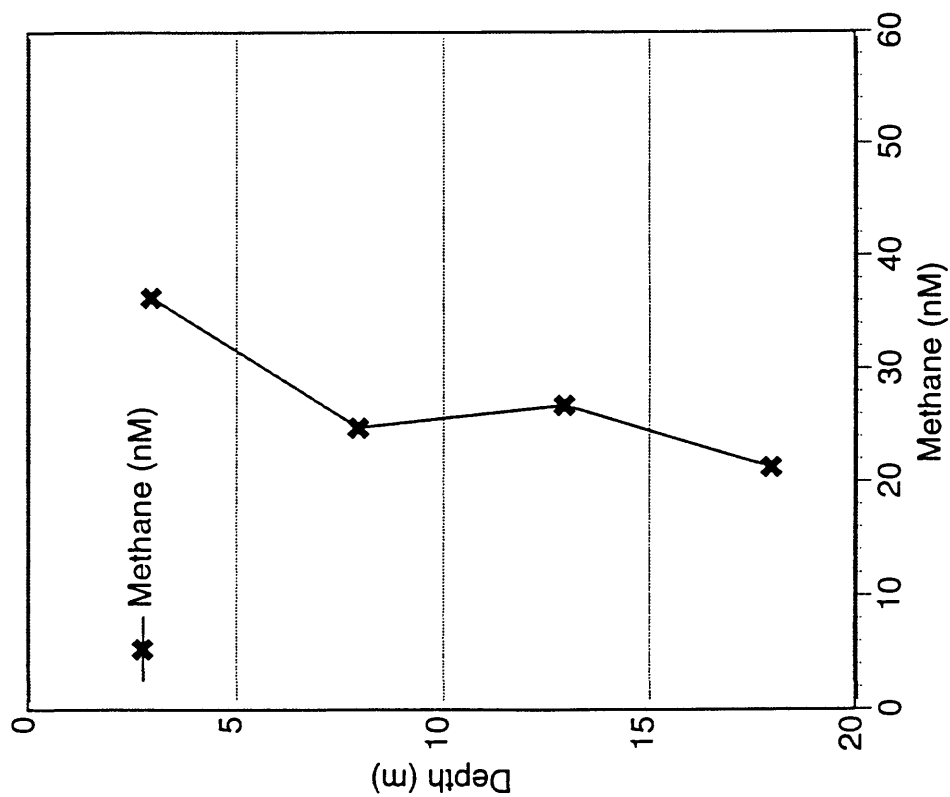
958118 T1 Oliktok Pt. 18m August 1995



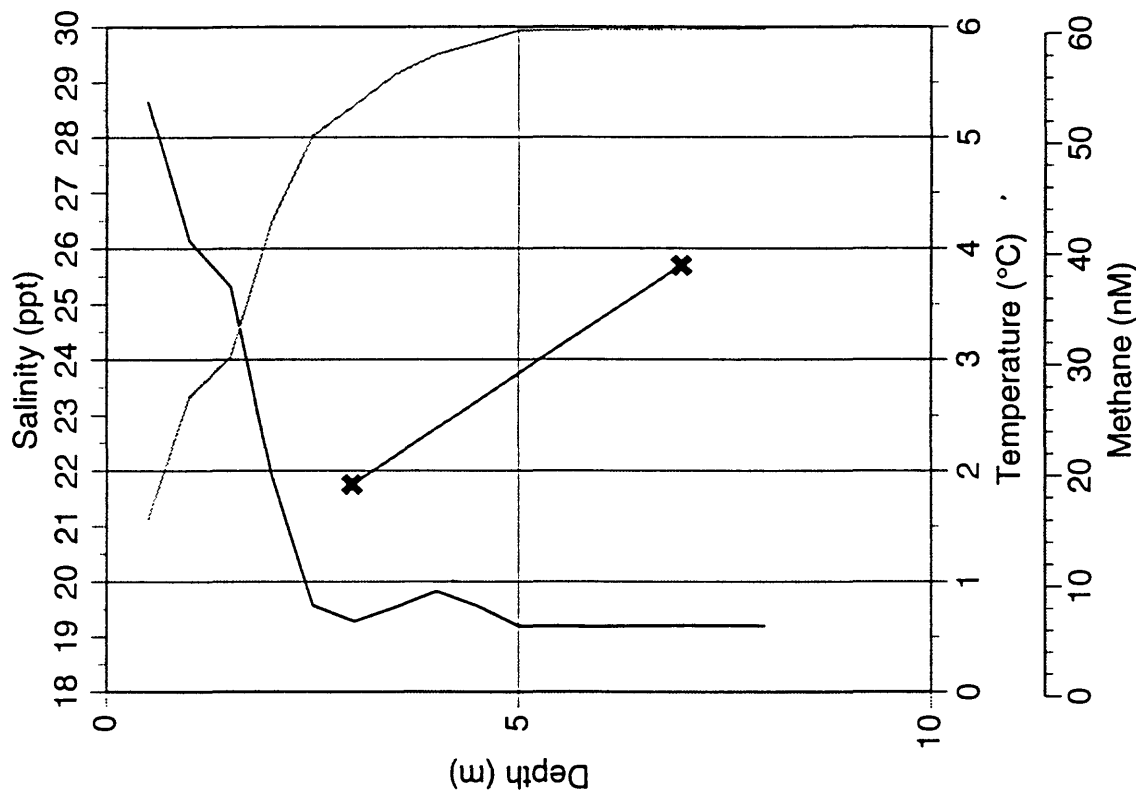
955120 T1 Oliktok Pt. 20m May 1995



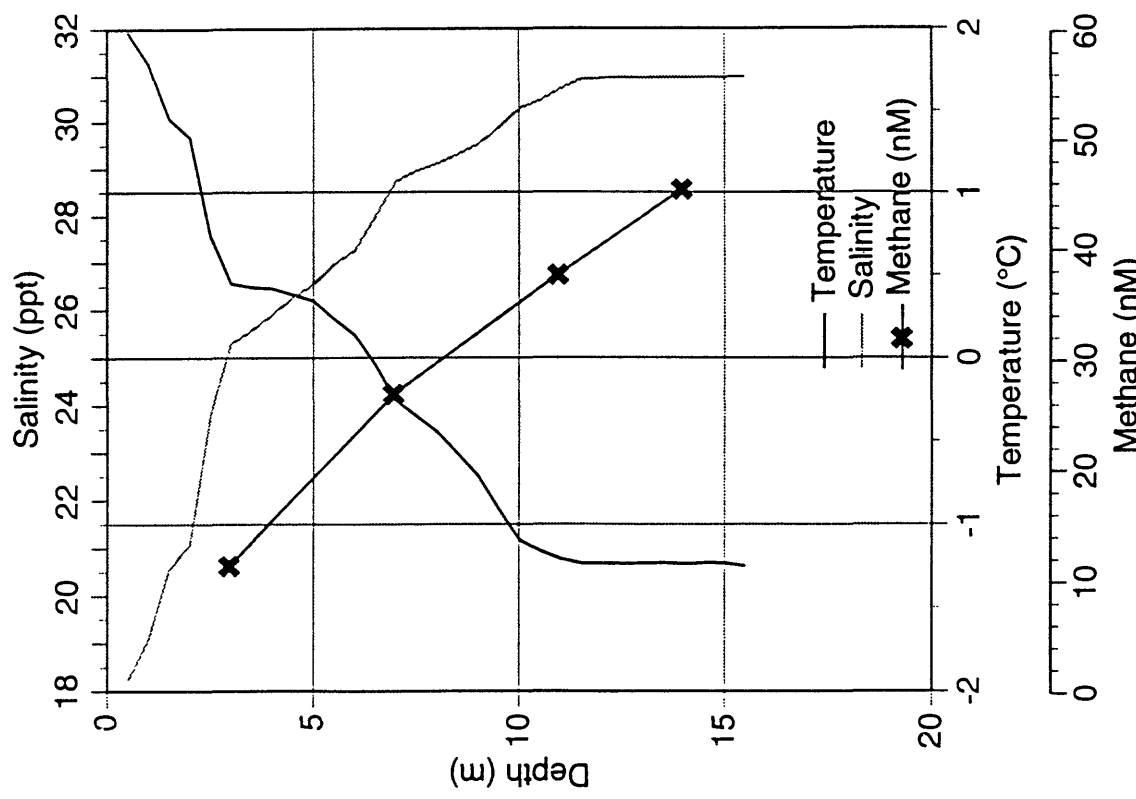
958120 T1 Oliktok Pt. 20m August 1995



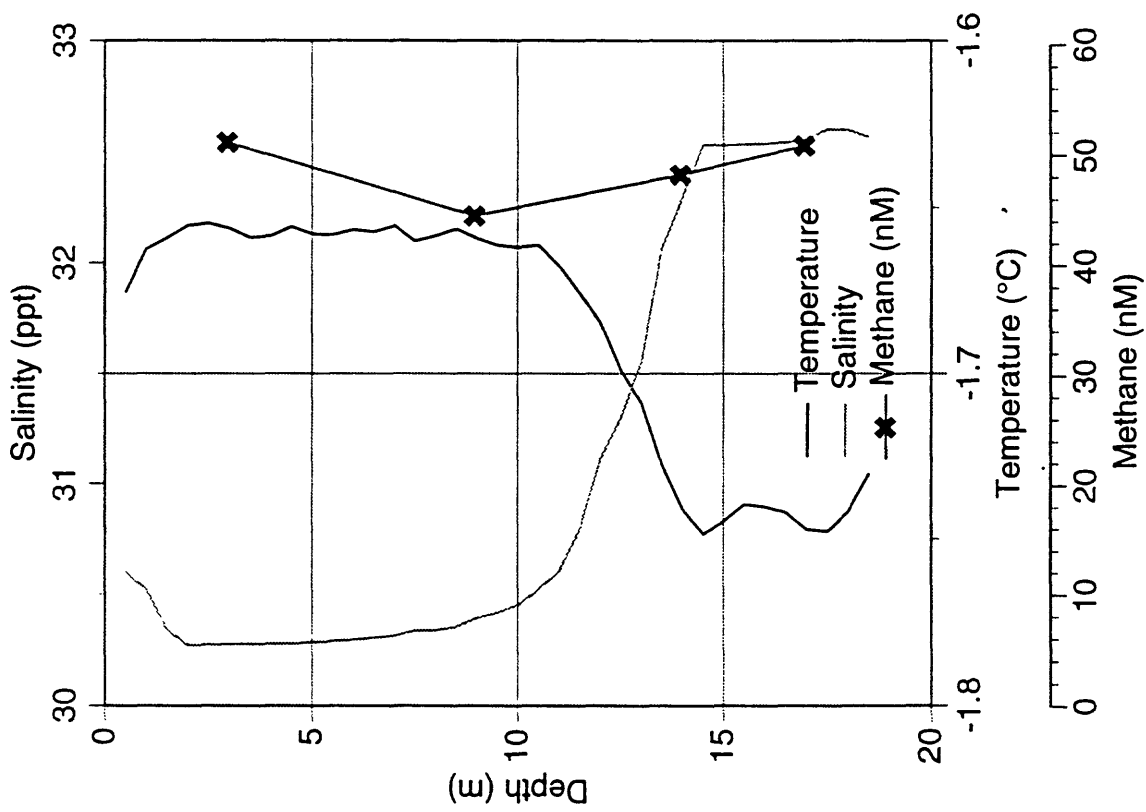
958210 T2 Colville River 10m August 1995



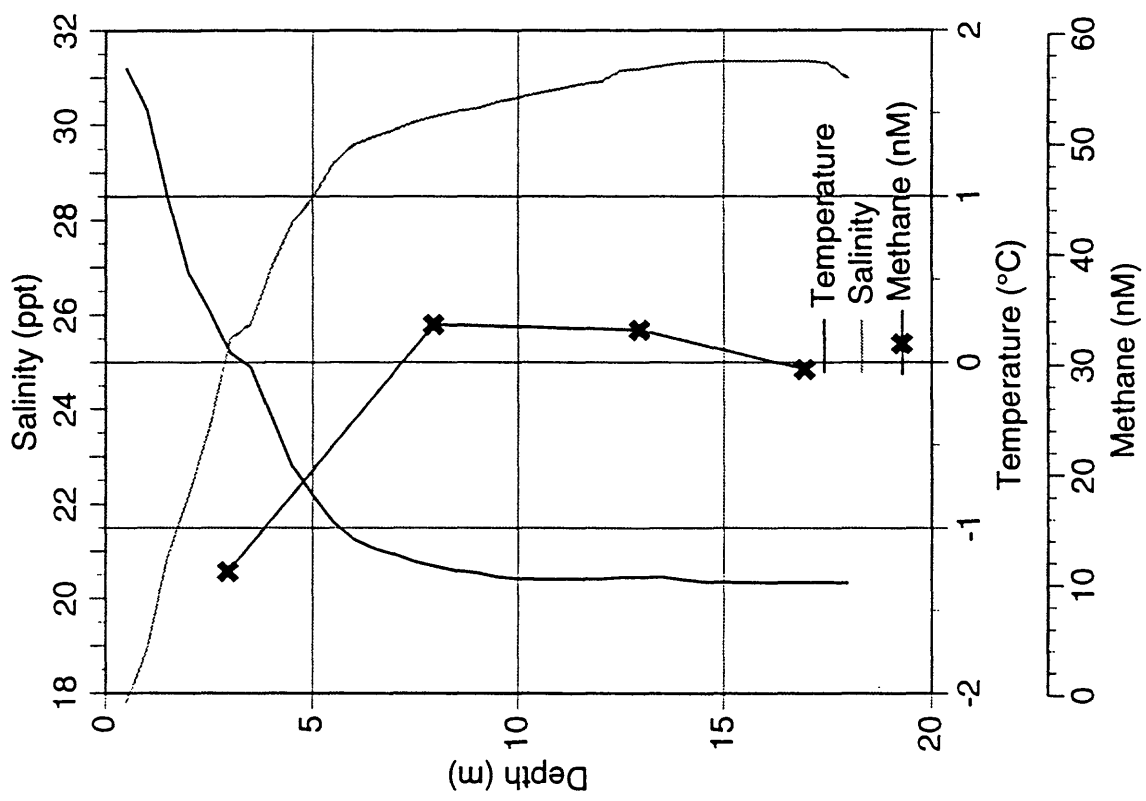
958215 T2 Colville River 15m August 1995



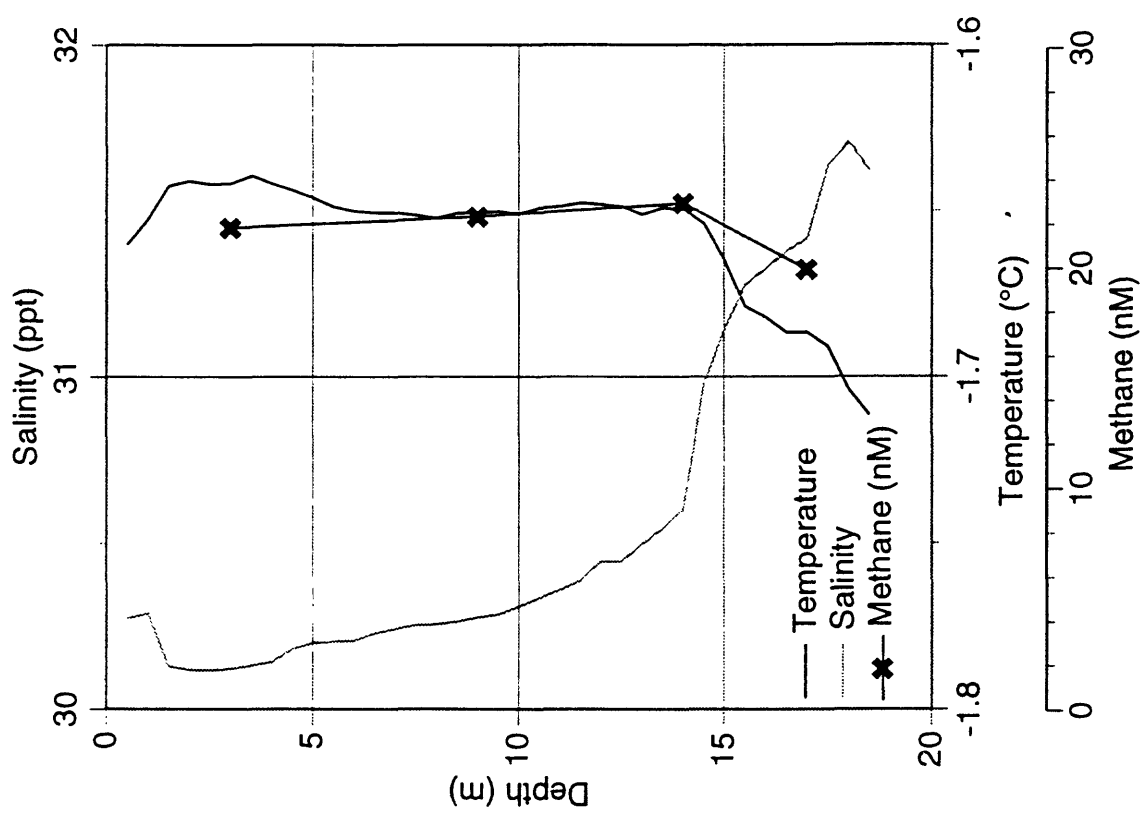
955218 T2 Colville River 18m May 1995



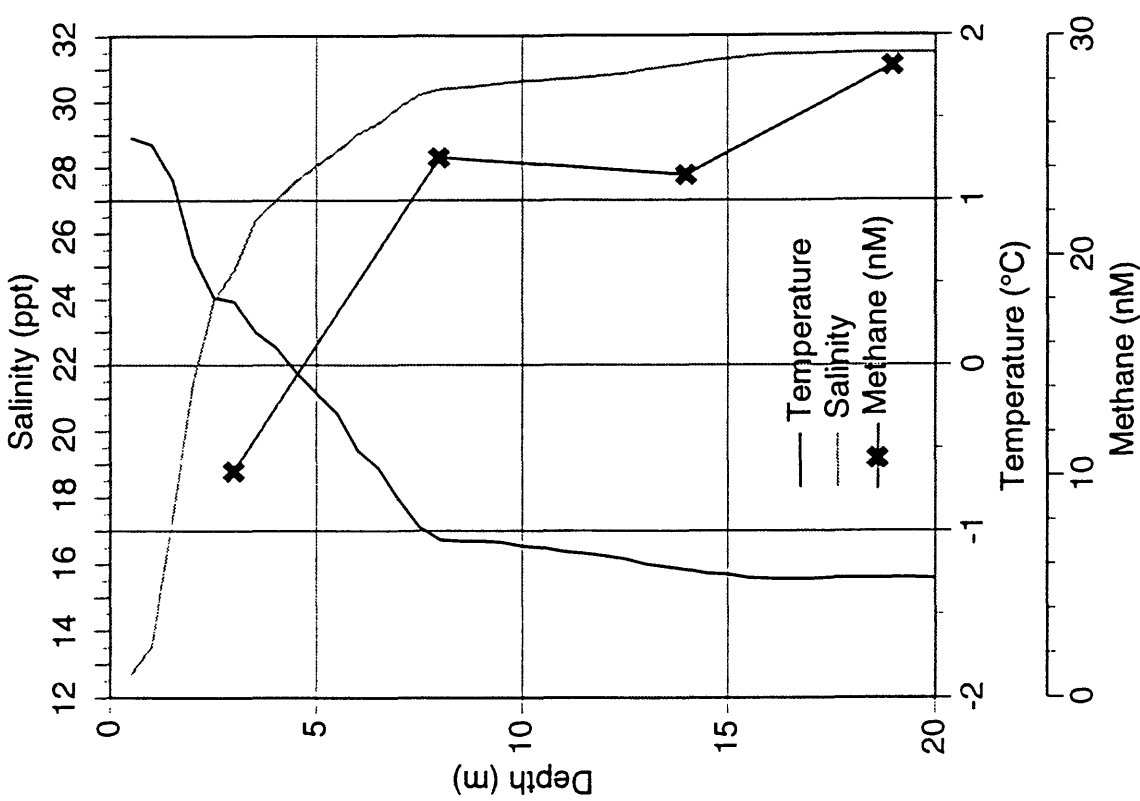
958218 T2 Colville River 18m August 1995



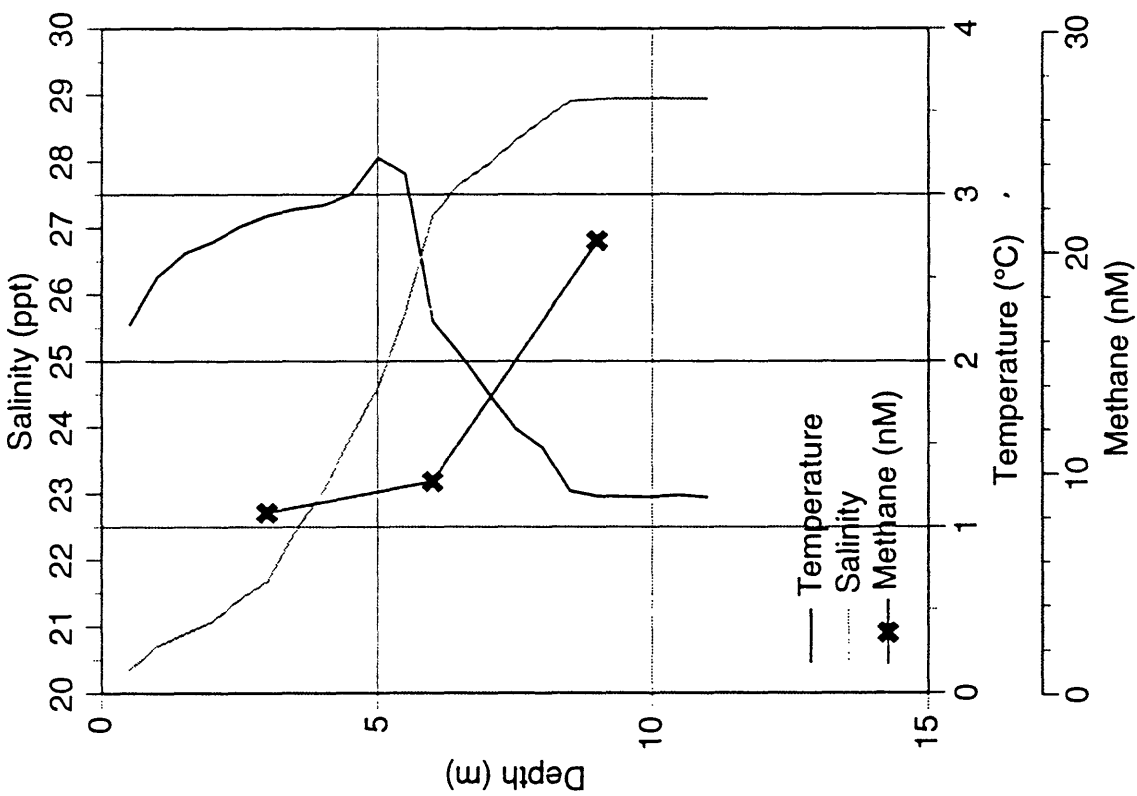
955418 T4 Kuparuk River 18m May 1995



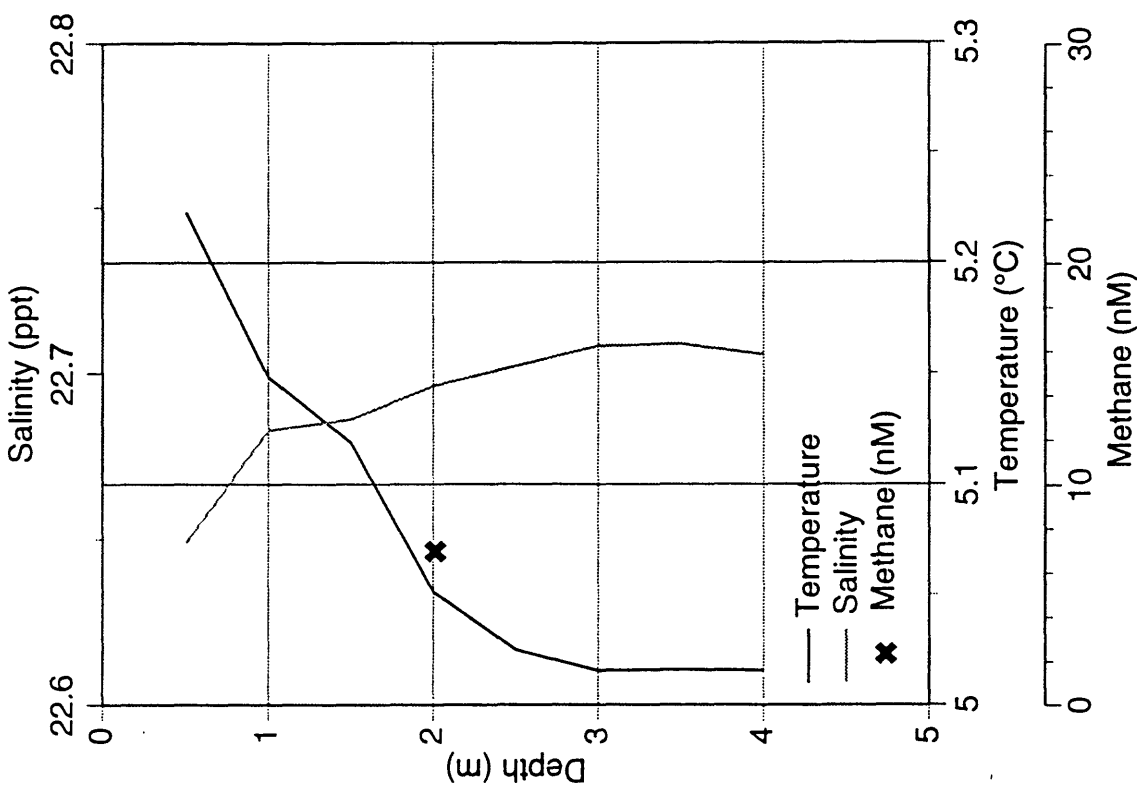
958420 T4 Kuparuk River 20m August 1995



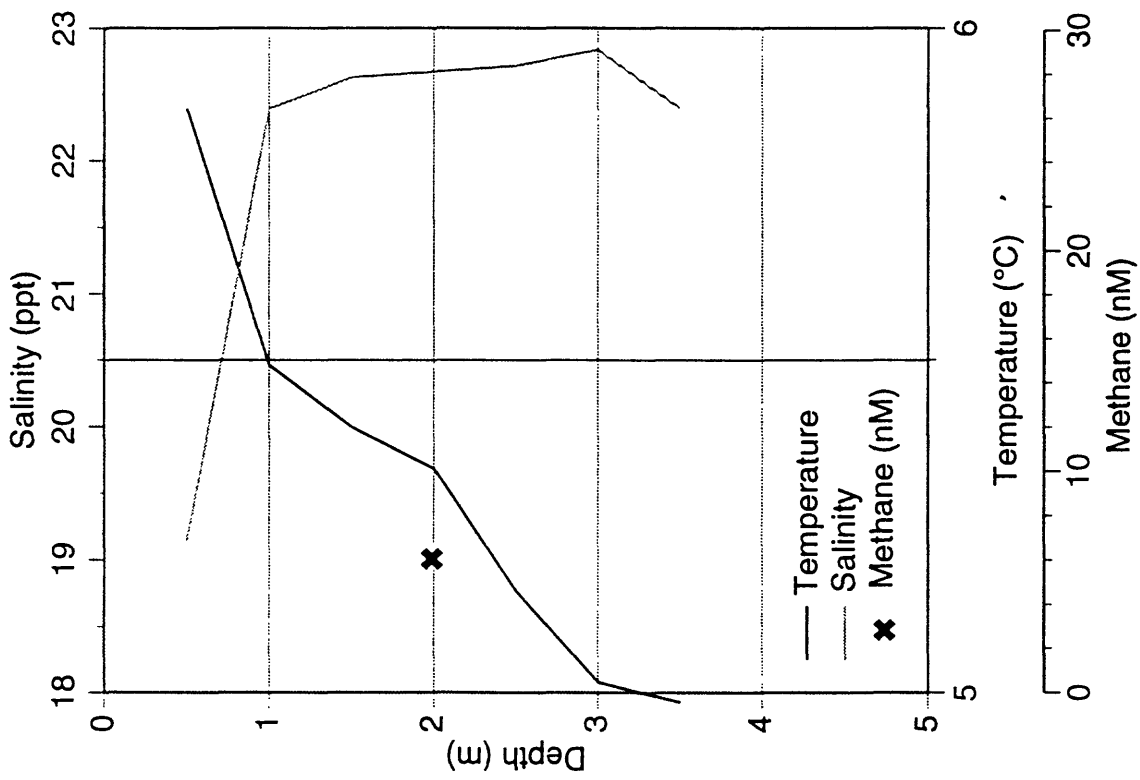
958410 T4 Kuparuk River 10m August 1995



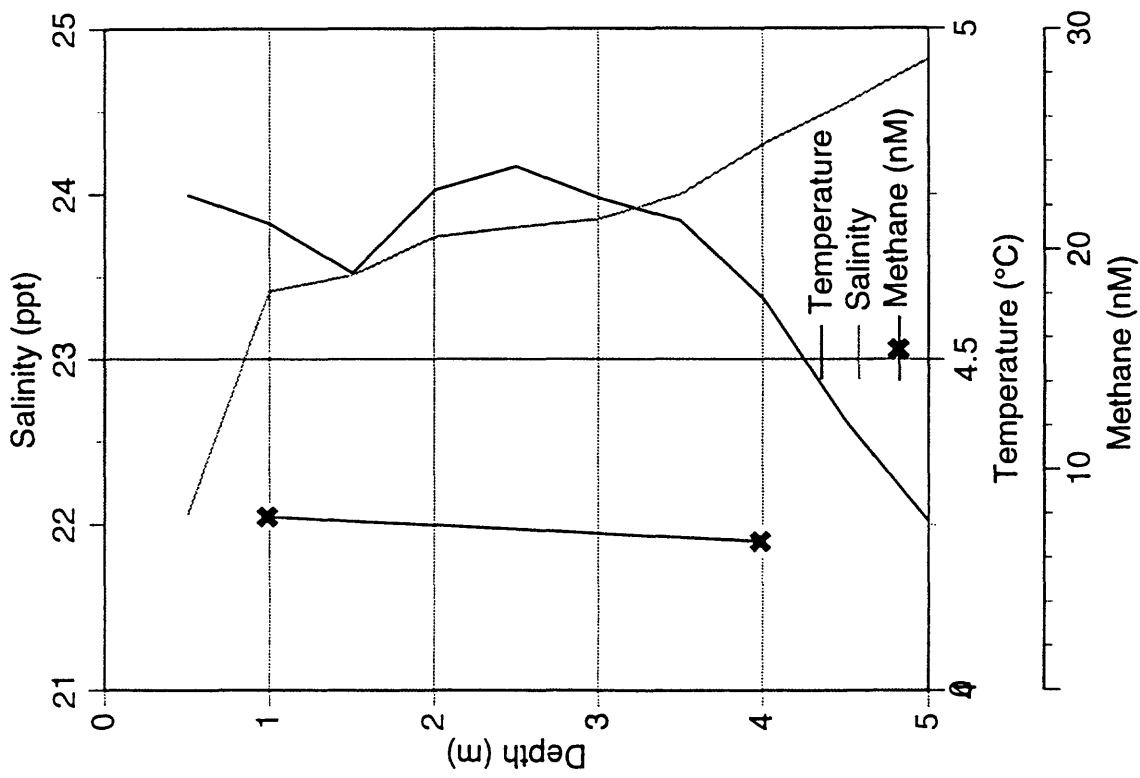
958503 Endicott Dock 3m August 1995



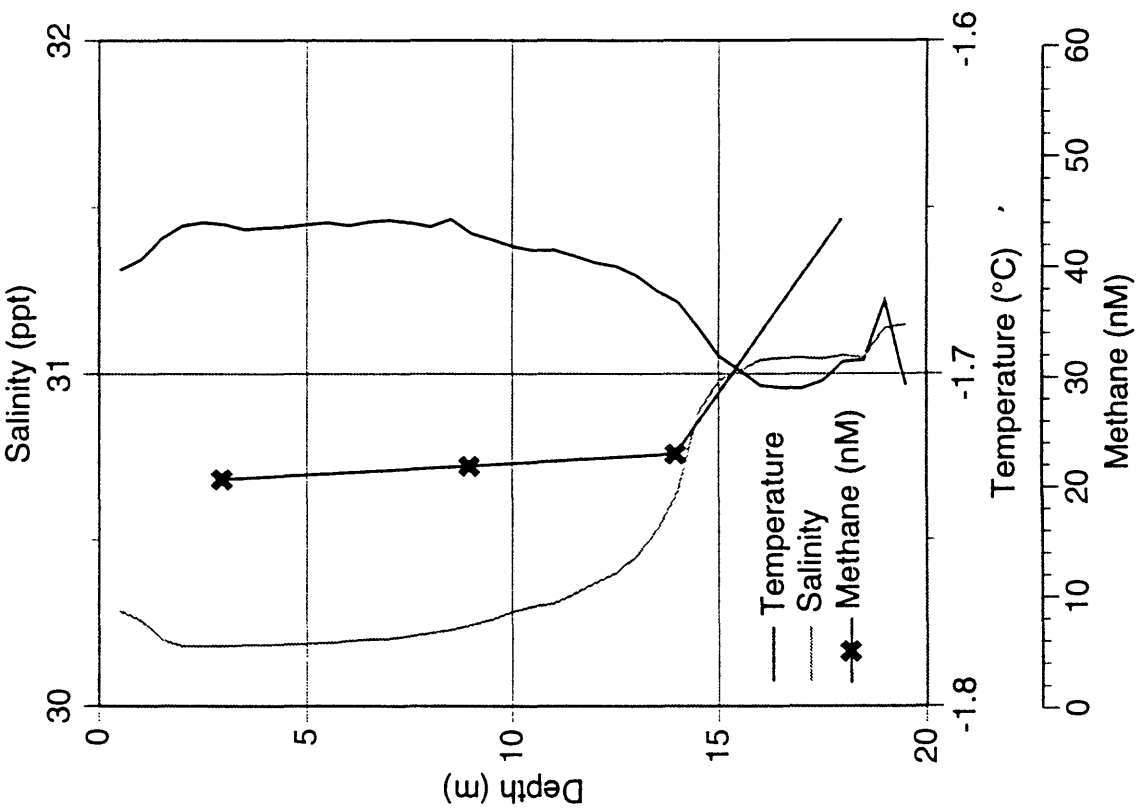
955502 T5 Endicott 2m May 1995



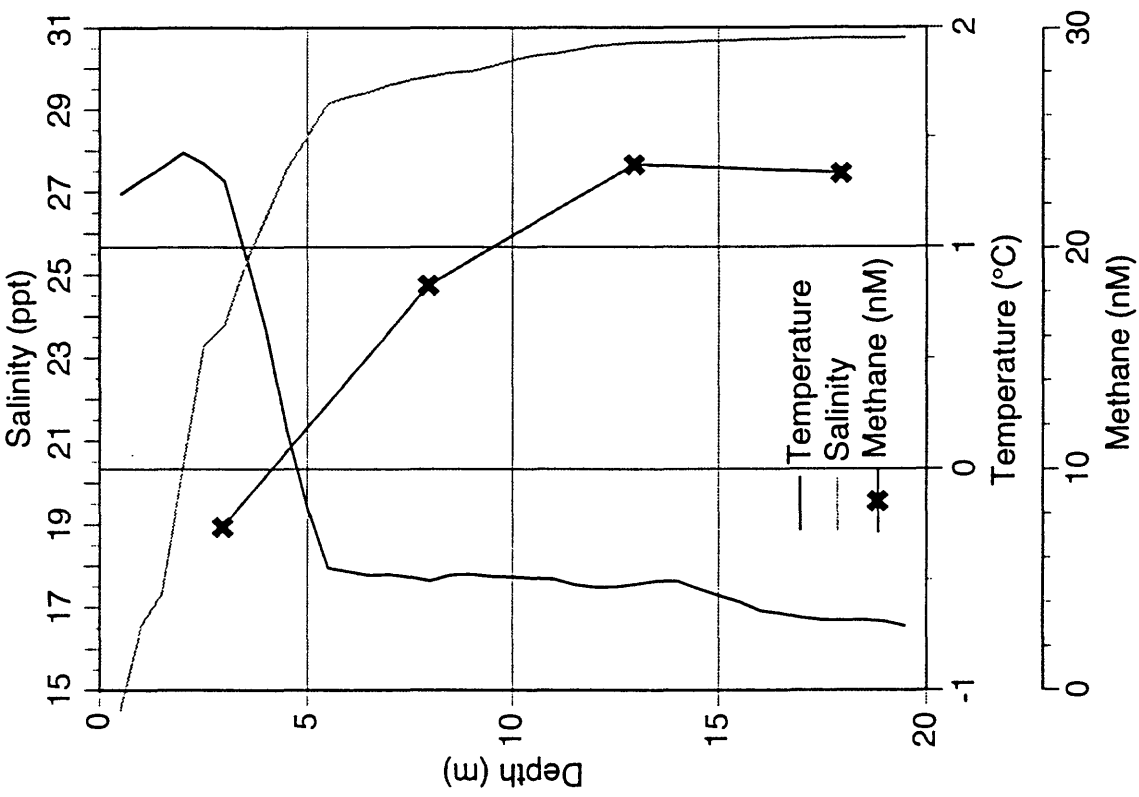
958505 T5 Endicott 5m August 1995



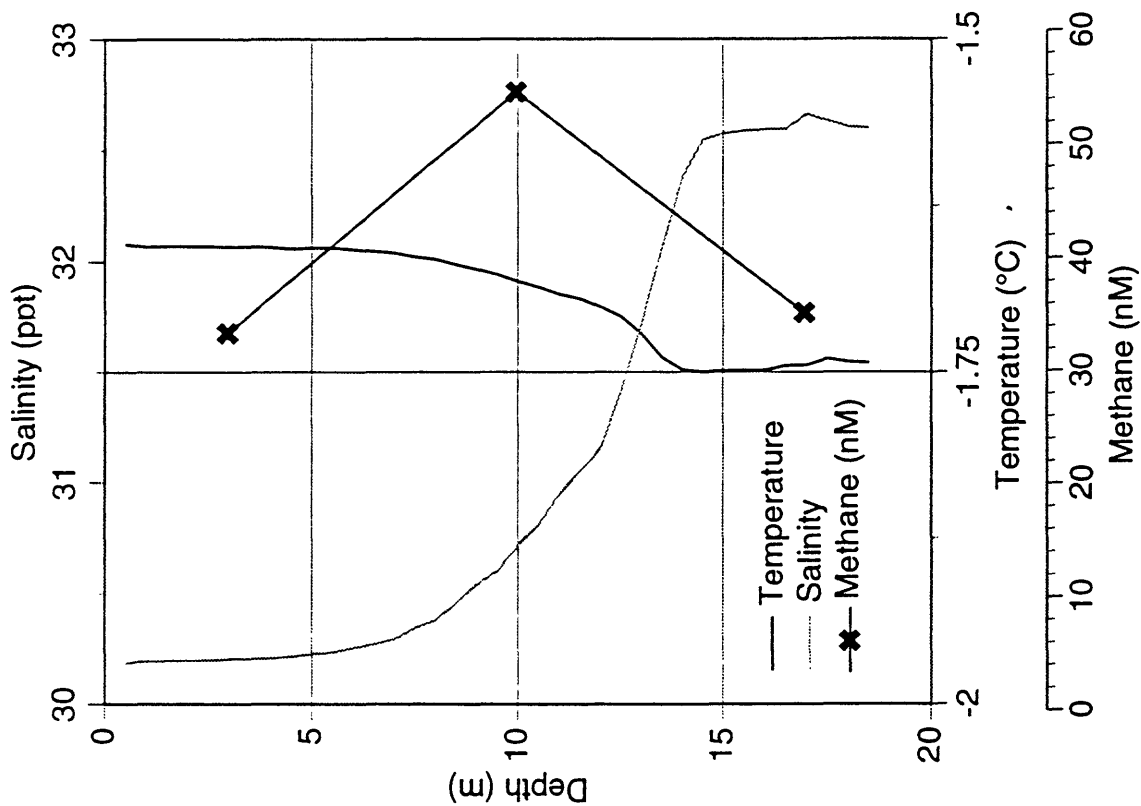
955518 T5 Endicott 18m May 1995



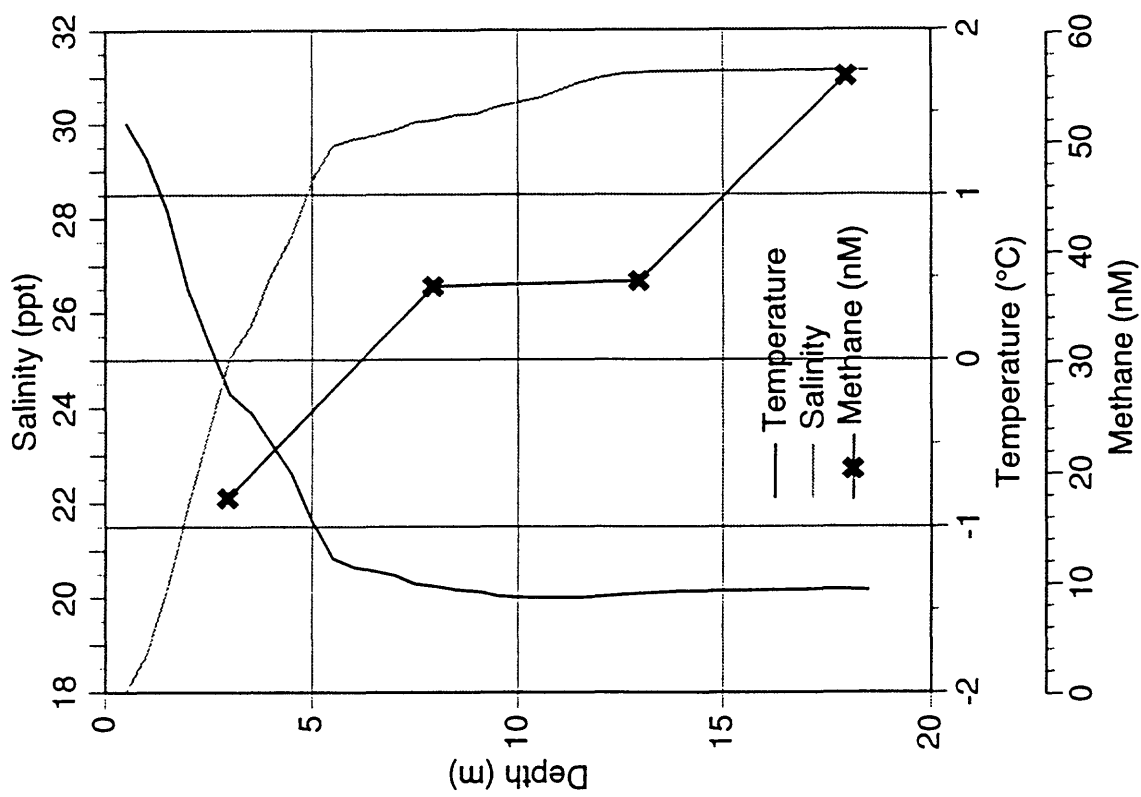
958518 T5 Endicott 18m August 1995



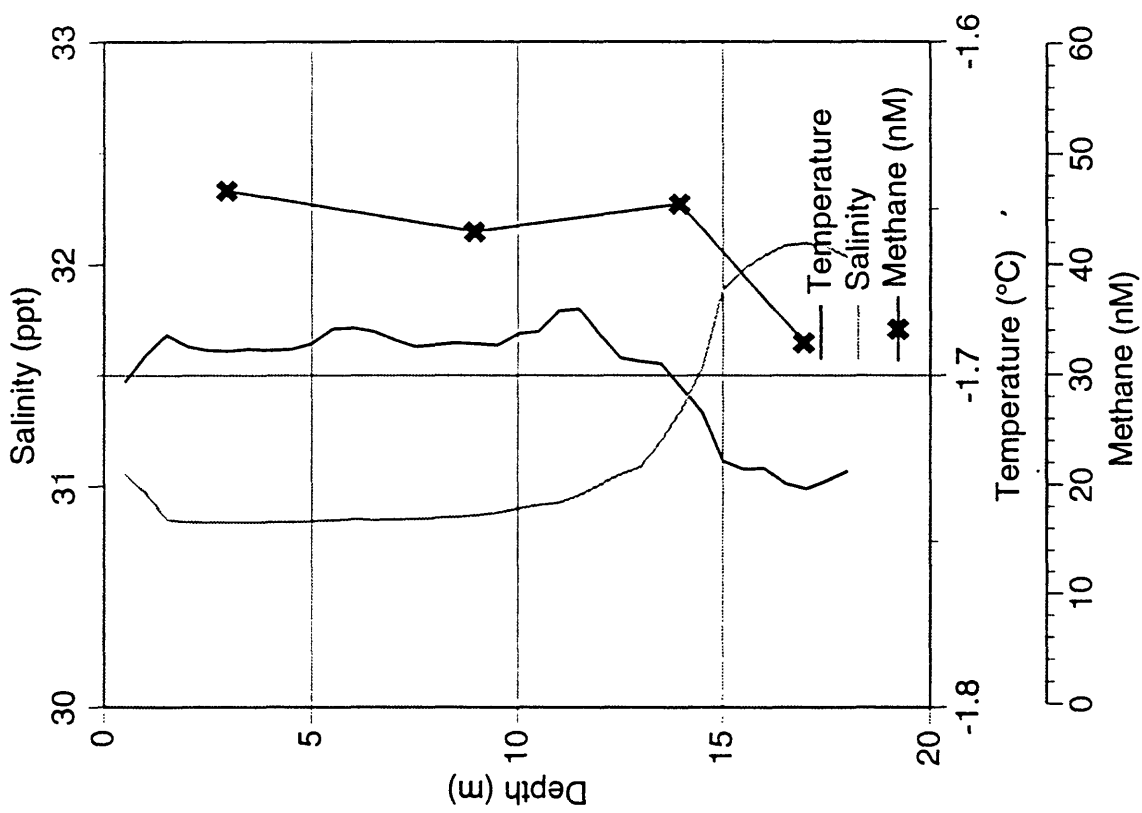
955040 18m May 1995



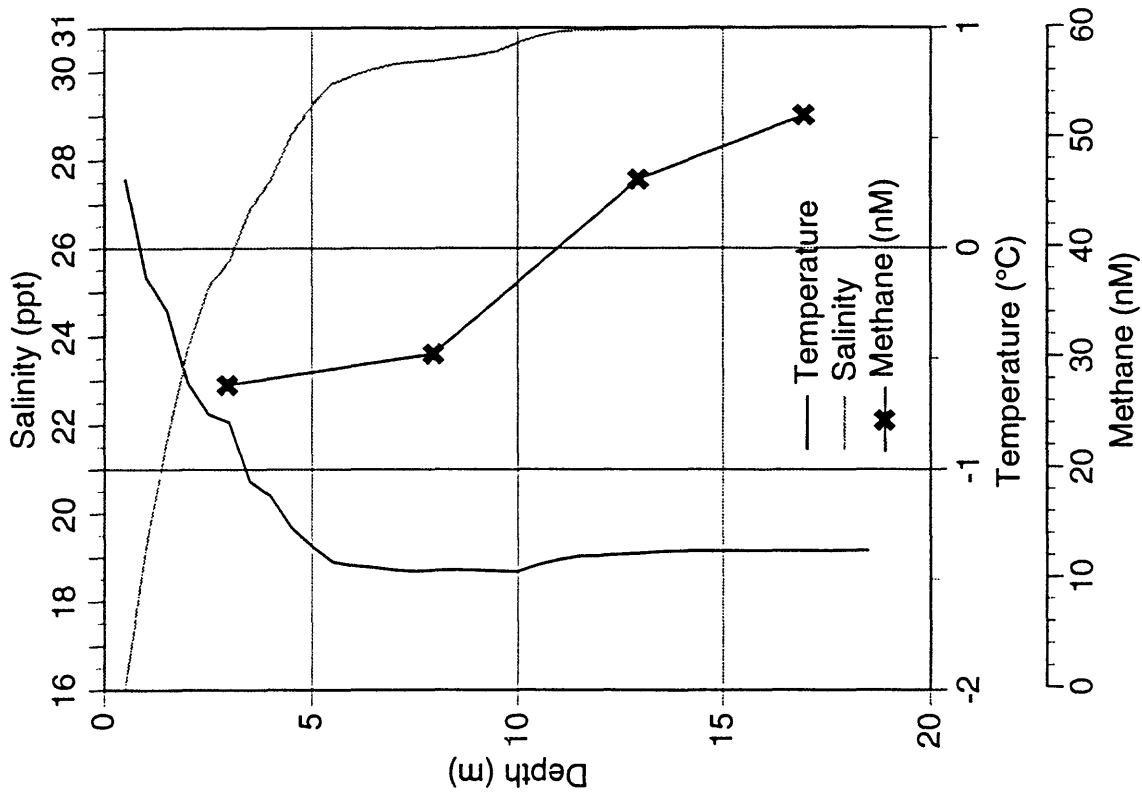
958040 18m August 1995



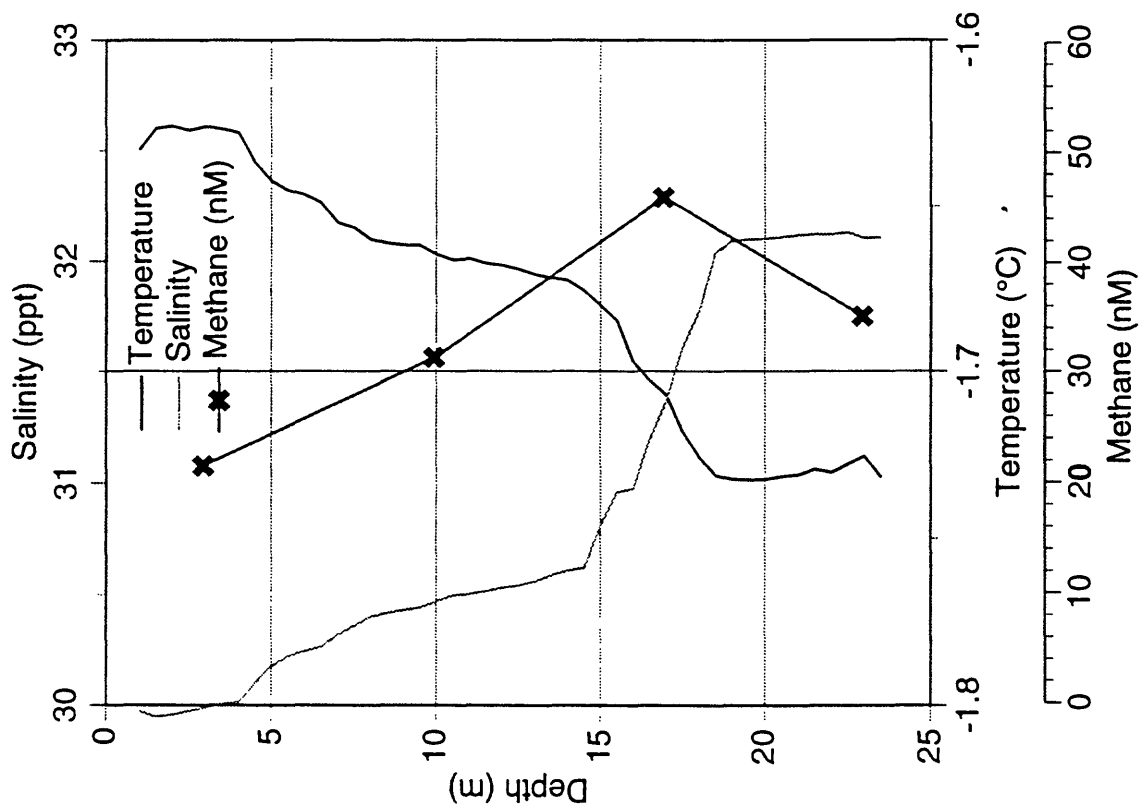
955041 18m May 1995



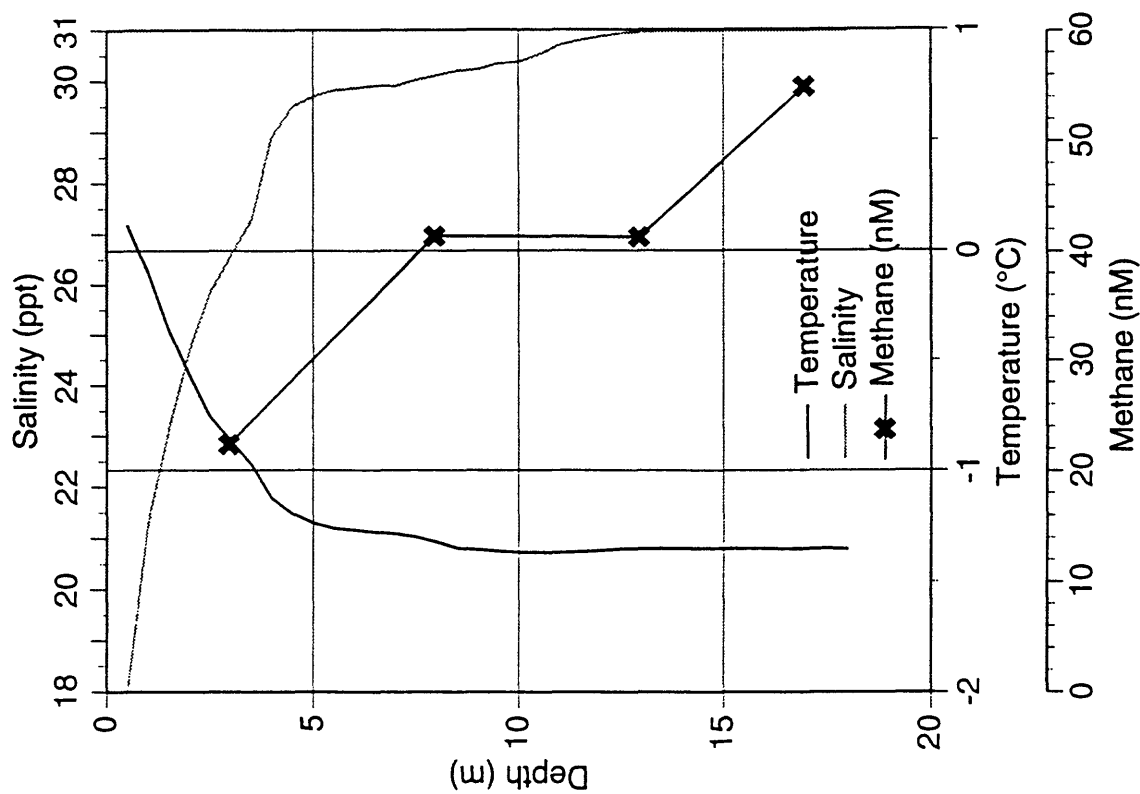
958041 18m August 1995



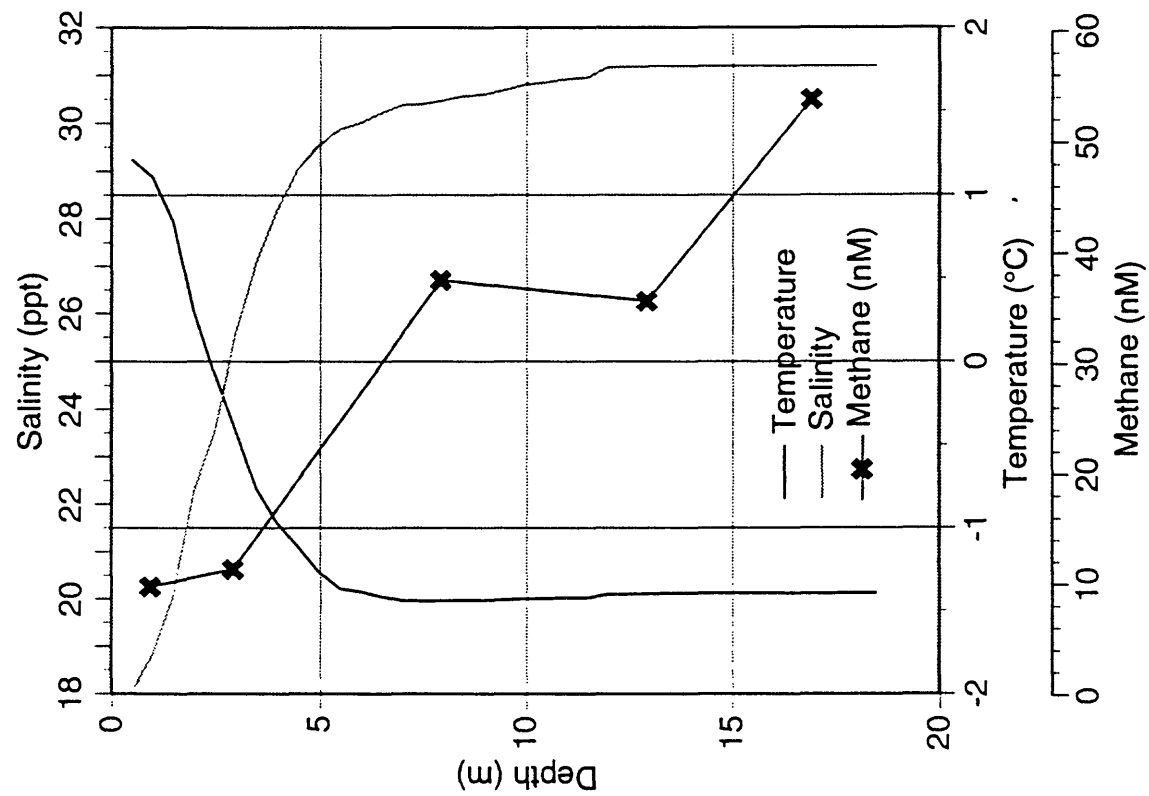
955042 24m May 1995



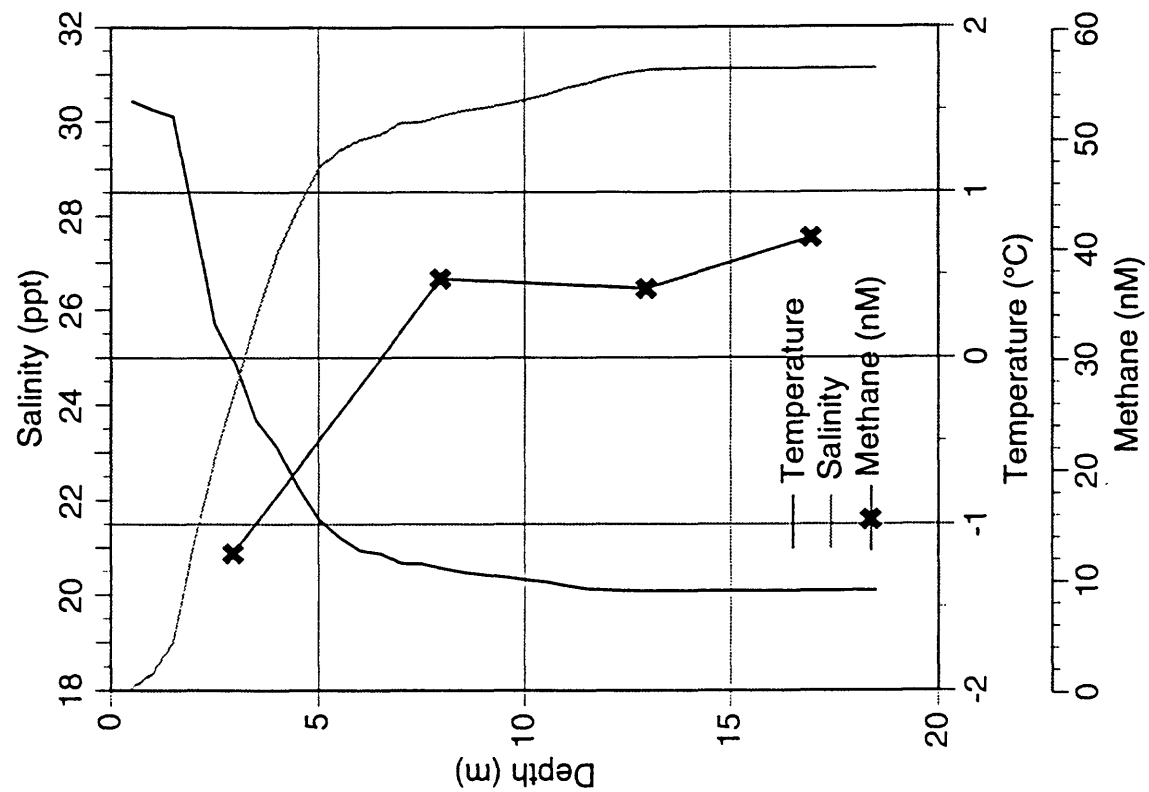
958044 18m August 1995



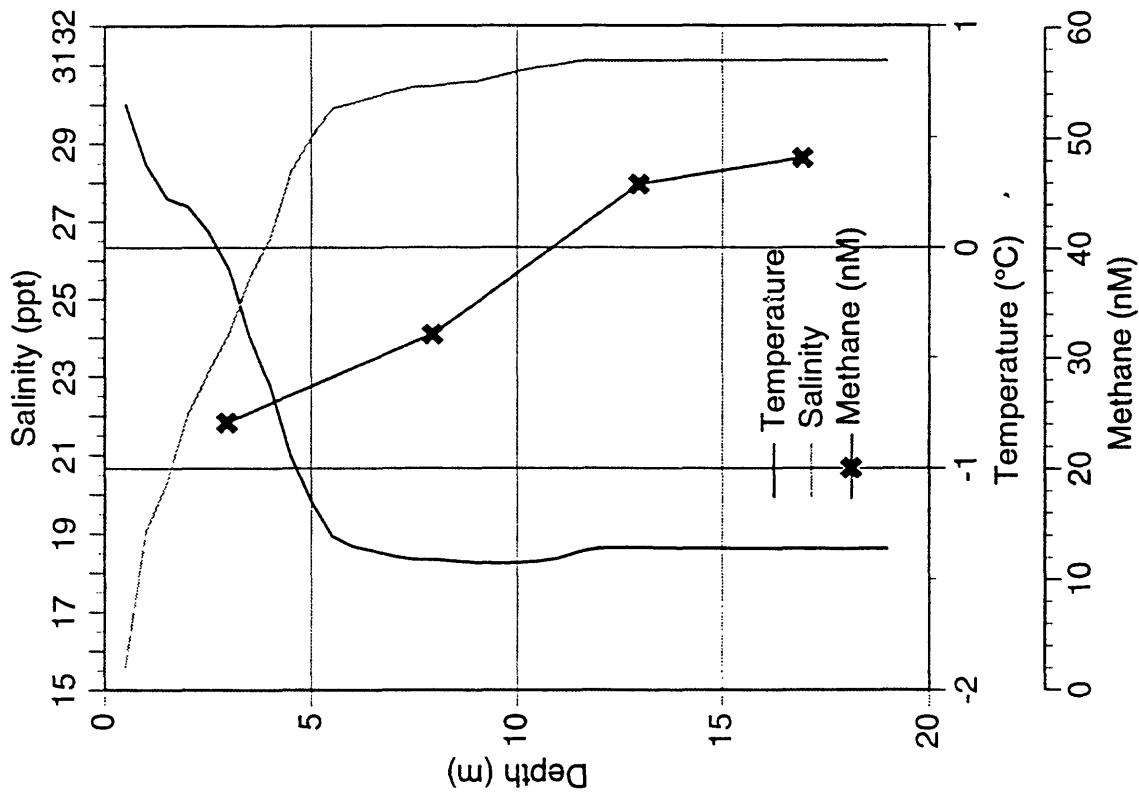
958043 18m August 1995



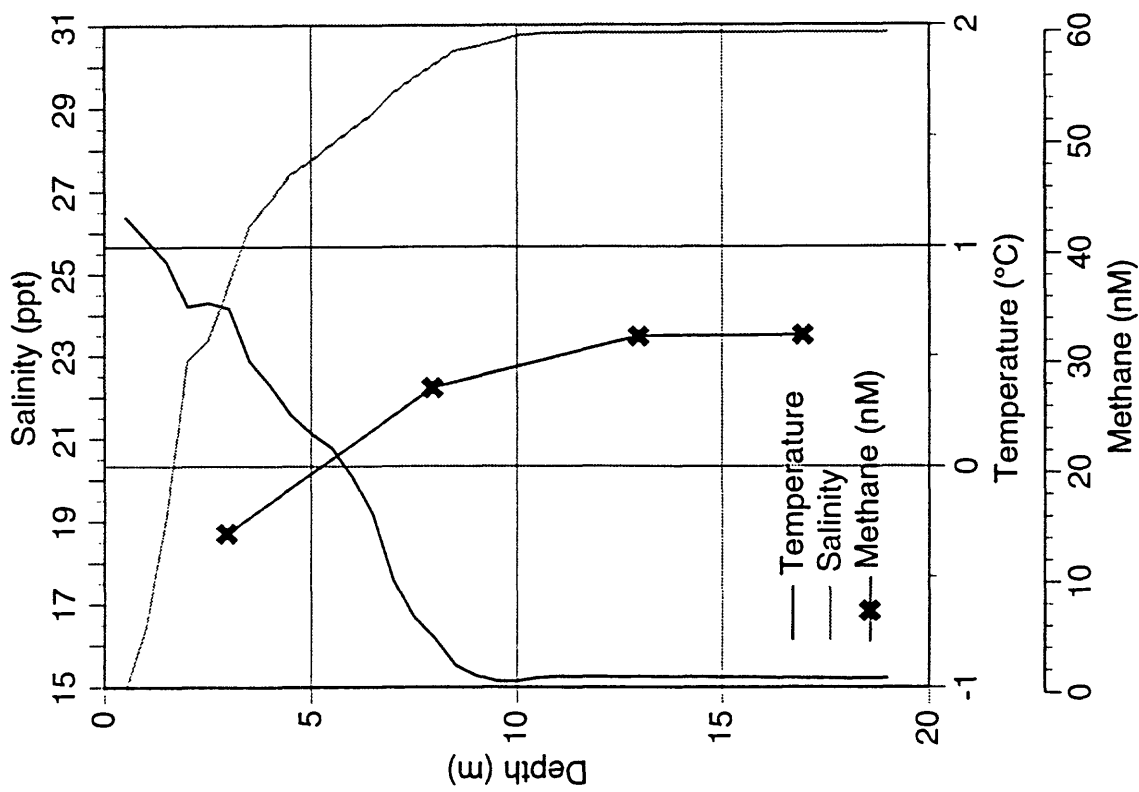
958045 18m August 1995



958046 18m August 1995



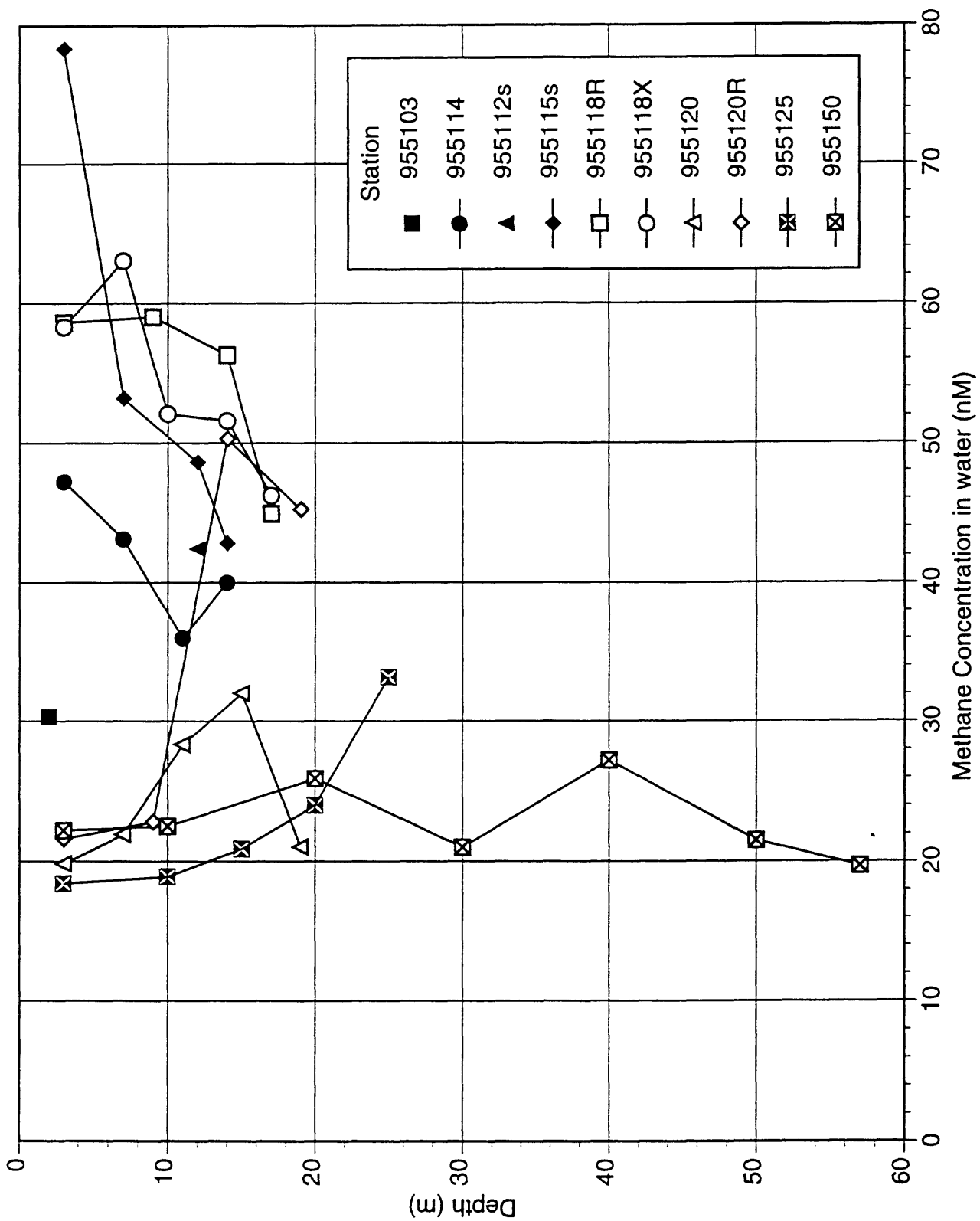
958047 18m August 1995



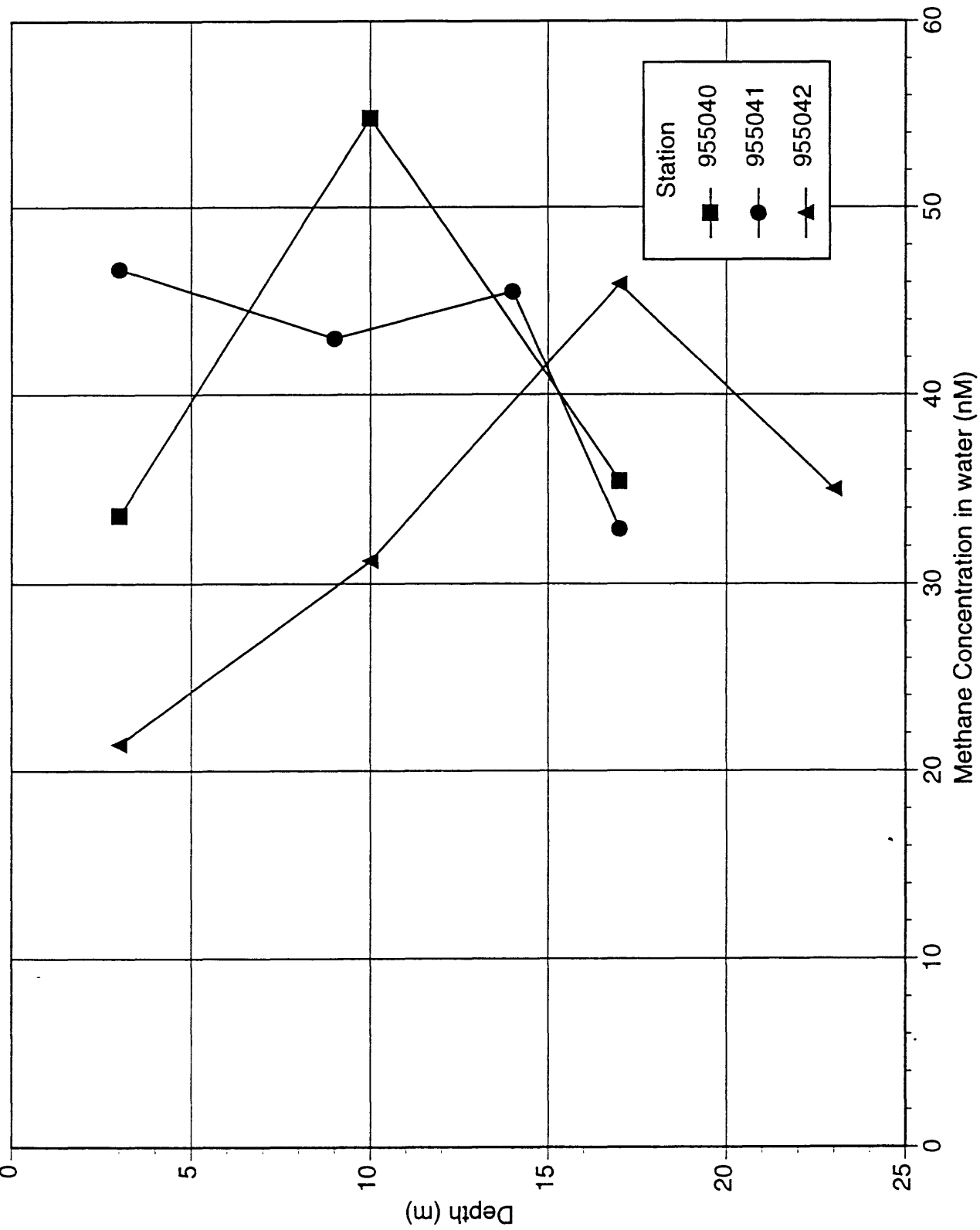
Appendix 2

Methane concentrations in water plotted with water depths grouped by transects from each survey

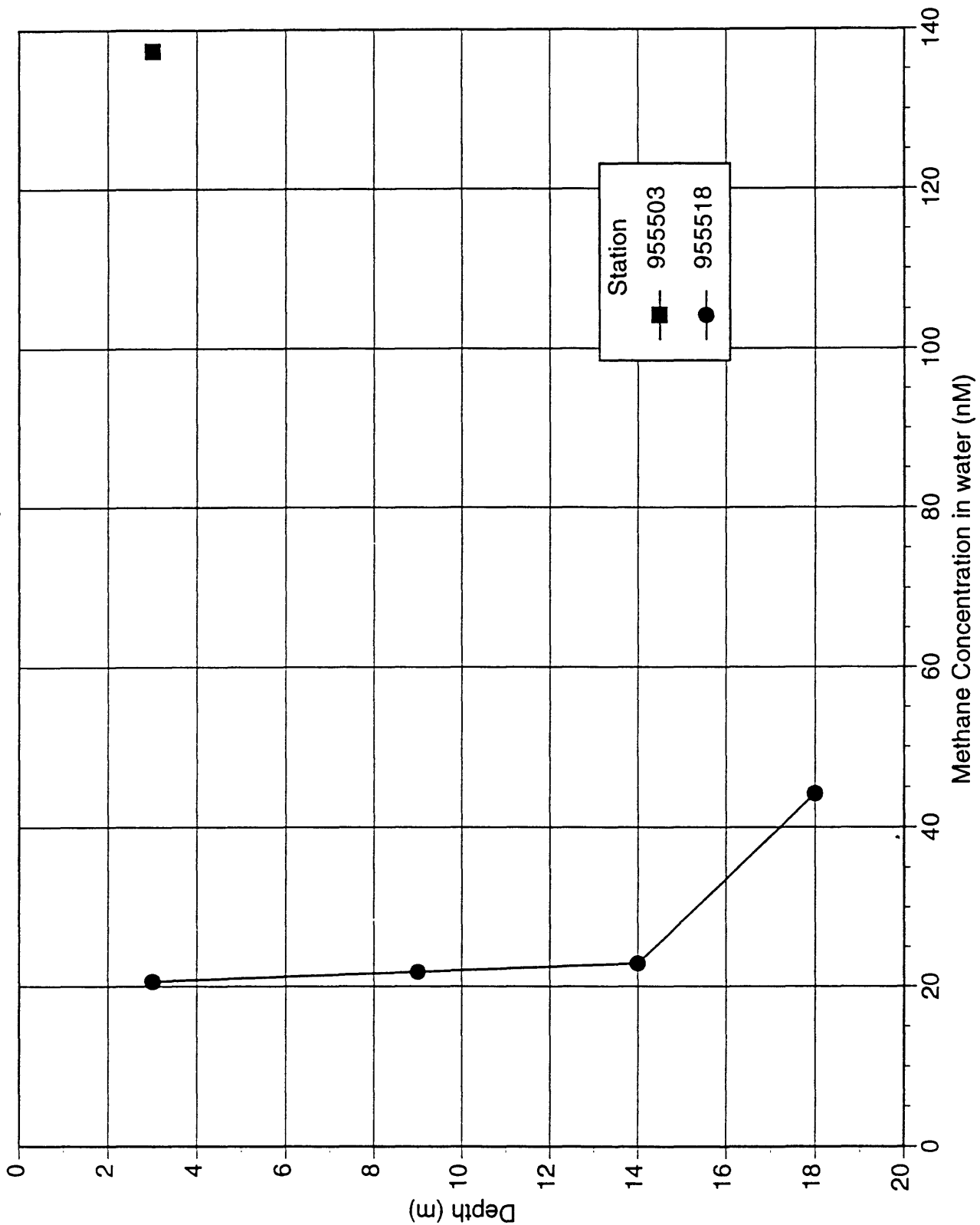
Transect 1 Oliktok Point May, 1995



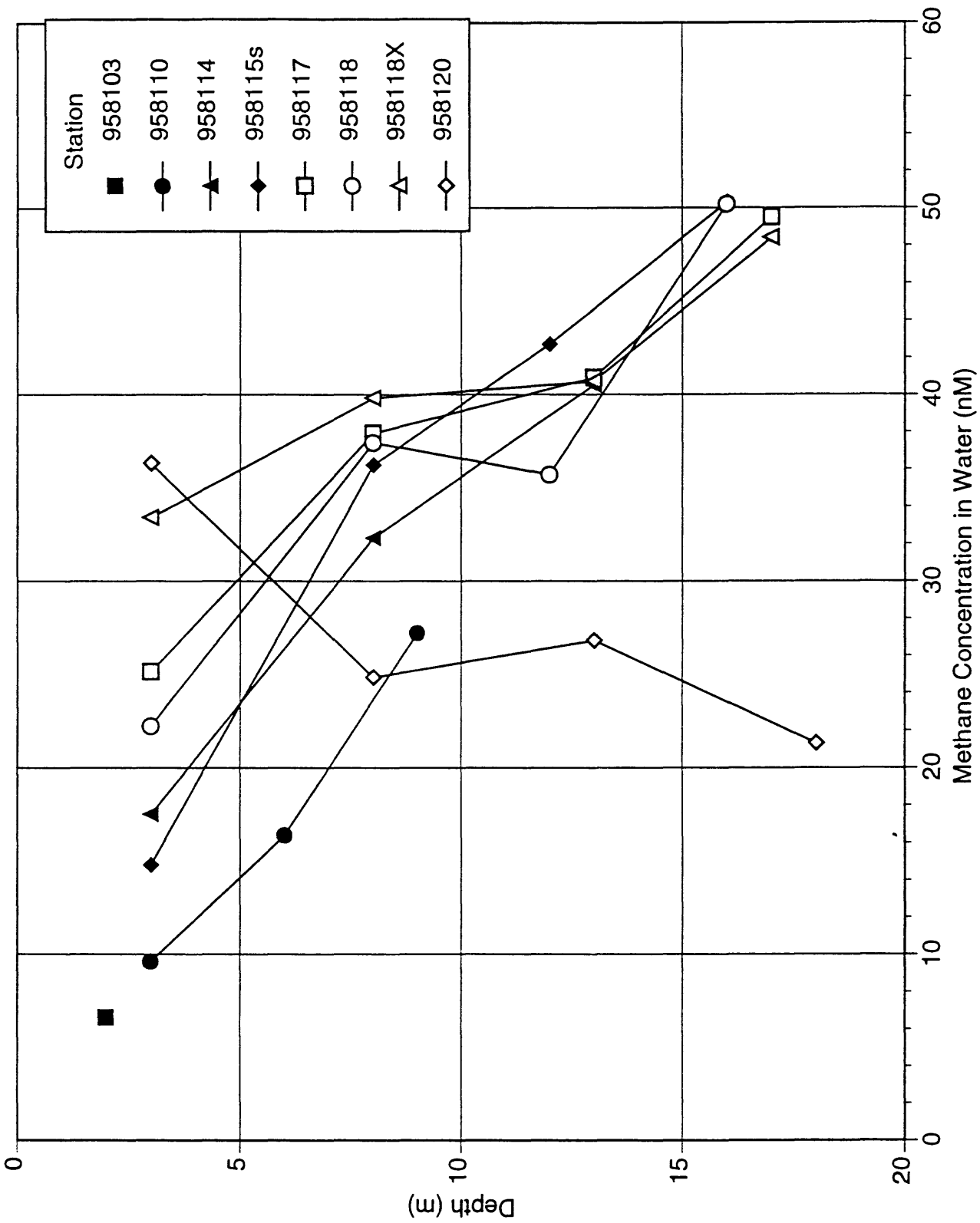
Stations near Transect 1 Oliktok Point May, 1995



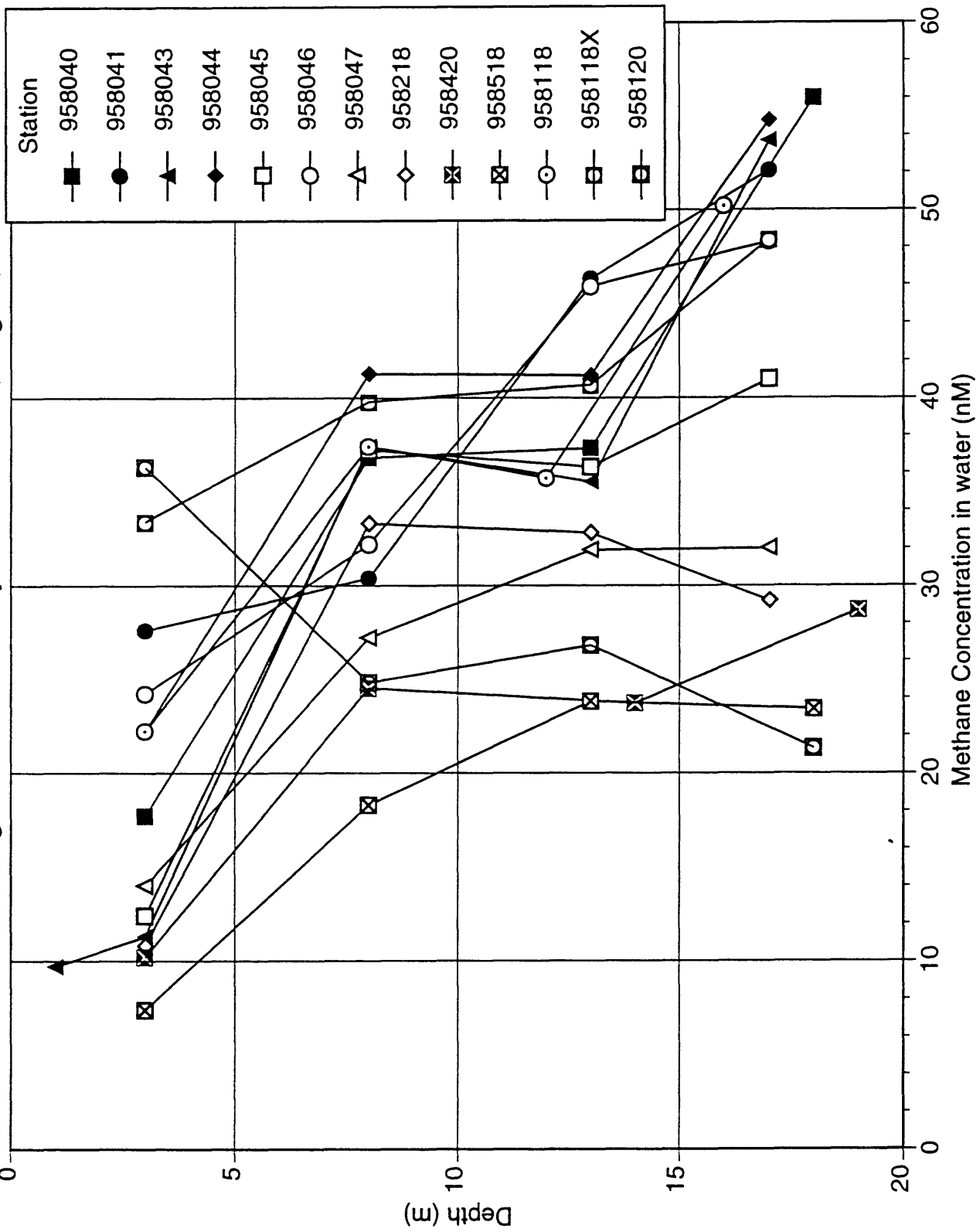
Transect 5 Endicott May, 1995



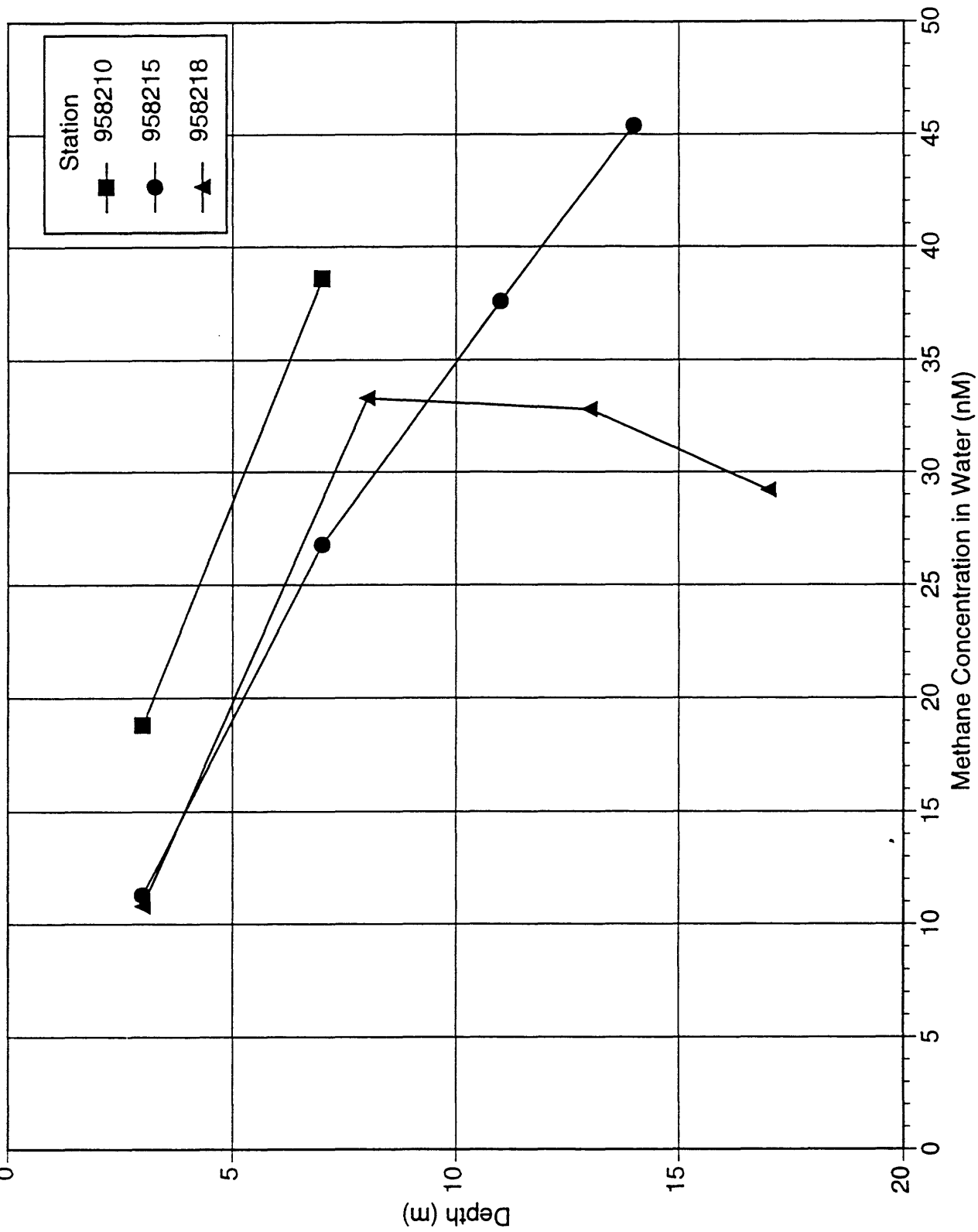
Transect 1 Oliktok Point August, 1995



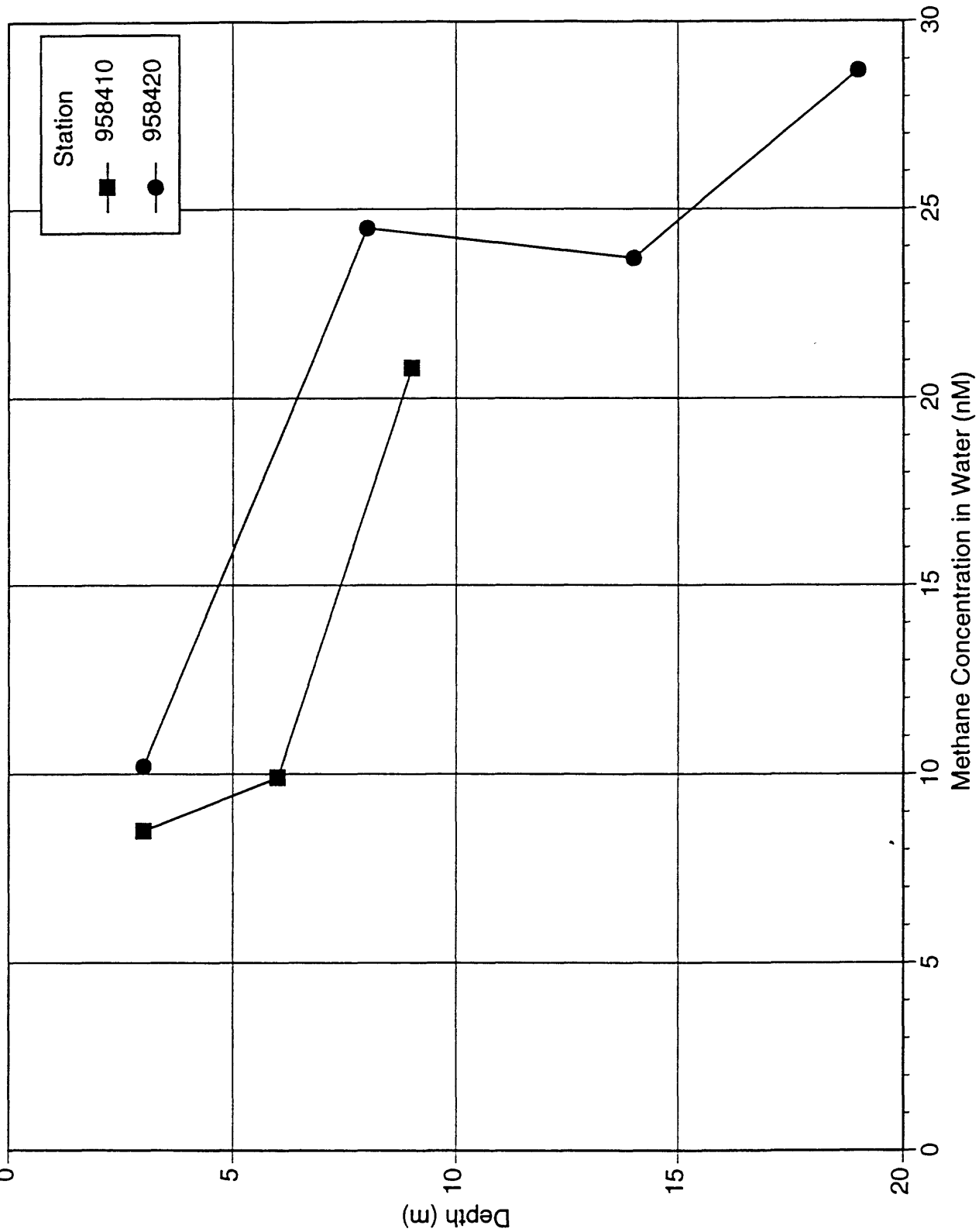
E-W Transect along the 18-20 m Bathymetric Contour, August, 1995



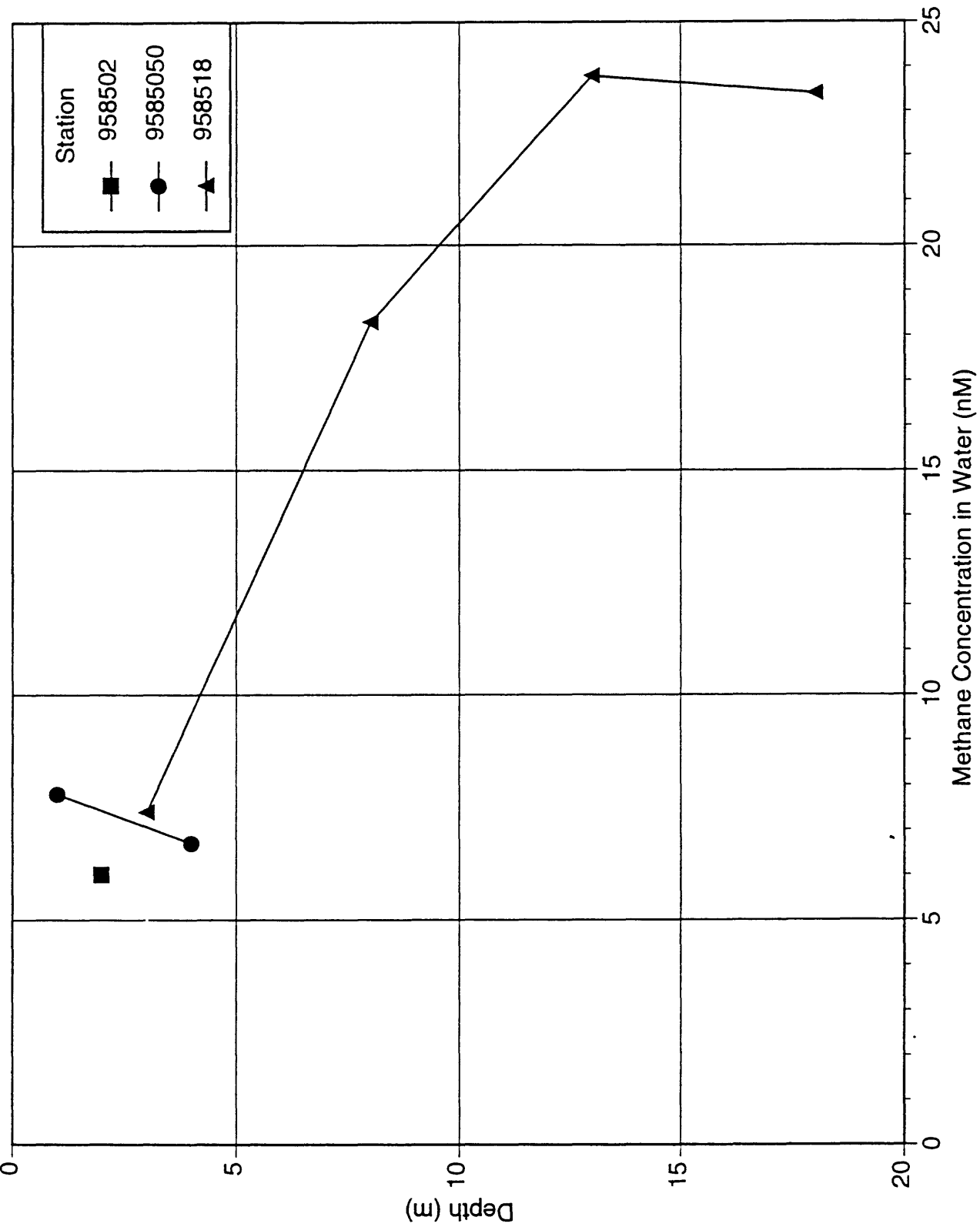
Transect 2 Colville River August, 1995



Transect 4 Kuparuk River August, 1995

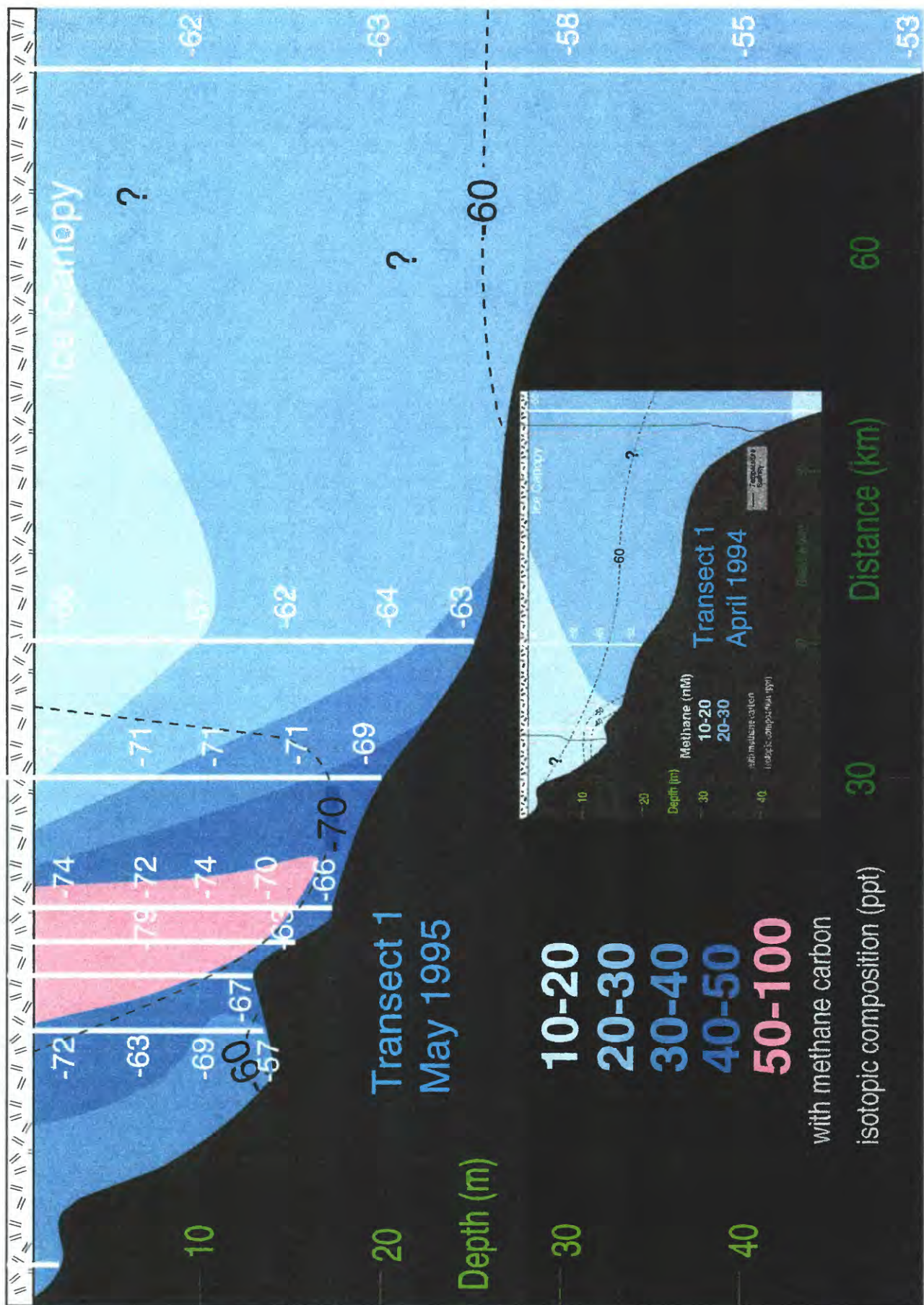


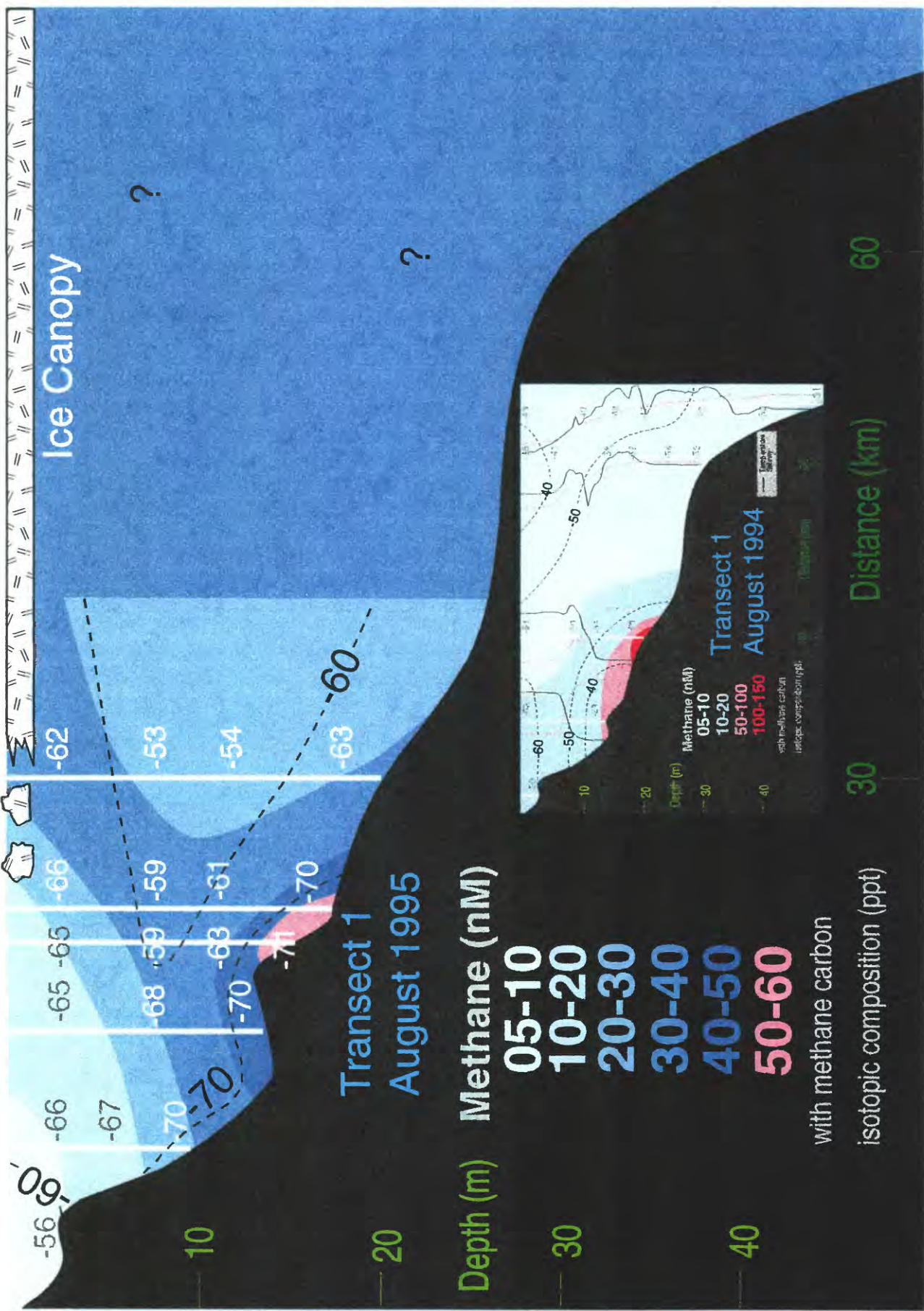
Transect 5 Endicott August, 1995

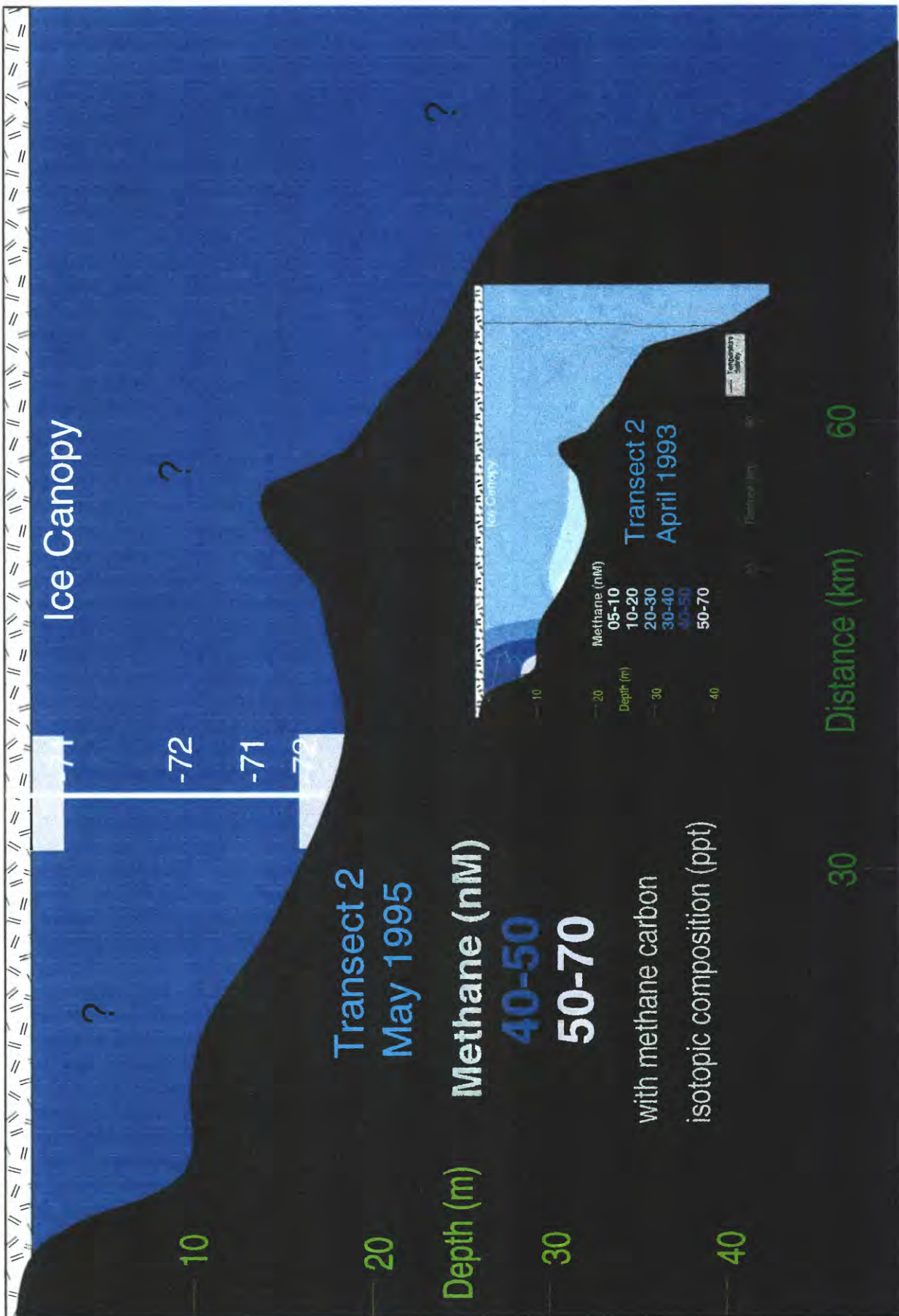


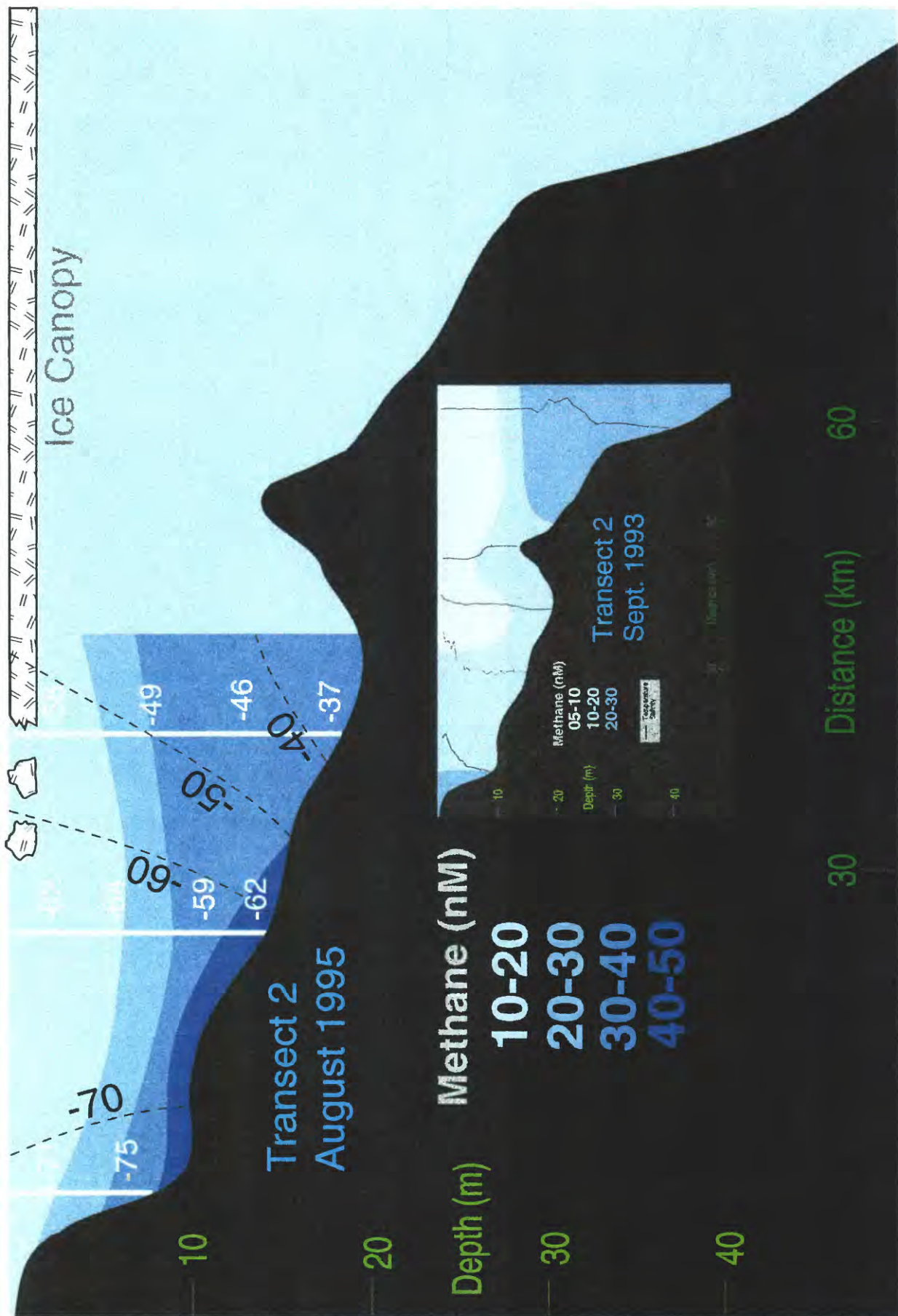
Appendix 3

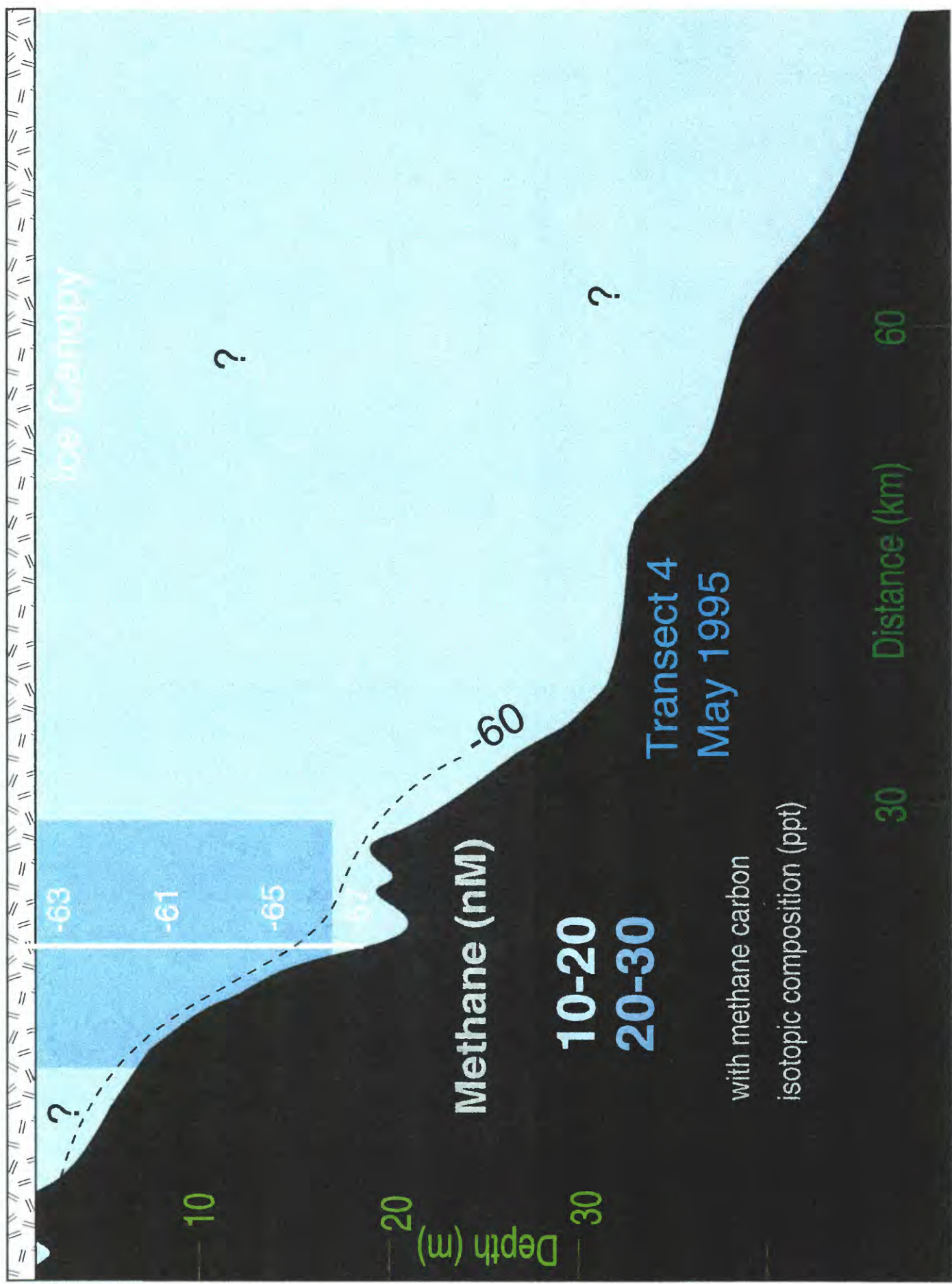
Water column cross sections of methane concentrations and carbon isotopic composition grouped by transects from each survey

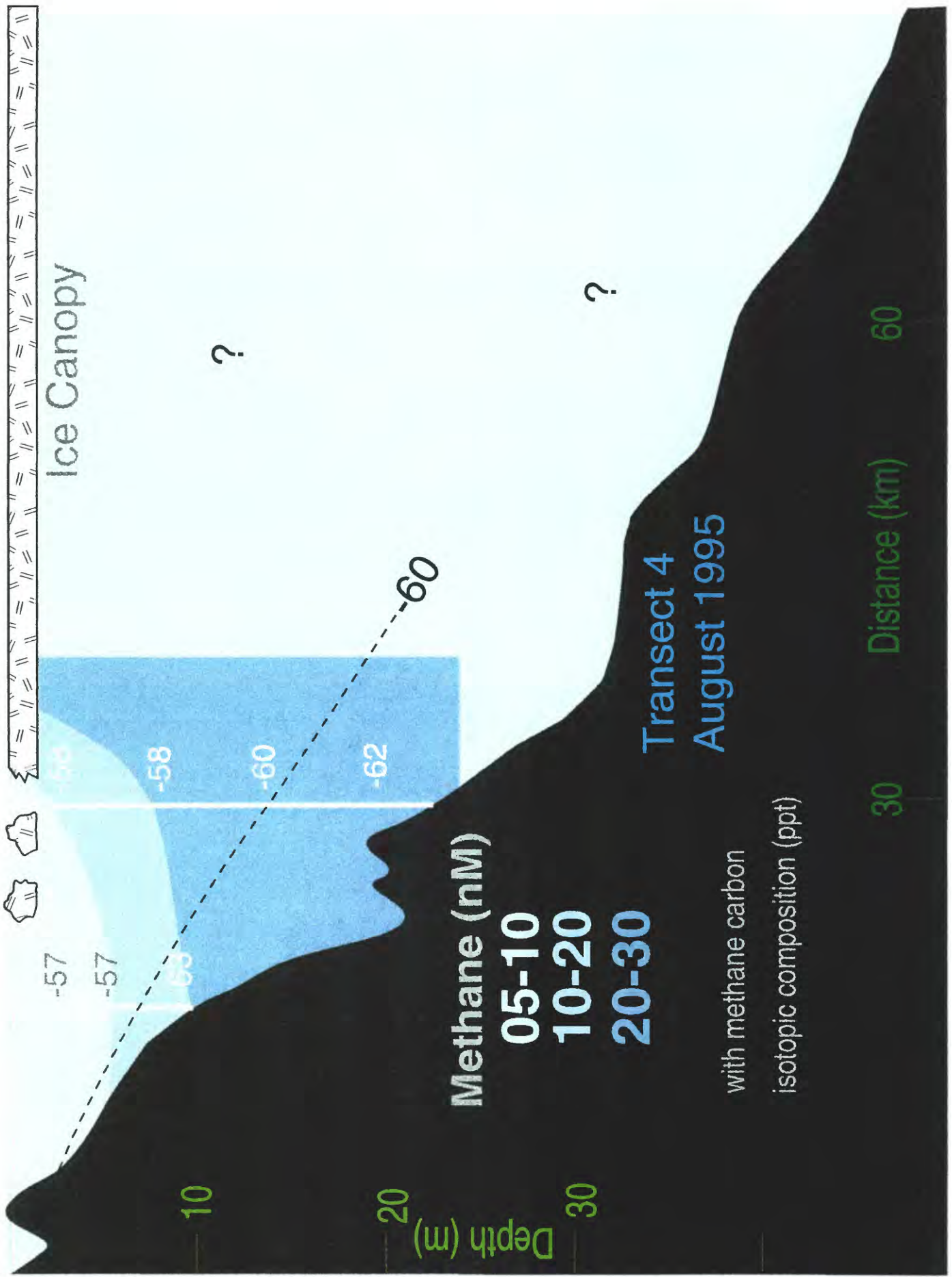




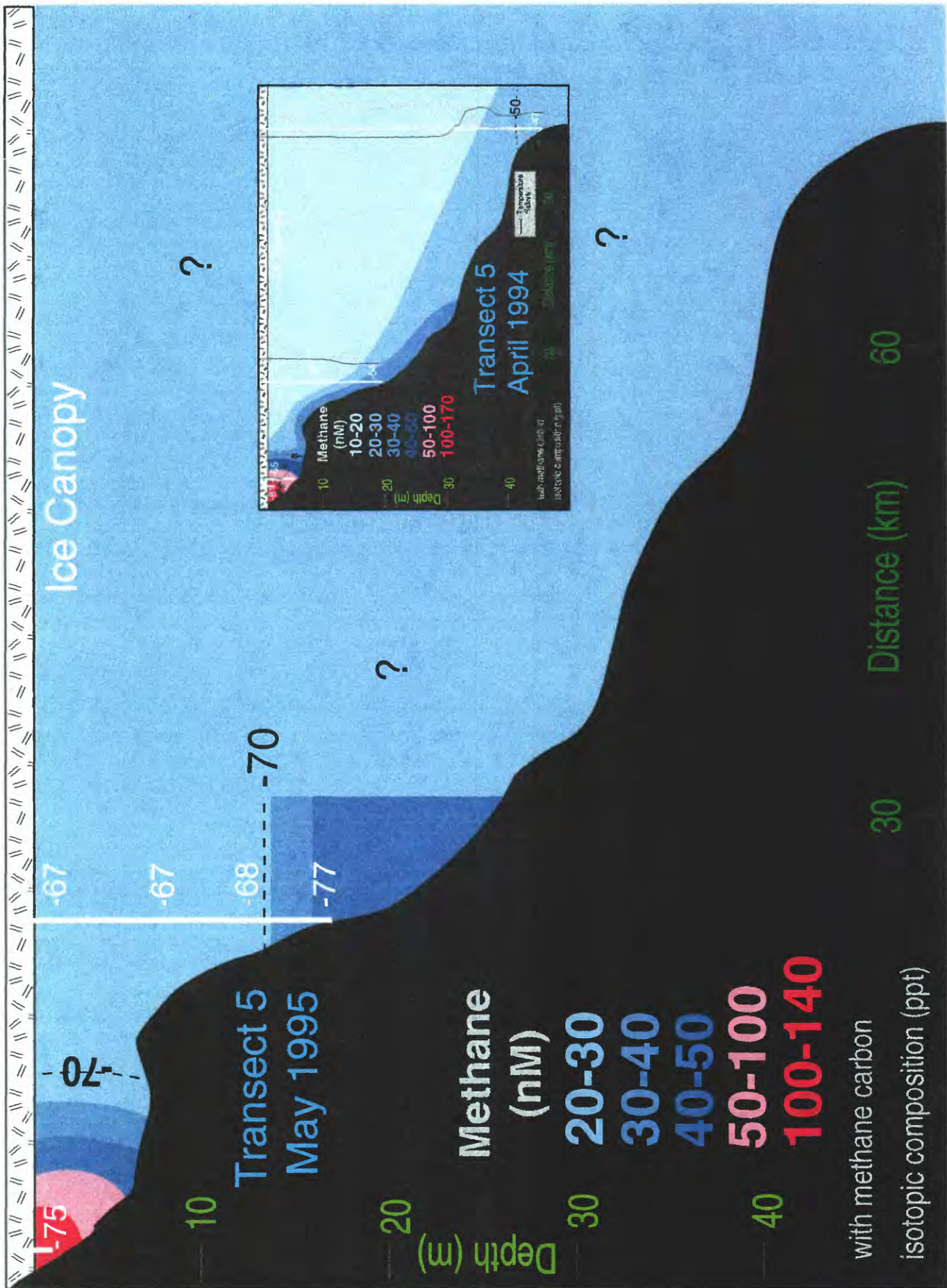




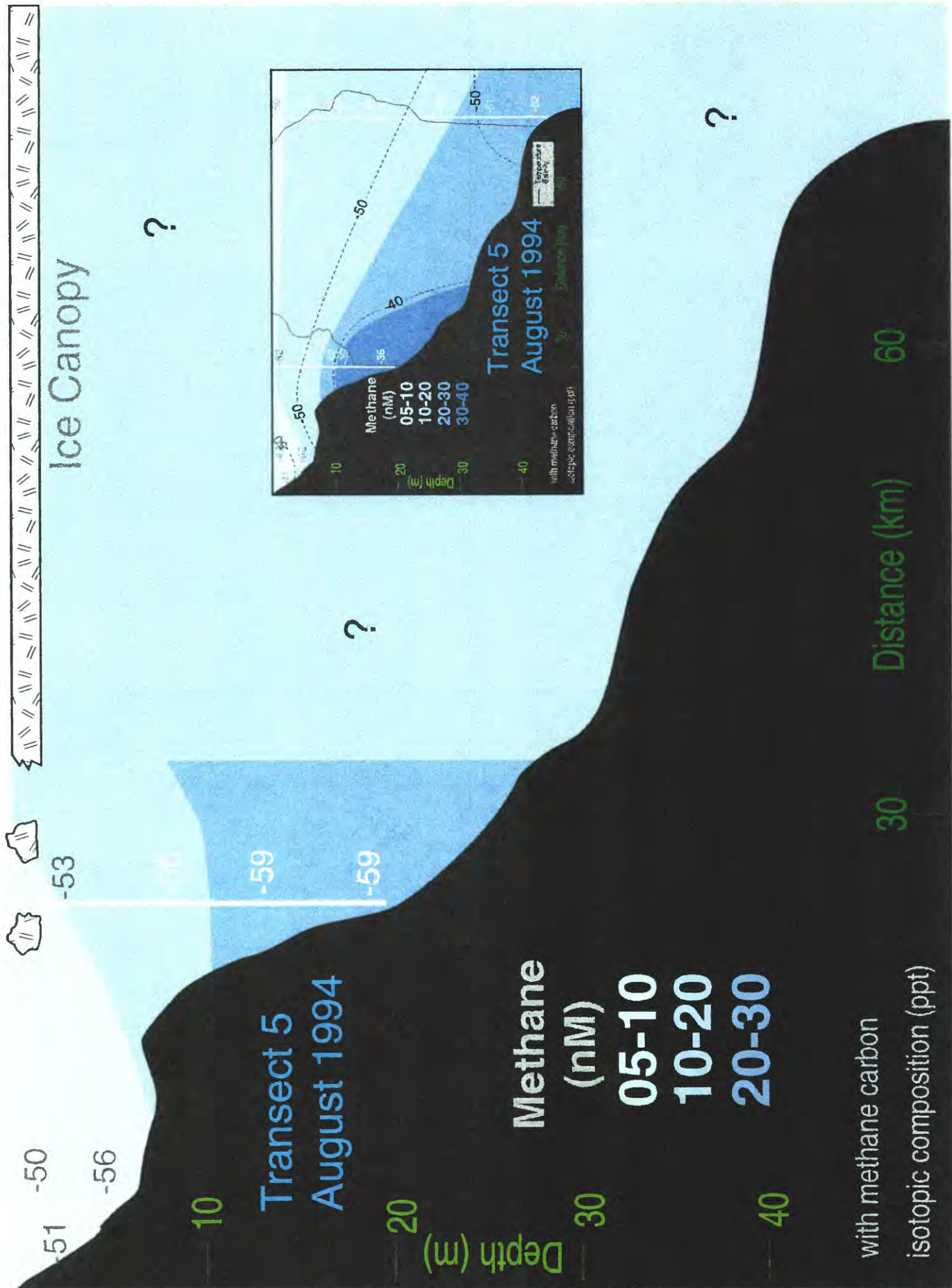




Ice Canopy



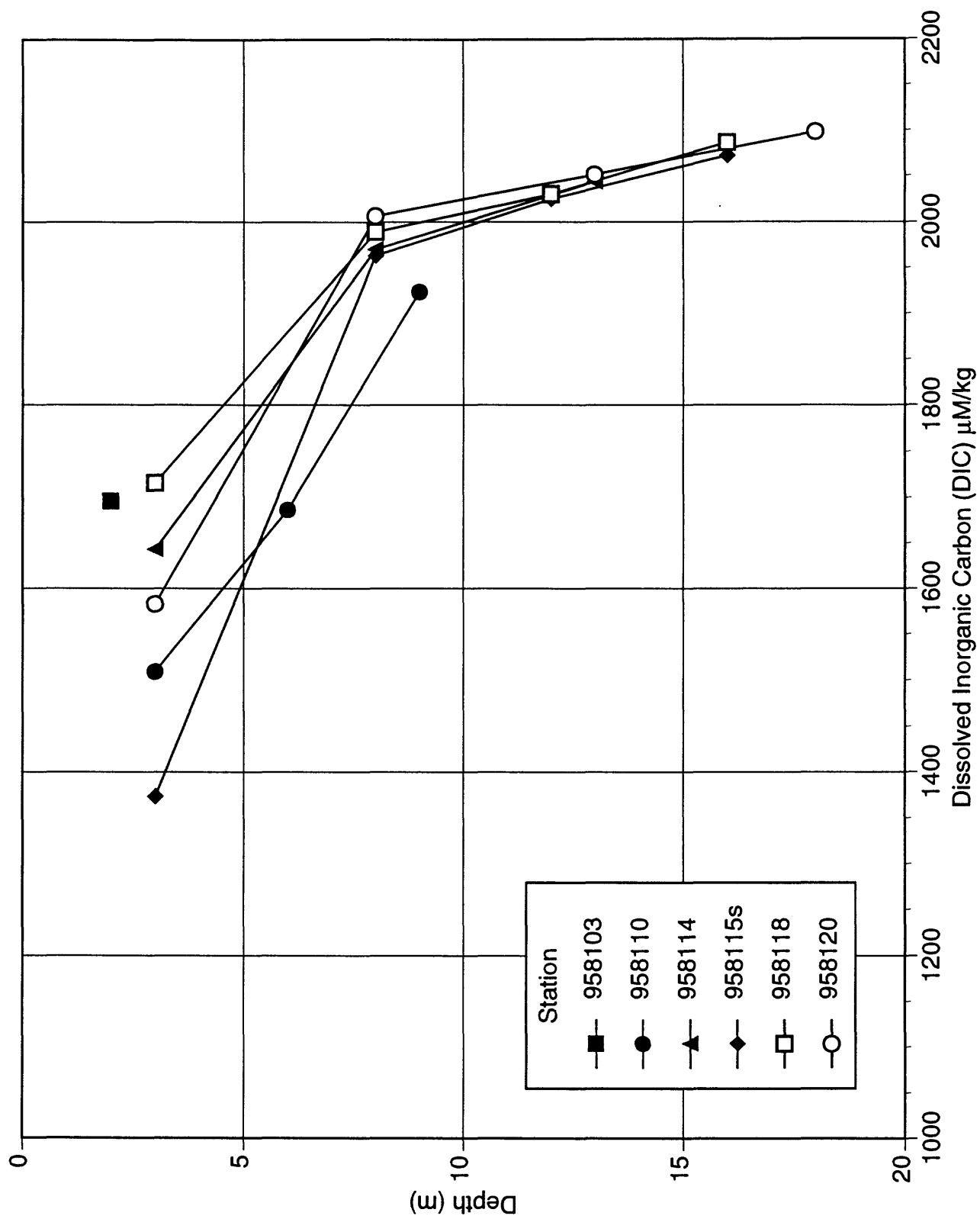
Ice Canopy

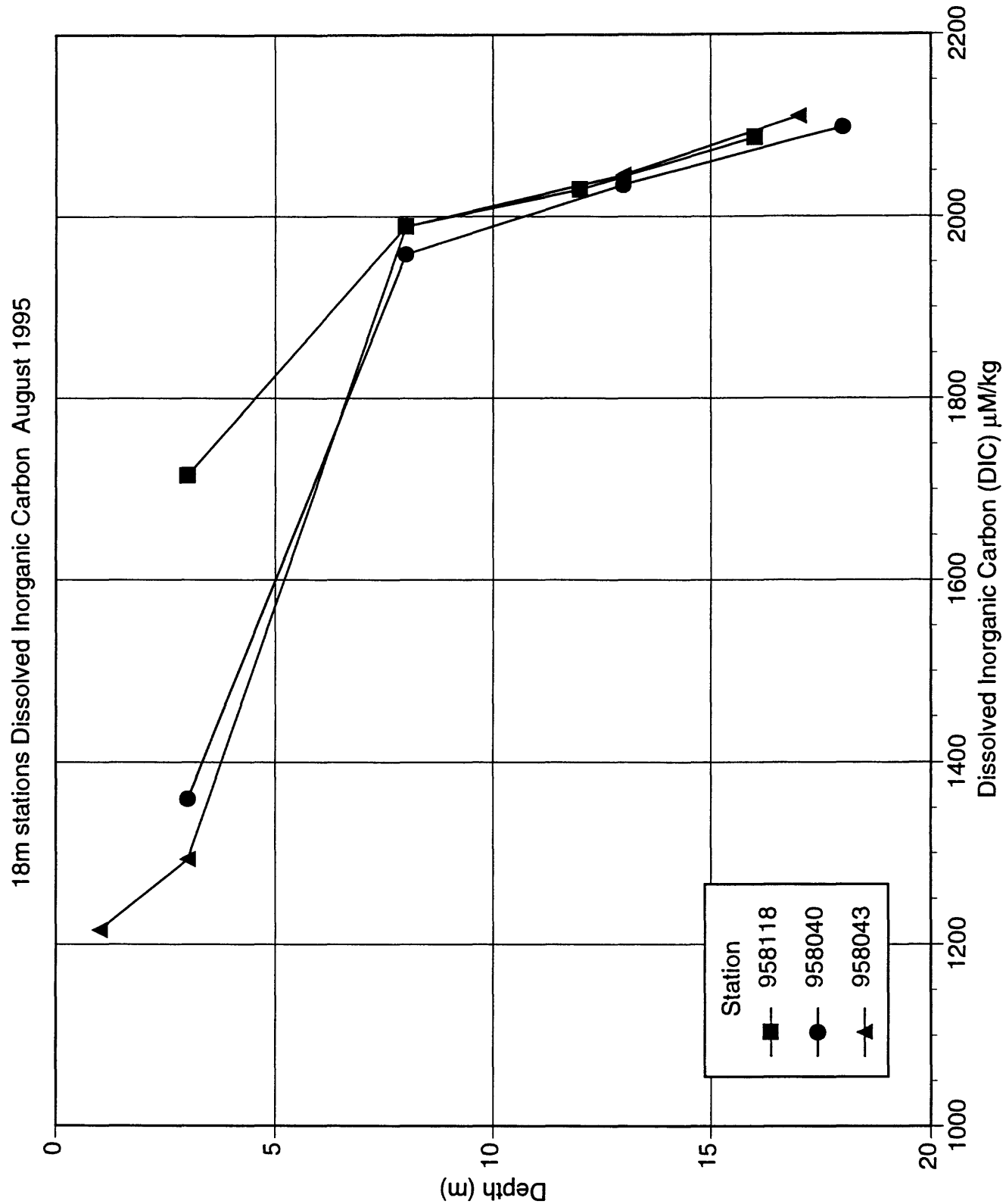


Appendix 4

Dissolved inorganic carbon in water plotted with water depth grouped in transects conducted In August 1995

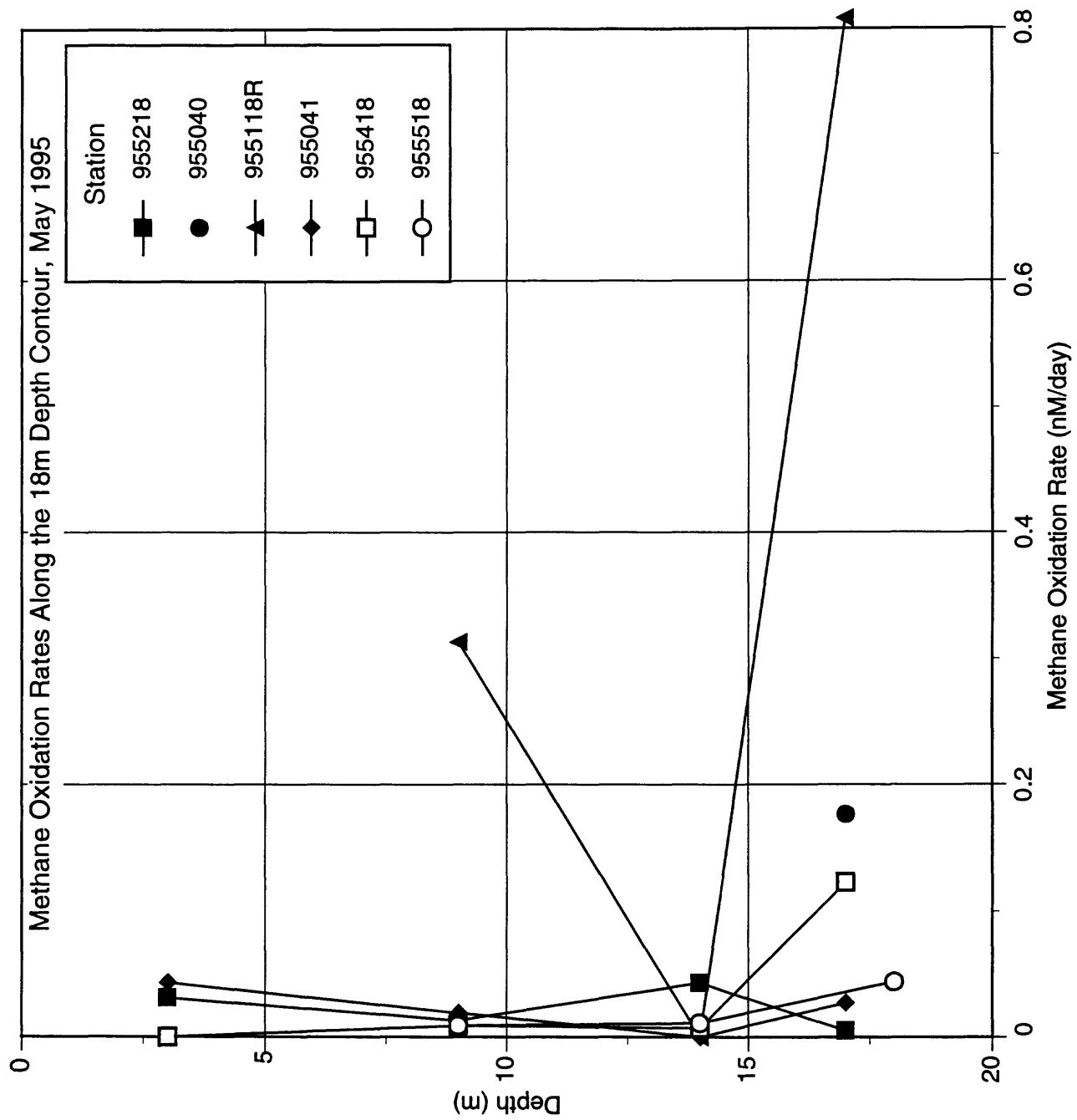
Transect 1 Oliktok Pt. Dissolved Inorganic Carbon August 1995

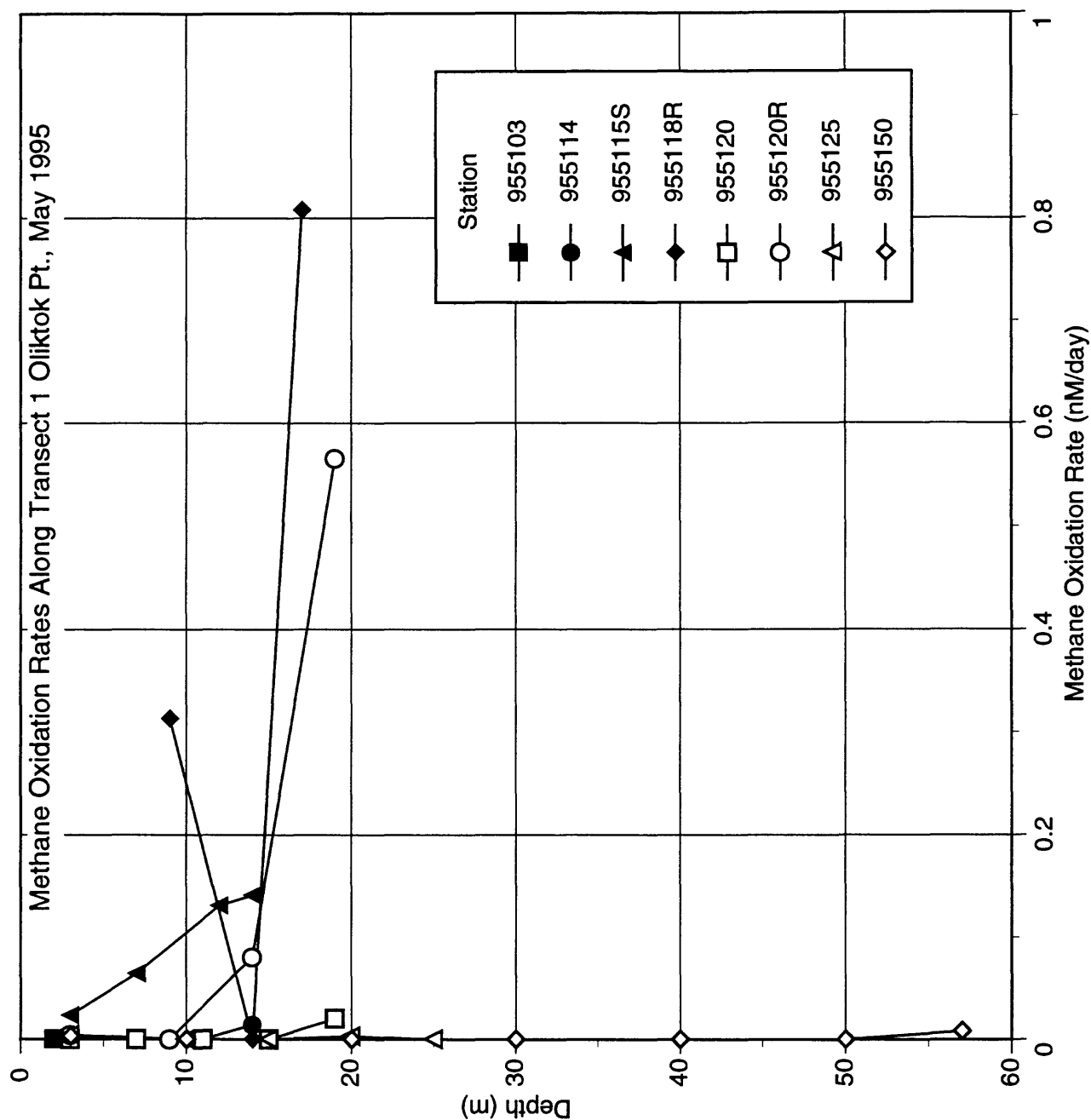




Appendix 5

Methane oxidation rates of water plotted with water depth grouped in transects conducted in each survey





Appendix 6

Methane concentrations of ice plotted with ice depth, grouped in transects

Transect 1 Oliktok Point May 1995

